University of Warsaw
Faculty of Physics

Kamil Serafin

Bound states of heavy quarks in renormalization group procedure for QCD

Doctoral thesis
under supervision of
Prof. dr hab. Stanisław D. Głazek

UNIVERSITY
OF WARSAW

Warsaw, July 2019

Acknowledgments

I would like to thank Professor Stanisław Głazek for his invaluable contribution to my education as a physicist, for the time he devoted to me, and for his patience.

I would also like to thank my parents for their support.

Contents

Chapter 1

Introduction

This thesis concerns a study of bound states of heavy quarks in heavy-flavor Quantum Chromodynamics (QCD). By heavy quarks I mean bottom and charm quarks. The light quarks, up, down, strange, and also top quark (whose mean lifetime is shorter than the typical timescale of hadronic interactions, hence, does not form bound states) are omitted from the theory. Reasons for limiting the theory to heavy and relatively stable quarks will be fully explained later. My main motivation is to contribute to the development of a Hamiltonian theory of hadrons. QCD of heavy-flavor quarks offers several simplifications. Thanks to the large quark masses one can use asymptotic freedom of QCD [1, 2, 3] and expand the Hamiltonian of the theory in powers of the coupling constant g. I perform the expansion explicitly up to order g^2 only. However, I use the fact that the coupling varies with the momentum scale of the renormalized theory once terms of third order and higher are included. Smallness of the coupling constant is related to the smallness of relative momenta of quarks in bound states. The fact that the relative momenta of bound quarks are small allows us to use the nonrelativistic approximation for description of their relative motion. Moreover, the phenomenon of dynamical chiral symmetry breaking is not significant for heavy quarks and does not complicate the theory. Therefore, from the theoretical point of view, heavy-flavor QCD is a good starting point when one seeks to gradually understand the QCD binding mechanism for quarks due to gluons.

The method that I use, which allows me to deal with divergent interactions of local quantum field theories, is called the renormalization group procedure for effective particles (RGPEP) [4, 5]. I present several applications of the method: calculation of masses of doubly-heavy mesons and triply-heavy baryons [6, 7], calculation of form factors in elastic scattering of electrons off heavy hadrons, and calculation of structure functions in deep inelastic scattering (DIS) of electrons off heavy hadrons. The results are approximate and preliminary. The purpose of the thesis is to show that the method can in principle be used for all of those applications.

Masses are usually calculated in the rest frame of a hadron, elastic scattering involves hadrons that move with small and moderate momenta (in comparison with the hadron mass, $\hbar = c = 1$), and DIS processes involve very large momenta. To describe in a unified way processes that involve momenta ranging from very small to very large, the method needs to be relativistic. RGPEP is formulated in the framework of the front form (FF) of Hamiltonian dynamics. This form seems to be best suited to that task among all known Hamiltonian formulations of quantum field theories [8]. The two main reasons are: the relativistic FF wave functions depend only on relative momenta of constituents; the vacuum state is treatable as simple [9, 10, 11, 5].

Several formulations of QCD are used by physicists to describe hadrons. Approaches utilizing Dyson-Schwinger equations [12, 13, 14, 15, 16] use path integral formulation of QCD in Euclidean space instead of the Minkowski space. Hence, the results for correlation functions need to be analytically continued from real Euclidean time to imaginary Euclidean time, which is the Minkowski time [14, 17, 18].

Another class of theoretical approaches, called Lattice QCD [19, 20, 21], uses computer Monte Carlo methods to estimate correlation functions on a finite grid of points in Euclidean space. Lattice

simulations have become recognized as a powerful tool for nonperturbative *ab initio* calculations of properties of hadrons. Using the Monte Carlo simulations, the lattice methods work best for studies of ground states, while extraction of properties of excited states may be difficult. The great progress in lattice studies [22, 23] stimulates also simulations of scattering processes, which are difficult to perform. In order to describe on a lattice a state of a hadron moving with a large momentum the lattice needs to be large enough and dense enough. Therefore, capabilities of lattice simulations depend on the available computer resources. Lattice QCD calculations currently give the best available reference points for the majority of other methods in the low-energy hadronic physics.

I use Lattice results on masses and charge radii of heavy mesons and baryons, wherever available, to compare with my results. The lattice results are very useful to me in the development of the FF Hamiltonian QCD because they allow me to assess the quality of approximations I make. Comparison of my approach results with the lattice simulation results suggests that these approximations may be justifiable, which is an encouraging result at this stage of development of the FF Hamiltonian approach.

Apart from the methods mentioned above there are also various other methods people use to learn more about hadrons. They include: phenomenological models like constituent quark models [24, 25, 26], bag models and Regge phenomenology, AdS/QCD correspondence model [27, 28, 29, 30], effective quantum field theories like nonrelativistic QCD (NRQCD) [31, 32], and the QCD sum rules [33, 34]. Basis Light Front Quantization (BLFQ) that also uses the FF of dynamics, should be mentioned here as the closest one in spirit, though considerably different in detail [35, 36].

An important ingredient of the method at this stage of its development is the assumption that gluons obtain an effective mass. When one derives from QCD an effective Hamiltonian that acts only on the states of quark-antiquark pairs in the case of quarkonia or on just three quarks for triply-heavy baryons, one has to explain how the infinite number of other components of these hadrons, including basis states of unlimited numbers of massless gluons [5], is accounted for. In the method developed in this thesis, the multiple gluon components are replaced by just one component with one gluon that is massive.

Gluon mass of some kind is expected on the basis of results of continuum methods (Dyson-Schwinger methods) [37, 38], lattice QCD studies [39], and phenomenology [40]. Therefore, the usage of gluon mass ansatz appears plausible. The effective Hamiltonian that I mentioned above should be obtained through some reduction procedure that guarantees that the effective Hamiltonian shares eigenvalues with the full Hamiltonian of QCD. Perturbative procedures, such as that of Bloch or Wilson [41, 42], are well-defined only in perturbation theory. Nonperturbative reduction procedures like Gaussian elimination, presented in Sec. 3.1, are difficult to formulate in a quantum field theory with massless particles.

The gluon mass ansatz is an assumption about the nonperturbative effects that some systematic account for gluons, if at all possible, induces on the degrees of freedom that are explicitly kept in the effective theory. In this thesis the small subspace in the space of all states that I explicitly work with is a space composed of a Fock sector with minimal quark content ($Q\bar{Q}$ for mesons and QQQ for baryons) and a sector with the same quarks and a single massive gluon. The gluon mass ansatz refers to the gluon in that second sector of the Fock space. The sector with the massive gluon is perturbatively eliminated, which results in a Hamiltonian eigenvalue equation similar to those written in quark models. This resulting finite effective theory is not sensitive to the details of the mass ansatz in the case of bound states of quarks (and antiquarks) with identical masses.

Future calculations that employ larger spaces, containing more sectors with gluons, may provide an *a posteriori* justification of the ansatz such as the one I use here. Another possibility is to develop nonperturbative calculations of renormalized QCD Hamiltonians. Such calculations are *a priori* possible in the RGPEP. It is not excluded that they produce a gluon mass in the renormalized Hamiltonian that acts still in the whole Fock space, *i.e.*, the one that is calculated in this thesis perturbatively and only up to terms order g^2. The key point I am making is that the gluon mass ansatz may be further studied and possibly validated within the same method of the RGPEP.

Using RGPEP and gluon mass ansatz I obtained masses and wave functions of heavy mesons and heavy baryons. The masses turn out to be in a quite good agreement with the estimates and predictions of other theoretical methods I mentioned earlier. The masses of spin-1 charmonia and bottomonia are used to fit the quark masses and renormalization-group scale parameters for mesons. Then, using an interpolation formula to identify the likely values of the renormalization group parameter for all considered baryon systems, I obtain spectra of heavy baryons that contain no new parameters. Therefore, the masses obtained in this thesis for heavy baryons may be treated as approximate predictions of heavy flavor QCD.

Comparison with Lattice QCD calculations, which are believed to be the best available benchmarks, reveals that not only the ground state masses of bbb and ccc baryons agree, but also their excited spectrum is qualitatively the same. This is rather surprising in view of crudeness of approximations that I used to arrive at the estimates of the masses. Note also that the Lattice calculations are rather complex while mine are largely analytic.

The masses of baryons composed of ccb and bbc quarks are also estimated. The mass of ground state of bbc is in agreement with lattice calculations. However, the ground state of ccb has mass about 300 MeV larger than Lattice QCD predicts. These results are obtained only if one neglects the gluon-mass-ansatz-dependent mass shift that appears only in mesons and baryons composed of quarks with different masses, see Chapter 4. The dependence of the mass shift on squares of masses of quarks, which significantly differ for b and c quarks, and the strong dependence of the shift on the gluon mass ansatz suggest that the shift is an artifact of the gluon mass ansatz. The ansatz may be too simple for describing systems with two significantly different scales. The scale setting in such case needs to be improved, *e.g.*, by introducing two different values of the RGPEP scale parameter in the Hamiltonian. Because the mass shift is the only effect that strongly depends on the gluon mass ansatz, because it can be as small as the spin splittings, and because it is likely to be artificial, I attempted to omit it in the calculation of masses and wave functions of hadrons built from different quarks.

I have used the calculated wave functions, in their approximate analytic forms, to compute form factors and charge radii of the heavy mesons and baryons. Lattice results for mesons and baryons composed of charm quarks (and antiquarks) are available and they agree with my results surprisingly well. Comparison with other methods, which also provide the radii of mesons containing bottom quarks, gives an agreement that is acceptable for a preliminary calculation like the one presented in this thesis when one takes into account that those methods disagree among themselves to a similar degree.

I also computed the magnetic moments of spin-1/2 and spin-1 hadrons. The agreement with results presented in literature is quite good for systems composed of quarks of one flavor, while the magnetic moments of hadrons containing two flavors of quarks are generally bigger than the magnetic moments reported in the literature.

The results for structure functions of heavy hadrons that I obtained are very preliminary. I neglected the huge difference between the scale of momentum transfer Q and the scale of quark binding in the hadron. For that reason the resulting structure functions do not evolve with Q, as they should [43, 44, 45, 46]. Appropriate account of the two vastly different scales using the RGPEP method is expected to give the proper Q-dependence of the structure functions in terms of the transformations it defines. Moreover, since the bound-state formation and scattering problem are described using the same framework, it is not excluded that the method will provide a unified description of evolution of structure functions in the momentum transfer Q and in the Bjorken x [47, 48]. Neglecting the scaling violation, I present my results for structure functions of the ground states of heavy quarkonia and heavy baryons and for a few excited quarkonia states. The structure functions of the excited states show some interesting features absent in the ground-state structure functions. These results are merely my elementary inspection of the starting point for developing the RGPEP application to the structure functions.

The pilot study of heavy mesons and heavy baryons presented in this thesis may be improved in several ways. First of all, perturbative calculation of the renormalized Hamiltonian can be extended

to the fourth order in the coupling constant. This will provide insight about the validity of the gluon mass ansatz and it will render spin-interaction terms and possibly other terms that produce mass shifts of the same order. A possible extension is a combination of the RGPEP methods with BLFQ techniques. A suitable combination might allow for nonperturbative diagonalization of effective Hamiltonians that act in spaces with states containing multiple constituents. Calculations of such type may be necessary to obtain reliable estimates of masses of highly excited states, which probably contain a large gluonic component.

Chapter 2

Hamiltonian formulation of quantum field theory

All of the work presented in this thesis is done using a framework called "the front form of Hamiltonian dynamics." The words front form are often abbreviated to FF. This chapter is intended to be a short introduction to that framework. Therefore, first I present some basic aspects of the Hamiltonian formulation of dynamics of fields, including different forms of dynamics, Poincare algebra of operators and distinction of kinematic and dynamic operators. I will describe some of the advantages of the FF as compared with the standard instant form of Hamiltonian dynamics. The general features of the framework are illustrated in the context of QCD – the theory of my main interest in this thesis. In the last part of the chapter I derive and present the canonical FF Hamiltonian of QCD.

2.1 Introduction

Quantum field theory is first of all a quantum theory. Ordinary quantum mechanics is usually formulated using Hamiltonian formalism, in which information about the state of a physical system is encoded in a vector from the Hilbert space of the theory[1] and evolution of state vectors (or operators, depending on the picture) is generated by the Hamiltonian – a self-adjoint operator on the Hilbert space. The main difference between quantum mechanics and quantum field theory is that the Hilbert space of QFT – the Fock space – is much "bigger" than Hilbert spaces of fixed-number-of-particles quantum theories, by which I mean that it has richer structure. For example, the Fock space is composed of infinitely many sectors, each of which contains a fixed number of particles of fixed types. The number of particles is not conserved because interactions can easily change the particle content. This means that physical states (asymptotic states in a scattering problem and bound states of the Hamiltonian) are linear combinations of states from different sectors of the Fock space. Hence, a vector from a sector of the Fock space is said to contain "bare particles." Even the ground state of the theory (vacuum) is typically believed to be a very complicated combination of bare particles' states. If the vacuum is so complicated, then excited states – states containing physical particles can only add to the complexity. For this reason, among others, people often choose to use noncanonical formulations of quantum field theories, for example path integrals. However, as I argue later, in the FF of Hamiltonian dynamics vacuum is kept simple in a regularized theory.

Classically, to set up the dynamical problem of fields one needs to provide equations of motion (conveniently by defining the density of Lagrangian) and initial and boundary conditions so that the values of fields in any point of interest can be found. Dirac distinguished three particular types of choices (see Fig. 2.1) for the hypersurface on which the initial condition is given and a dynamical system is built [8]. The corresponding forms in which relativistic dynamical theories

[1] More generally, it is encoded in a density matrix.

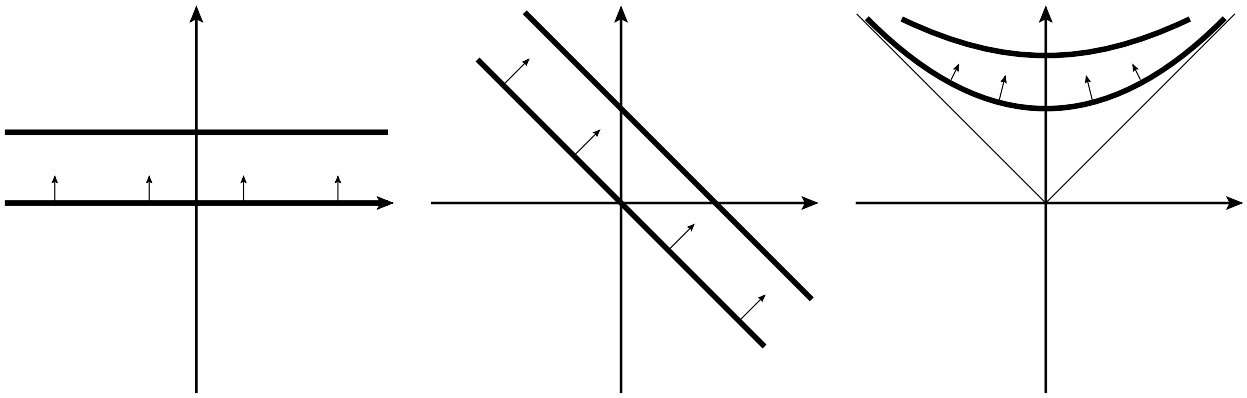

Figure 2.1: Three forms of dynamics. Instant form on the left, point form on the right. The central one is the front form. The usual time, instant-form time, flows upwards. In each form two successive hypersurfaces of constant "time" are shown, appropriately to the form of dynamics. Arrows point in the direction of evolution in "time."

may be put are called "instant form," "point form," and "front form." The central role in Dirac's analysis play "the ten fundamental quantities," which may be organized into a fourvector P^μ and an antisymmetric tensor $M^{\mu\nu}$. In quantum field theory in the instant form these are the operators of energy (Hamiltonian), P^0, three-momentum, P^i, angular momentum, $M^{12} = L^3$, $M^{23} = L^1$, $M^{31} = L^2$, and three boost operators, M^{0i}. They serve the purpose of generating changes of states and operators induced by specific changes in the coordinate system: translation in time, translation in space, rotations, and boosts, respectively. The changes will be consistent with principle of relativity if the ten fundamental quantities fulfill the set of relations,

$$[P^\mu, P^\nu] = 0 \,, \tag{2.1}$$

$$-i\,[M^{\mu\nu}, P^\rho] = -g^{\mu\rho}P^\nu + g^{\nu\rho}P^\mu \,, \tag{2.2}$$

$$-i\,[M^{\mu\nu}, M^{\rho\sigma}] = -g^{\mu\rho}M^{\nu\sigma} + g^{\nu\rho}M^{\mu\sigma} - g^{\mu\sigma}M^{\rho\nu} + g^{\nu\sigma}M^{\rho\mu} \,, \tag{2.3}$$

which define the Poincare algebra. Construction of a representation of this algebra in a noninteracting quantum field theory is known and relatively easy. In the presence of interactions it is a difficult task because some of the conditions in Eqs. (2.1)–(2.3) are quadratic in interactions and they have to be fulfilled by operators acting on a Hilbert space (of which, as it turns out, the Hamiltonian and boost operators can change particle content of a state). One can divide the ten operators, P^μ and $M^{\mu\nu}$, into two groups. Operators in the first group, formed by P^i and M^{ij}, are called kinematic, because their form is the same in the free theory and in the interacting theory. They are the operators whose corresponding coordinate changes leave the hypersurface of an instant time invariant. The operators of the other group, composed of P^0 and M^{0i}, are called dynamic because their form depends on the interactions and they are difficult to construct. In the next section I discuss in some detail the FF of Hamiltonian dynamics and its advantages.

2.2 Front form of Hamiltonian dynamics

Front form of Hamiltonian dynamics is set on a hypersurface tangent to a light cone (see Fig. 2.1) and features seven kinematic generators of Poincare algebra, which is one more than in instant form and point form. Spatial coordinates used in the FF include,

$$x^\pm = x^0 \pm x^3 \,. \tag{2.4}$$

The initial condition is given on the hypersurface defined by $x^+ = 0$. The usual parametrization of the hypersurface is given by the longitudinal coordinate x^- (along the distinguished direction) and transverse coordinates $x^\perp$ (perpendicular to x^3), where I treat symbol $\perp$ as an index that can

take values 1 or 2 (or x and y). [2] The evolution of a system means progression in parameter x^+, a change from one hypersurface of constant x^+ to another one. Therefore, x^+ is the "FF time" – an analogue of the usual time in the instant form.

FF components of tensors can be determined in a similar manner, *e.g.*, $g^{+-} = g^{+0} - g^{+3} = g^{00} + g^{30} - g^{03} - g^{33} = 2$. The lower component, $g_{+-} = 1/2$. If the order of components of four-vectors is (x^+, x^-, x^1, x^2), then,

$$g_{\mu\nu} = \begin{pmatrix} 0 & \frac{1}{2} & 0 & 0 \\ \frac{1}{2} & 0 & 0 & 0 \\ 0 & 0 & -1 & 0 \\ 0 & 0 & 0 & -1 \end{pmatrix} . \tag{2.5}$$

It follows from Eq. (2.5) that

$$p_\mu x^\mu = \frac{1}{2}p^- x^+ + \frac{1}{2}p^+ x^- - p^\perp x^\perp , \tag{2.6}$$

$$p_\mu p^\mu = p^+ p^- - (p^\perp)^2 . \tag{2.7}$$

Component p^- of four-momentum, being conjugate to x^+, is the "FF energy". Hence, the energy-momentum relation for a particle of mass m on the front is,

$$p^- = \frac{m^2 + (p^\perp)^2}{p^+} . \tag{2.8}$$

This is the analogue of instant-form relation $p^0 = \sqrt{m^2 + \vec{p}^2}$. Note that the sign of "energy," p^-, is determined by the sign of longitudinal momentum p^+. Therefore, the positive-energy solutions of the classical equations of motion can be distinguished on the basis of the value of kinematic variable p^+ (as opposed to the instant form, where to every positive energy solution with some three-momentum there is a negative energy solution with the same three-momentum). Condition $p^- \geq 0$ implies

$$p^+ \geq 0 . \tag{2.9}$$

This fact is of a profound importance, because plus component of momentum is conserved at every interaction vertex. Hence, particles (and antiparticles) cannot couple to the vacuum unless they have $p^+ = 0$, which is the value of p^+ that vacuum state should have. States with $p^+ = 0$ are called zero modes. In a regularized theory states with $p^+ = 0$ are excluded. **Therefore, the vacuum in a regularized theory in FF is the same as the Fock vacuum, hence, simple.**

Whenever one deals with a set of particles it is advantageous to define various relative momenta. Suppose we have two particles with momenta p_1^+, $p_1^\perp$ and p_2^+, $p_2^\perp$. The total momentum of the system is $P^+ = p_1^+ + p_2^+$, $P^\perp = p_1^\perp + p_2^\perp$. Longitudinal momentum fraction x_1 (not to be confused with four-vector x^μ or its components) and transverse relative momentum κ_1 of particle 1 are,

$$x_1 = \frac{p_1^+}{P^+} , \tag{2.10}$$

$$\kappa_1^\perp = p_1^\perp - x_1 P^\perp . \tag{2.11}$$

Similarly, one defines relative momenta of particle 2 by replacing indices 1 with 2. Momentum conservation implies $\kappa_2^\perp + \kappa_1^\perp = 0$ and $x_1 + x_2 = 1$, while $1 \geq x_1 \geq 0$ and $1 \geq x_2 \geq 0$ due to

[2] It is a frequent practice to use symbol $\perp$ as characterizing objects with only two transverse components [9]. In that case $\perp$ is written as a subscript and individual components may be further specified by adding a component index. For me the placement of $\perp$ is informative – upper index $\perp$ indicates that the object is a component of some four vector (unless stated otherwise), while the lower index $\perp$ would indicate a component of a covector. In order not to introduce unnecessary confusion, whenever the components of four-vectors are explicitly written, I use only upper-index components.

Eq. (2.9). The total momentum P is also called "parent" momentum, while p_1 is called "child" momentum. It may be convenient to indicate in the notation the parent momentum, for example: $x_1 = x_{1/12}$, $\kappa_1^\perp = \kappa_{1/12}^\perp$, where 12 indicates the parent momentum $P^{+,\perp} = p_1^{+,\perp} + p_2^{+,\perp}$. It is important that the total FF energy is,

$$P^- = p_1^- + p_2^- = \frac{\mathcal{M}_{12}^2 + (P^\perp)^2}{P^+} , \tag{2.12}$$

where $\mathcal{M}_{12}$ is the invariant mass of the system and depends only on the relative variables:

$$\mathcal{M}_{12}^2 = \frac{m_1^2 + \kappa_1^2}{x_1} + \frac{m_2^2 + \kappa_2^2}{x_2} . \tag{2.13}$$

Equations (2.12) and (2.13) show that *the motion of the system as a whole and the relative motion of its constituents are separated* – the energy of the system depends on the momentum of the system and on the mass of the system, while the mass of the system depends only on the relative motion of the constituents. Such separation is not possible in the instant form. Due to this separation bound state problem can be written for the system of particles whose motion as a whole is arbitrary. As is illustrated in Sec. 4.3.1, **wave functions of bound states depend only on the relative momenta, hence, are the same for a bound state at rest and for a bound state moving with the speed close to the speed of light**. In the instant form bound states are sought for primarily in the rest frame of the system and recoil effects present a problem to solve. Where does this difference come from? To boost a state in the instant form – to transform a state at rest into a state in motion – one needs to use boost generators M^{0i}, which are dynamic and depend on interactions. The situation is complicated, because interactions can change number of particles, hence, boosting a state can also change the number of particles. On the other hand, in the FF one of the boost generators $M^{+-} = -2M^{03}$ is kinematic and does not depend on interactions.

There are several problems that one has to face using the FF of Hamiltonian dynamics. First of all, only rotations around z axis are kinematic, hence, one cannot readily use the usual algebra of angular momentum operators. Because rotations around other axes involve interactions it is a dynamic problem to obtain physical manifestations of rotational invariance like angular-momentum degeneracies of states or relativistic form factors in scattering processes. However, equipped with renormalization group procedure to deal with divergent interactions, one can construct all of dynamic operators of the Poincare algebra. An example of such construction up to second order in the interaction in scalar ϕ^3 theory in $1+3$ dimensions can be found in Ref. [49]. One may also be worried that FF cannot describe effects of symmetry breaking that people usually associate with complex structure of the vacuum, *e.g.*, chiral symmetry breaking. While the regularization disconnects the theory from the zero modes it may be necessary to add counterterms to the Hamiltonian that will reproduce the physical effects of the zero modes. Moreover, it is argued that chiral symmetry breaking should be connected with in-hadron condensates instead of condensates that fill all of space [10, 50] and hence, it is a property of the hadron states instead of the vacuum.

2.3 Canonical Front-Form Hamiltonian of QCD

2.3.1 Density of Lagrangian

The starting point for defining the Hamiltonian of QCD is the usual density of Lagrangian. I am interested in the theory with heavy quarks only (c and b), therefore,

$$\mathcal{L} = \sum_{f=b,c} \bar{\psi}_f (i\not{D} - m_f)\psi_f - \frac{1}{4} F^{\mu\nu\,a} F^a_{\mu\nu} , \tag{2.14}$$

where covariant derivative acting on a quark field ψ_f is $D^\mu = \partial^\mu + igG^\mu$ with g the coupling constant of color interactions. $G^\mu = G^{\mu\,a} T^a$ is the four-potential of the color field

$$F^{\mu\nu\,a} = \partial^\mu G^{\nu\,a} - \partial^\nu G^{\mu\,a} - g f^{abc} G^{\mu\,b} G^{\nu\,c} , \tag{2.15}$$

where T^a are the generators of $SU(3)$ – eight 3 by 3 matrices satisfying $[T^a, T^b] = if^{abc}T^c$, $\mathrm{Tr}(T^aT^b) = \delta^{ab}/2$. Conventionally, the color matrices are $T^a = \lambda^a/2$, where λ^a are the Gell-Mann matrices. Lorentz indices denoted by Greek letters run from 0 to 3. Color indices a, b, c run from 1 to 8, color indices i, j run from 1 to 3. Moreover, in FF of Hamiltonian dynamics the directions perpendicular to z axis are also denoted by i, j and run from 1 to 2.

Euler-Lagrange equations are

$$\left(i\not{D} - m_f\right)\psi_f = 0 \,, \tag{2.16}$$

$$D_\mu F^{\mu\nu\,a} = j^{\nu\,a} = \sum_{f=b,c} j_f^{\nu\,a} \,, \tag{2.17}$$

where color currents are

$$j_f^{\nu\,a} = g\,\bar{\psi}_f \gamma^\nu T^a \psi_f \,, \tag{2.18}$$

and the covariant derivative of color field tensor is

$$D_\mu F^{\mu\nu\,a} = \partial_\mu F^{\mu\nu\,a} - g f^{abc}\, G_\mu^b\, F^{\mu\nu\,c} \,. \tag{2.19}$$

2.3.2 Constraint equations

Before one can write down the Hamiltonian, one needs to determine what degrees of freedom this Hamiltonian is supposed to describe. In the FF of dynamics half of fermion field components are dynamic, the other half is constrained. To see this, one first defines projection operators $\Lambda^\pm = \frac{1}{2}\gamma^0\gamma^\pm$. They satisfy $(\Lambda^\pm)^2 = \Lambda^\pm$ and $\Lambda^+ + \Lambda^- = 1$. Now, multiplying Eq. (2.16) by either Λ^+ or Λ^- one obtains two equations:

$$iD^-\psi_{f+} = \left(i\alpha^\perp D^\perp + \beta m_f\right)\psi_{f-} \,, \tag{2.20}$$

$$iD^+\psi_{f-} = \left(i\alpha^\perp D^\perp + \beta m_f\right)\psi_{f+} \,, \tag{2.21}$$

where $\psi_{f\pm} = \Lambda^\pm\psi_f$, $\beta = \gamma^0$, and $\alpha^\perp = \gamma^0\gamma^\perp$. The second of these equations is a constraint on the field ψ_f, because it relates ψ_{f+} and ψ_{f-} components and does not contain any FF-time derivative. Such derivative, $\partial^- = 2\frac{\partial}{\partial x^+}$, acts in the first equation on ψ_{f+}. Therefore, ψ_{f+} is dynamic, while ψ_{f-} is constrained. In gauge $G^+ = 0$ Eq. (2.21) can be formally solved,

$$\psi_{f-} = \frac{1}{i\partial^+}\left(i\alpha^\perp D^\perp + \beta m_f\right)\psi_{f+} \,, \tag{2.22}$$

where $1/(i\partial^+)$ is defined in such a way that Fourier transform of ψ_{f+} is simply divided by momentum p^+. Therefore, ψ_{f-} is completely determined by ψ_{f+} and $G^\perp$, which is there in $D^\perp$.

The second of the Euler-Lagrange equations also contains constraints. In $G^+ = 0$ gauge, putting $\nu = +$ in Eq. (2.17) gives,

$$-\frac{1}{2}(\partial^+)^2 G^- + \partial^+\partial^\perp G^\perp + ig\left[G^\perp, \partial^+ G^\perp\right] = j^+ \,. \tag{2.23}$$

One can formally solve it to express G^- through other fields,

$$G^- = \frac{2}{i\partial^+} i\partial^\perp G^\perp + g\frac{2}{(i\partial^+)^2}\left[i\partial^+ G^\perp, G^\perp\right] + \frac{2}{(i\partial^+)^2} j^+ \,. \tag{2.24}$$

Note that $j_f^{+\,a} = 2g\psi_{f+}^\dagger T^a \psi_{f+}$, hence, depends only on the dynamic components of the quark field. Therefore, G^- is completely determined by the dynamic fields ψ_{f+} and $G^{\perp a}$.

2.3.3 Density of the canonical Hamiltonian

One defines canonical stress-energy tensor,

$$T^{\mu}_{\ \nu} = \sum_{f=b,c} \frac{\partial \mathcal{L}}{\partial(\partial_\mu \psi_f)} \partial_\nu \psi_f + \partial_\nu \psi_f^\dagger \frac{\partial \mathcal{L}}{\partial(\partial_\mu \psi_f^\dagger)} + \frac{\partial \mathcal{L}}{\partial(\partial_\mu G^{\alpha\, a})} \partial_\nu G^{\alpha\, a} - \delta^{\mu}_{\ \nu} \mathcal{L} \tag{2.25}$$

$$= \sum_{f=b,c} \bar{\psi}_f i\gamma^\mu \partial_\nu \psi_f - \delta^{\mu}_{\ \nu} \bar{\psi}_f \left(i\not{\partial} - m_f \right) \psi_f + \frac{1}{4} \delta^{\mu}_{\ \nu} F^{\alpha\beta\, a} F^a_{\alpha\beta} - F^{\mu\ \ a}_{\ \alpha}\ \partial_\nu G^{\alpha\, a} \ . \tag{2.26}$$

The second term is zero for fields satisfying Eq. (2.16). In the instant form T^{00} would be chosen as the density of energy and integrated over space to yield the canonical Hamiltonian of QCD. In the FF the density of canonical Hamiltonian is given by T^{+-} component,

$$\mathcal{H} = \frac{1}{2} T^{+-} \ . \tag{2.27}$$

and, after integration over $x^+ = 0$ hypersurface, gives the canonical FF Hamiltonian, *cf.* Eq. (2.38). In anticipation of that integration one can manipulate the form of T^{+-} in a way that corresponds to integration by parts in Eq. (2.38) with omission of boundary terms. After tedious manipulations, which additionally involve using Euler-Lagrange equations, the density of the canonical FF Hamiltonian can be cast in the following form,

$$\mathcal{H} = \mathcal{H}_{\psi^2} + \mathcal{H}_{G^2} + \mathcal{H}_{G^3} + \mathcal{H}_{G^4} + \mathcal{H}_{\psi G \psi} + \mathcal{H}_{\psi G G \psi} + \mathcal{H}_{[\partial GG]^2} + \mathcal{H}_{[\partial GG](\psi\psi)} + \mathcal{H}_{(\psi\psi)^2} \ , \tag{2.28}$$

where

$$\mathcal{H}_{\psi^2} = \sum_{f=b,c} \bar{\psi}_f \frac{\gamma^+}{2} \frac{(i\partial^\perp)^2 + m_f^2}{i\partial^+} \psi_f \ , \tag{2.29}$$

$$\mathcal{H}_{G^2} = \frac{1}{2} G^{i\, a} (i\partial^\perp)^2 G^{i\, a} \ , \tag{2.30}$$

$$\mathcal{H}_{G^3} = g \left(i\partial_\alpha G^a_\beta \left[G^\alpha, G^\beta \right]^a \right) \Big|_{g=0} \ , \tag{2.31}$$

$$\mathcal{H}_{G^4} = -\frac{1}{4} g^2 \left[G_\alpha, G_\beta \right]^a \left[G^\alpha, G^\beta \right]^a \ , \tag{2.32}$$

$$\mathcal{H}_{\psi G \psi} = (j^a_\mu)_{g=0} G^{\mu\, a} \ , \tag{2.33}$$

$$\mathcal{H}_{\psi G G \psi} = \frac{1}{2} g^2 \sum_{q=b,c} \bar{\psi}_q \not{G} \frac{\gamma^+}{i\partial^+} \not{G} \psi_q \ , \tag{2.34}$$

$$\mathcal{H}_{[\partial GG]^2} = \frac{1}{2} g^2 \left[i\partial^+ G^\perp, G^\perp \right]^a \frac{1}{(i\partial^+)^2} \left[i\partial^+ G^\perp, G^\perp \right]^a \ , \tag{2.35}$$

$$\mathcal{H}_{[\partial GG](\psi\psi)} = j^{+\, a} \frac{1}{(i\partial^+)^2}\ g \left[i\partial^+ G^\perp, G^\perp \right]^a \ , \tag{2.36}$$

$$\mathcal{H}_{(\psi\psi)^2} = \frac{1}{2} j^{+\, a} \frac{1}{(i\partial^+)^2}\ j^{+\, a} \ . \tag{2.37}$$

The first two terms correspond to free propagation of quarks and gluons. The next three terms are similar to interaction vertices in a Lagrangian theory. The last four terms are called instantaneous interactions and arise due to constraints in the Hamiltonian theory. In all but two terms – $\mathcal{H}_{G^3}$

and $\mathcal{H}_{\psi G\psi}$ – only the dynamical components of the fields are present. For example, $j^{+\,a}$ contains only ψ_{f+} part of the field and in $\mathcal{H}_{G^4}$ whenever there appears G^- it is multiplied by G^+, which is zero due to the gauge choice. Only terms that are products of three fields contain ψ_{f-} and G^-. These parts of quark and gluon fields in Eqs. (2.22) and (2.24) are obtained by solving the constraint equations with $g = 0$.

2.3.4 Canonical Hamiltonian

The canonical Hamiltonian is defined as an integral of the density Eq. (2.28) with classical fields replaced by quantum operators,

$$H = \int dx^- d^2x^\perp : \mathcal{H} : \ . \tag{2.38}$$

Quantum fields are expanded in terms of their Fourier transforms. Quark fields are

$$(\psi_f)_{g=0} \ = \ \int_1 \left[\chi_1 u_1 b_{f1} e^{-ip_1 x} + \chi_1 v_1 d^\dagger_{f1} e^{ip_1 x}\right]\Big|_{x^+=0} \ , \tag{2.39}$$

where χ denotes three-vector in color space, u and v are particle and antiparticle spinors, and b_f and d_f are annihilation operators of quark and antiquark of flavor f. Very compact notation, which I use, means,

$$\int_1 \ = \ \sum_{\sigma_1 i_1} \int [p_1] \ , \tag{2.40}$$

$$\begin{aligned}
\chi_1 &= \chi_{i_1} \ , && (2.41)\\
u_1 &= u_{m_f}(p_1^\perp, p_1^+, \sigma_1) \ , && (2.42)\\
v_1 &= v_{m_f}(p_1^\perp, p_1^+, \sigma_1) \ , && (2.43)\\
b_{f1} &= b_f(p_1^\perp, p_1^+, \sigma_1, i_1) \ , && (2.44)\\
d_{f1} &= d_f(p_1^\perp, p_1^+, \sigma_1, i_1) \ , && (2.45)
\end{aligned}$$

where f is the flavor of quark and m_f, p_1, σ_1, i_1 are its mass, four-momentum, spin projection on z axis and color index respectively. Moreover,

$$\int [p_1] \ = \ \int_0^\infty \frac{dp_1^+}{4\pi p_1^+} \int \frac{d^2p_1^\perp}{(2\pi)^2} \ . \tag{2.46}$$

The only nonzero anticommutation relations between creation and annihilation operators are,

$$\begin{aligned}
\left\{b_{f_1 1}, b^\dagger_{f_2 2}\right\} &= p_1^+ \delta_{f_1 f_2} \delta_{i_1 i_2} \delta_{\sigma_1 \sigma_2} \tilde{\delta}_{1.2} \ , && (2.47)\\
\left\{d_{f_1 1}, d^\dagger_{f_2 2}\right\} &= p_1^+ \delta_{f_1 f_2} \delta_{i_1 i_2} \delta_{\sigma_1 \sigma_2} \tilde{\delta}_{1.2} \ , && (2.48)
\end{aligned}$$

where

$$\tilde{\delta}_{1.2} \ = \ 2(2\pi)^3 \delta^2(p_1^\perp - p_2^\perp)\delta(p_1^+ - p_2^+) \ , \tag{2.49}$$

The spinors are [11],

$$\begin{aligned}
u_m(p^\perp, p^+, \sigma) &= \frac{1}{\sqrt{p^+}} \begin{bmatrix} p^+ \\ i\sigma^\perp \times p^\perp + m \end{bmatrix} \chi_\sigma \ , && (2.50)\\
v_m(p^\perp, p^+, \sigma) &= \frac{1}{\sqrt{p^+}} \begin{bmatrix} -p^+ \\ -i\sigma^\perp \times p^\perp + m \end{bmatrix} \chi_{-\sigma} \ , && (2.51)
\end{aligned}$$

where

$$i\sigma^\perp \times p^\perp \;=\; \det\begin{bmatrix} i\sigma^1 & p^1 \\ i\sigma^2 & p^2 \end{bmatrix} = -i\sigma^2 p^1 + i\sigma^1 p^2 \;, \tag{2.52}$$

and $\sigma^\perp$ are Pauli matrices. The quantized gluon field is

$$G^\mu|_{g=0} \;=\; \int_1 \left(\varepsilon_1^\mu a_1 e^{-ip_1 x} + \varepsilon_1^{\mu *} a_1^\dagger e^{ip_1 x}\right) T^a \;, \tag{2.53}$$

where

$$\int_1 \;=\; \sum_{\sigma_1 c_1} \int [p_1] \;, \tag{2.54}$$

$$a_1 \;=\; a(p_1^\perp, p_1^+, \sigma_1, c_1) \;, \tag{2.55}$$

and the nonzero commutation relations are,

$$\left[a_1, a_2^\dagger\right] \;=\; p_1^+ \delta_{c_1 c_2} \delta_{\sigma_1 \sigma_2} \tilde{\delta}_{1.2} \;. \tag{2.56}$$

The gluon polarization vector is

$$\varepsilon_1^\mu \;=\; \varepsilon^\mu_{p_1 \sigma_1} \;, \tag{2.57}$$

where,

$$\varepsilon^\mu_{p\sigma} \;=\; \begin{bmatrix} \varepsilon^+ = 0 \\ \varepsilon^-_{p\sigma} = \frac{2p^\perp \varepsilon_\sigma^\perp}{p^+} \\ \varepsilon_\sigma^\perp \end{bmatrix} \;. \tag{2.58}$$

Using the notation established above the canonical Hamiltonian of QCD is,

$$H^{\rm can}_{\rm QCD} \;=\; H_0 + g H_1^{\rm can} + g^2 H^{\rm can}_{Q\bar{Q}\,\rm inst} + g^2 H^{\rm can}_{QQ\,\rm inst} + \dots \;, \tag{2.59}$$

where the dotted terms are not needed in their explicit form at this point. The free Hamiltonian is,

$$H_0 \;=\; \sum_{f=b,c} \int_1 p_1^- \left(b^\dagger_{f\,1} b_{f\,1} + d^\dagger_{f\,1} d_{f\,1}\right) + \int_1 p_1^- a_1^\dagger a_1 \;. \tag{2.60}$$

Eigenstates of H_0 are the multiparticle states obtained by action of products of creation operators $b_f^\dagger$, $d_f^\dagger$ and $a^\dagger$ on the free vacuum state $|0\rangle$. Action of any of the annihilation operators on $|0\rangle$ gives zero. The first order interaction terms are,

$$H_1^{\rm can} \;=\; \sum_{f=b,c} \int_{123} \left[B_{21.3}\; t^1_{23}\; b^\dagger_{f2} a_1^\dagger b_{f3} + D_{21.3}\; t^1_{32}\; d^\dagger_{f2} a_1^\dagger d_{f3} + \text{H.c.}\right] \;, \tag{2.61}$$

where

$$t^1_{23} \;=\; \chi^\dagger_{i_2} T^{c_1} \chi_{i_3} \;, \tag{2.62}$$

and

$$B_{21.3} \;=\; +\tilde{\delta}_{21.3} \bar{u}_2 \not{\varepsilon}_1^* u_3 \;=\; +\tilde{\delta}_{21.3}\; j^\mu_{23} \varepsilon^*_{1\,\mu} \;, \tag{2.63}$$

$$D_{21.3} \;=\; -\tilde{\delta}_{21.3} \bar{v}_3 \not{\varepsilon}_1^* v_2 \;=\; -\tilde{\delta}_{21.3}\; \bar{j}^\mu_{32}\, \varepsilon^*_{1\,\mu} \;, \tag{2.64}$$

$$j^\mu_{12} \;=\; \bar{u}_1 \gamma^\mu u_2 \;, \tag{2.65}$$

$$\bar{j}^\mu_{21} \;=\; \bar{v}_2 \gamma^\mu v_1 \;. \tag{2.66}$$

Terms that are second order in the coupling constant are divided in two parts. The first consists of interactions between quarks b and c, including terms that involve only one flavor and terms that involve both charm and bottom quarks:

$$\begin{aligned} H^{\rm can}_{QQ\,\rm inst} &= \sum_{f=b,c} \frac{1}{2} \int_{121'2'} \tilde{\delta}_{12.1'2'} \ {\rm Asym}\Big\{ \frac{j^+_{11'} j^+_{22'}}{(p^+_1 - p^+_{1'})^2} \ t^a_{11'} t^a_{22'} \Big\} \ b^\dagger_{f\,1} b^\dagger_{f\,2} b_{f\,2'} b_{f\,1'} \\ &+ \int_{121'2'} \tilde{\delta}_{12.1'2'} \ \frac{j^+_{11'} j^+_{22'}}{(p^+_1 - p^+_{1'})^2} \ t^a_{11'} t^a_{22'} \ b^\dagger_{b\,1} b^\dagger_{c\,2} b_{c\,2'} b_{b\,1'} \ . \end{aligned} \tag{2.67}$$

Note that single-flavor terms have extra $1/2$, which cancels in matrix elements of $H^{\rm can}_{QQ\,\rm inst}$ with a factor of 2 that appears due to two possible ways one can contract the annihilation and creation operators. Moreover, the function of momenta, spins and colors of quarks that stands in front of the creation and annihilation operators is antisymmetrized in indexes 1 and 2, because only the antisymmetric part survives the integration. For any function $V(1,2;1',2')$,

$$ {\rm Asym}\Big\{ V(1,2;1',2') \Big\} \ = \ \frac{1}{2} \left[V(1,2;1',2') - V(2,1;1',2') \right] \ . \tag{2.68}$$

If $V(1,2;1',2') = V(1',2';1,2)$, then antisymmetrization of indexes 1 and 2 also automatically ensures antisymmetry in indexes $1'$ and $2'$. The function that is antisymmetrized in Eq. (2.67) fulfills that condition.

The other second order term of the canonical Hamiltonian consists of interactions between a quark and an antiquark in all possible flavor combinations:

$$ H^{\rm can}_{Q\bar{Q}\,\rm inst} \ = \ - \sum_{f_1,f_2=b,c} \int_{121'2'} \tilde{\delta}_{12.1'2'} \ \frac{j^+_{11'} \bar{j}^+_{2'2}}{(p^+_1 - p^+_{1'})^2} \ t^a_{11'} t^a_{2'2} \ b^\dagger_{f_1\,1} d^\dagger_{f_2\,2} d_{f_2\,2'} b_{f_1\,1'} \ . \tag{2.69}$$

As compared with $H^{\rm can}_{QQ\,\rm inst}$ this term has inverted direction of flow of color and spin and j^+ replaced by $-\bar{j}^+$.

2.4 Need for regularization of the canonical Hamiltonian

The canonical Hamiltonian of QCD is not well-defined. For example, the second order correction to the energy of a free quark state $b^\dagger_{f\,1}|0\rangle$ involves the product of two $H^{\rm can}_1$ Hamiltonians and is divergent – the integral over all intermediate states does not exist. Regularization is, therefore, necessary to have mathematically well-defined integrals in perturbation theory and eigenvalue equations like the ones I write in Chapter 4. Renormalization solves the problem of dependence of observables on unphysical regularization parameters. In its essence, it does it by introducing into vertices its own regulating functions, like the RGPEP form factors Eq. (3.31, that regulate the divergent interactions [51]. But the regularization should be chosen in such a way, that it does not spoil too much the symmetries one wants to have in the theory. For example, regularization by removing states with high momenta breaks the Lorentz symmetry, because there is a highest available momentum in the theory, while Lorentz boosts can make momentum arbitrarily large. It is more advantageous to use a regularization that does not break Lorentz symmetry, because then, *e.g.*, the construction of relativistically covariant amplitudes should be easier [51]. Therefore, instead of, *e.g.*, restricting the range of Fourier components of fields that are used, I restrict the interactions that are allowed in the theory [6]. Moreover, using sharp cutoff functions like Heaviside step function introduces nonanaliticities, which may be hard to handle. Therefore, it is better to use smooth regulating functions.

The regulating functions that I use are introduced according to the following prescription. Suppose we have an interaction vertex and the total momentum annihilated (or created) in the vertex is $P^{+,\perp}$. The momentum of a particle annihilated (or created) in the interaction is $p^{+,\perp}$,

and relative momentum of that particle with respect to other particles annihilated (or created) in the interaction is $x = p^+/P^+$, $\kappa^\perp = p^\perp - xP^\perp$. If that particle is a quark then a factor of

$$\exp\left(-\frac{m^2+\kappa^2}{x\Delta^2}\right) \tag{2.70}$$

is associated with that quark, where m is its mass. If the particle is a gluon then the factor is,

$$\exp\left(-\frac{\delta^2+\kappa^2}{x\Delta^2}\right) \ . \tag{2.71}$$

Δ is called the ultraviolet cutoff and it regulates the difference between the invariant mass of the state before interaction and the invariant mass of the state after the interaction. δ regulates divergences that may appear for small values of gluon x, so-called small-x divergences. The regulating function associated with the interaction vertex is a product of factors for all particles involved in the interaction. The instantaneous interaction terms, which are of order g^2 are regulated as if they were products of first-order interaction vertices.

Therefore, the regulated Hamiltonian of QCD is,

$$H^{\rm R}_{\rm QCD} \ = \ H_0 + gH^{\rm R}_1 + g^2 H^{\rm R}_{Q\bar{Q}\,\rm inst} + g^2 H^{\rm R}_{QQ\,\rm inst} + \dots \ , \tag{2.72}$$

where H_0 in not regulated, because it does not involve interactions. The first-order regulated Hamiltonian term is

$$H^{\rm R}_1 \ = \ \sum_{f=b,c} \int_{123} \Big[r_{21.3}\ B_{21.3}\ t^1_{23}\ b^\dagger_{f2} a^\dagger_1 b_{f3} + r_{21.3}\ D_{21.3}\ t^1_{32}\ d^\dagger_{f2} a^\dagger_1 d_{f3} + \text{H.c.} \Big] \ , \tag{2.73}$$

where

$$r_{21.3} \ = \ e^{-\frac{m_f^2+\kappa^2_{2/3}}{x_{2/3}\Delta^2}} e^{-\frac{\delta^2+\kappa^2_{1/3}}{x_{1/3}\Delta^2}} e^{-\frac{m_f^2}{\Delta^2}} \ = \ e^{-\frac{\mathcal{M}^2_{21}+m_f^2}{\Delta^2}} e^{-\frac{\epsilon^2}{x_{1/3}}} \ , \tag{2.74}$$

where $\epsilon = \delta/\Delta$. Regularized terms that are second order in the coupling constant are,

$$\begin{aligned} H^{\rm R}_{QQ\,\rm inst} \ &= \ \sum_{f=b,c} \frac{1}{2} \int_{121'2'} \tilde{\delta}_{12.1'2'}\ \text{Asym}\Big\{ r_{C\,12.1'2'}\ \frac{j^+_{11'} j^+_{22'}}{(p^+_1 - p^+_{1'})^2}\ t^a_{11'} t^a_{22'} \Big\}\ b^\dagger_{f\,1} b^\dagger_{f\,2} b_{f\,2'} b_{f\,1'} \\ &+ \ \int_{121'2'} \tilde{\delta}_{12.1'2'}\ r_{C\,12.1'2'}\ \frac{j^+_{11'} j^+_{22'}}{(p^+_1 - p^+_{1'})^2}\ t^a_{11'} t^a_{22'}\ b^\dagger_{b\,1} b^\dagger_{c\,2} b_{c\,2'} b_{b\,1'} \ , \end{aligned} \tag{2.75}$$

$$H^{\rm R}_{Q\bar{Q}\,\rm inst} \ = \ -\sum_{f_1,f_2=b,c} \int_{121'2'} \tilde{\delta}_{12.1'2'}\ r_{C\,12.1'2'}\ \frac{j^+_{11'} \bar{j}^+_{2'2}}{(p^+_1 - p^+_{1'})^2}\ t^a_{11'} t^a_{2'2}\ b^\dagger_{f_1\,1} d^\dagger_{f_2\,2} d_{f_2\,2'} b_{f_1\,1'} \ , \tag{2.76}$$

where

$$r_{C\,12.1'2'} \ = \ \theta(x_{1'} - x_1) r_{14.1'} r_{2'4.2} + \theta(x_1 - x_{1'}) r_{1'4.1} r_{24.2'} \ , \tag{2.77}$$

and 4 denotes the momentum of would-be exchanged gluon, see the left diagram in Fig. 3.5.

Chapter 3

Renormalization group procedures for Hamiltonians

Canonical Hamiltonian of QCD is ill-defined and needs to be regularized and renormalized. In this chapter I review two kinds of renormalization group procedures for Hamiltonians. In Wilsonian renormalization group procedure one integrates out high-energy degrees of freedom to obtain finite effective theory of only low-energy degrees of freedom. I present it on a quantum-mechanical example of a divergent potential $1/r^2$. Then I discuss the idea that instead of integrating out high-energy degrees of freedom one can, in a sense, integrate out interactions that cause big jumps in invariant masses of states. This idea is the cornerstone of renormalization group procedure for effective particles (RGPEP), which is the method I use to study bound states in QCD. Its central concept is the concept of effective particles with nonzero size. The effective theory of such particles involves non-local interactions, yet the theory may still be relativistic, because the renormalization group equations preserve all kinematic symmetries of the front form of Hamiltonian dynamics. After theoretical introduction to RGPEP I present the renormalized Hamiltonian of QCD obtained using RGPEP equations solved up to second order.

3.1 Renormalization by integrating out large-energy degrees of freedom

3.1.1 Illustrative example: Schrödinger particle in potential $-\alpha/r^2$

The purpose of this section is to illustrate on a simple example the general principles of Wilsonian renormalization group procedure. The example is a quantum-mechanical potential $1/r^2$, which is known to be divergent [52]. The renormalization of this model was studied in Ref. [53], where prior literature on the subject is extensively discussed. The Hamiltonian is,

$$H \;=\; -\frac{\Delta}{2m} - \frac{g}{r^2}\;, \tag{3.1}$$

where m is the mass of the particle and r is the distance from the center. The eigenvalue problem, the usual Schrödinger equation, written in momentum space reads,

$$\frac{p^2}{2m}\phi(\vec{p}) - \frac{g}{4\pi}\int \frac{d^3q}{(2\pi)^3}\frac{1}{|\vec{p}-\vec{q}|}\phi(\vec{q}) \;=\; E\phi(\vec{p})\;. \tag{3.2}$$

Since the potential is formally spherically symmetric it should be possible for the eigenstates, if they exist, to write them as states with definite total angular momentum and its z component. We define $\phi(\vec{q}) = \sum_{lm}\psi_{lm}(|\vec{p}|)Y_{lm}(\hat{p})$, where Y_{lm} are spherical harmonics and then cast Eq. (3.2) on each of the components of the angular decomposition. As a result we obtain for each $l = 0, 1, 2, ...$ and $m = -l, ..., l$ an equation,

$$p^2\psi_{lm}(p) + \int_0^\infty dq\; q^2\; V_l(p,q)\;\psi_{lm}(q) \;=\; \mathcal{E}\psi_{lm}(p)\;, \tag{3.3}$$

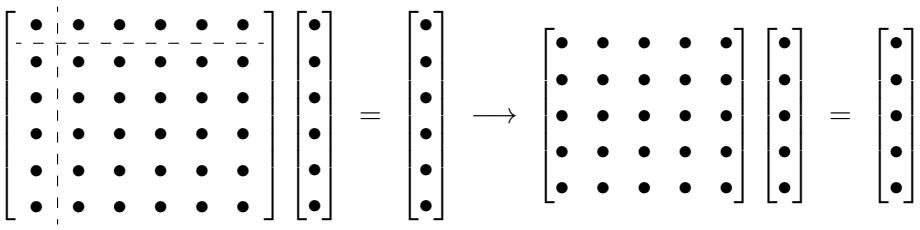

Figure 3.1: Schematic illustration of Gaussian elimination method used in solving systems of equations written in a matrix form.

where $\mathcal{E} = 2mE$,

$$V_l(p,q) \;=\; -\frac{\alpha}{2l+1}\left[\theta(p-q)\frac{q^l}{p^{l+1}} + \theta(q-p)\frac{p^l}{q^{l+1}}\right] , \tag{3.4}$$

and $\alpha = 2mg$. Therefore, we have a separate eigenvalue equation for each angular momentum l. The potentials V_l do not depend on the magnetic number m (not to be confused with the mass also denoted by m), therefore, the eigenvalues $\mathcal{E}$ cannot depend on it and from now on I drop subscript m.

3.1.2 Gaussian elimination and renormalization group equations

Equations (3.3) are regularized, by replacing ∞ in the upper limit of the integral by cutoff Δ. The Wilsonian idea of integrating out large-energy degrees of freedom is realized step by step by Gaussian elimination of one infinitesimal momentum shell at a time, see Fig. 3.1. To make the analogy with matrices more apparent I write the regularized Eq. (3.3) in two lines,

$$\Delta^2\psi_l(\Delta) + d\Delta\ \Delta^2\ V_l(\Delta,\Delta)\ \psi_l(\Delta) + \int_0^{\Delta-d\Delta} dq\ q^2\ V_l(\Delta,q)\ \psi_l(q) \;=\; \mathcal{E}\psi_l(\Delta)\ , \tag{3.5}$$

$$p^2\psi_l(p) + d\Delta\ \Delta^2\ V_l(p,\Delta)\ \psi_l(\Delta) + \int_0^{\Delta-d\Delta} dq\ q^2\ V_l(p,q)\ \psi_l(q) \;=\; \mathcal{E}\psi_l(p)\ , \tag{3.6}$$

where the upper equation represents the equation obtained form the highest row of the matrix, while the lower equation represents equations obtained from all other rows. Moreover, the integral is split into two parts: the integral from 0 to $\Delta - d\Delta$ that represents all columns except the one furthest to the left, and integral from $\Delta - d\Delta$ to Δ, which is represented by the second term in each of the equations and where the integration was performed assuming that the integrand is constant between $\Delta - d\Delta$ and Δ. Now, the upper equation is solved for $\psi_l(\Delta)$ in order to insert it into the lower equation. We have,

$$\psi_l(\Delta) \;=\; \frac{1}{\mathcal{E} - d\Delta\ \Delta^2\ V_l(\Delta,\Delta) - \Delta^2}\int_0^{\Delta-d\Delta} dq\ q^2\ V_l(\Delta,q)\ \psi_l(q)\ . \tag{3.7}$$

The term proportional to $d\Delta$ in the denominator of the fraction can be neglected. Moreover, if we restrict our attention to the eigenvalues that are much smaller than the cutoff, $\mathcal{E} \ll \Delta^2$, then $\mathcal{E}$ can also be omitted. Putting $\psi_l(\Delta)$ into Eq. (3.6) we complete the first step of Gaussian elimination, and obtain an equation in a smaller space of momenta,

$$p^2\,\psi_l(p) + \int_0^{\Lambda} dq\ q^2\ \tilde{V}_l(p,q)\ \psi_l(q) \;=\; \mathcal{E}\ \psi_l(p)\ , \tag{3.8}$$

where $\Lambda = \Delta - d\Delta$ and

$$\tilde{V}_l(p,q) \;=\; V_l(p,q) - d\Delta\ V_l(p,\Delta)\ V_l(\Delta,q) \tag{3.9}$$

$$\;=\; -\frac{\alpha}{2l+1}\left[\theta(p-q)\frac{q^l}{p^{l+1}} + \theta(q-p)\frac{p^l}{q^{l+1}}\right] - d\Delta\frac{\alpha^2}{(2l+1)^2}\frac{p^l}{\Delta^{l+1}}\frac{q^l}{\Delta^{l+1}}\ . \tag{3.10}$$

With respect to V_l the new interaction kernel $\tilde{V}_l$ contains extra term that is different from the terms in V_l. It corresponds to a different kind of interactions, because its momentum dependence is different from momentum dependence of V_l. We should now perform another step of integrating-out an infinitesimal shell of the largest momentum. For generality, we write the new kernel, Eq. (3.10), in the form,

$$V_l(p,q,\Lambda) \;=\; -\frac{\alpha}{2l+1}\left[\theta(p-q)\frac{q^l}{p^{l+1}}+\theta(q-p)\frac{p^l}{q^{l+1}}\right]+\gamma_\Lambda p^l q^l \;, \tag{3.11}$$

where γ_Λ is the coupling constant of the new interaction. The step of Gaussian elimination from the equation with momentum range up to Λ to the equation with momentum range up to $\Lambda - d\Lambda$ proceeds exactly as before, therefore,

$$\begin{aligned} V_l(p,q,\Lambda-d\Lambda) \,=\, \tilde{V}_l(p,q) \;&=\; -\frac{\alpha}{2l+1}\left[\theta(p-q)\frac{q^l}{p^{l+1}}+\theta(q-p)\frac{p^l}{q^{l+1}}\right] \\ &+\; \gamma_\Lambda p^l q^l - d\Lambda\left(-\frac{\alpha}{2l+1}\frac{1}{\Lambda^{l+1}}+\gamma_\Lambda\Lambda^l\right)^2 p^l q^l \;. \end{aligned} \tag{3.12}$$

In this step no new interaction appeared. The extra term that was produced by the elimination only shifts the coupling constant γ_Λ to some new coupling constant $\gamma_{\Lambda-d\Lambda}$. The subsequent steps will also produce only shift in the coupling constant γ. The shift may be described by a differential equation, a renormalization group equation:

$$\frac{d\gamma}{d\Lambda} \;=\; \left[\gamma\Lambda^l-\frac{\alpha}{(2l+1)\Lambda^{l+1}}\right]^2 \;. \tag{3.13}$$

There is also another renormalization group equation, for the coupling constant α,

$$\frac{d\alpha}{d\Lambda} \;=\; 0 \;. \tag{3.14}$$

It is convenient, especially for the purpose of solving Eq. (3.13), to define a dimensionless coupling constant f by the relation $\gamma_\Lambda = f/\Lambda^{2l+1}$. The renormalization group equation for that coupling constant is,

$$\Lambda\frac{\partial f}{\partial\Lambda} \;=\; (f-A)^2+B^2 \;, \tag{3.15}$$

where

$$A \,=\, \frac{\alpha}{2l+1}-l-\frac{1}{2} \;, \quad B \,=\, \sqrt{\alpha-\left(l+\frac{1}{2}\right)^2} \;. \tag{3.16}$$

Because A and B depend on l, there is in fact one coupling f for each l and *a priori* they are independent. However, it suffices to provide one observable per one partial wave l to fix the value of f for all $\Lambda \gg \mathcal{E}$. In other words one has to provide some initial condition to Eq. (3.15), the value $f = f_0$ at some Λ_0. Λ_0 is arbitrary and may be chosen, *e.g.*, in such a way that makes calculation of observables especially easy. Once an appropriate observable is calculated it should be compared with experiment, which will fix f_0. Equation (3.15), although simple, admits several interesting kinds of solutions. I present them in the next section.

3.1.3 Classification of solutions of renormalization group equations

The behavior of solutions to Eq. (3.15) is largely determined by the value of B. For $B^2 > 0$ the general solution for f is given by a log-periodic function,

$$f \;=\; B\,\tan\left(\varphi+B\log\frac{\Lambda}{\Lambda_0}\right)+A \;, \tag{3.17}$$

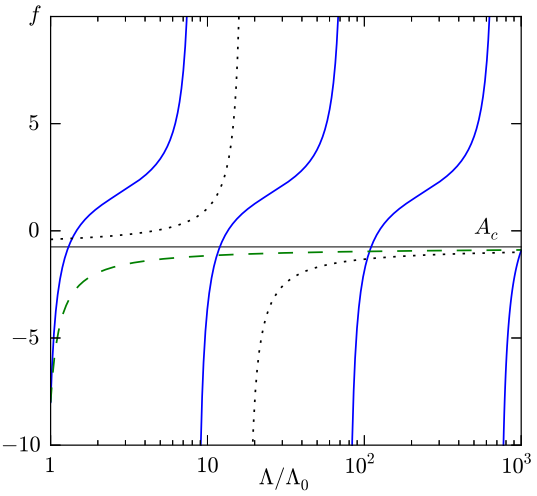

(a) For $l = 0$ with $f_0 = -8.0$ the coupling constant f develops a limit cycle (solid line). Dashed line shows behavior of f for $l = 1$, which is asymptotic-freedom-like ($f_0 = -8.0$). Dotted line is also a solution for $l = 1$, but with $f_0 = -0.4$, which implies the Landau pole.

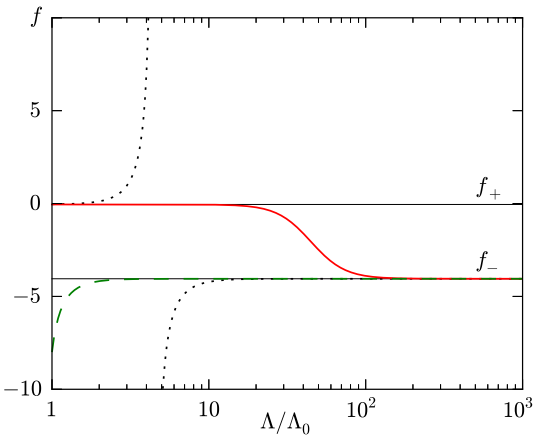

(b) Different possible behaviors of $l = 2$ coupling constant f for different initial value f_0. The fixed points are $f_+ = -0.05$, and $f_- = -4.05$. For solid line $f_0 = f_+ - 10^{-6}$, for dotted line $f_0 = f_+ + 10^{-2}$, and for dashed line $f_0 = -8.0$.

Figure 3.2: Examples of behavior of coupling constants f for angular momenta $l = 0, 1, 2$ [53]. Coupling constant $\alpha = 9/4$, which is the critical value of the coupling constant for $l = 1$ coupling constant f with $A_c = -3/4$.

where $\varphi = \arctan \frac{f_0 - A}{B}$. This kind of solution is called limit cycle. The condition $B > 0$ implies that $\alpha > (l + 1/2)^2$. In other words, the potential has to be attractive and sufficiently strong. If $\alpha < 1/4$ then there are no solutions of the limit cycle kind. If $\alpha > 1/4$, then f follows the limit cycle at least for $l = 0$, but possibly also for other partial waves. Another kind of solution is obtained when the coupling constant α takes the critical value for some partial wave, that is if $B = 0$ for some l. In that case, for the distinguished l, coupling constant f approaches slowly the critical value $A_c = -l - 1/2$,

$$f - A_c \;=\; \frac{f_0 - A_c}{1 - (f_0 - A_c)\log\frac{\Lambda}{\Lambda_0}} \,. \tag{3.18}$$

If $f_0 - A_c < 0$, then the equation resembles the running of the QCD coupling constant. Therefore, this kind of solution is called asymptotic-freedom-like. For $f_0 - A_c > 0$, as we evolve f to larger and larger values of Λ, it will develop a pole, which we call the Landau pole, since the running of the coupling f resembles the running of electromagnetic coupling constant. There is of course also $f = A_c = \text{const}$ solution. Finally, for $B^2 < 0$ there are two fixed points $f_\pm = A \pm |B|$. Both are negative and $f_+ > f_-$. The solution may be written in the following way,

$$f \;=\; A + |B|\,\frac{f_0 - f_- + (f_0 - f_+)\left(\frac{\Lambda}{\Lambda_0}\right)^{2|B|}}{f_0 - f_- - (f_0 - f_+)\left(\frac{\Lambda}{\Lambda_0}\right)^{2|B|}} \,. \tag{3.19}$$

As we increase Λ the coupling constant f is repelled from f_+ and attracted to f_-, but depending on the initial value f_0 it may do different things on the way. If f_0 is smaller than f_-, then f quickly approaches f_-. If f_0 is between f_+ and f_- then f also flows to f_-, but if f_0 is really close to f_+, but still below it, f may stick to f_+ for a large range of Λ until it suddenly jumps to f_-. For $f_0 > f_+$, the coupling constant f quickly grows, develops a pole, and reappears from the negative side to finally come close to the attractive fixed point f_-. Figure 3.2 presents all types of solutions

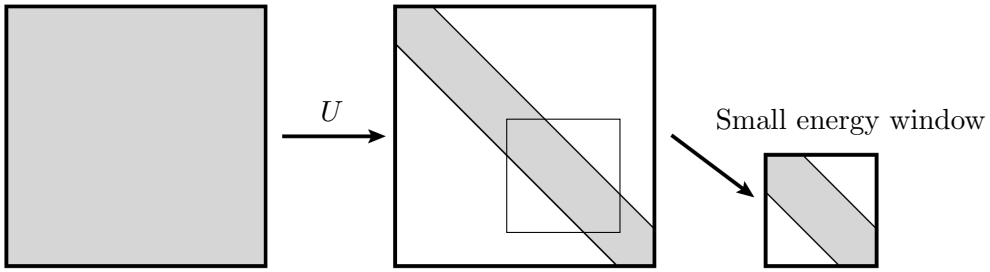

Figure 3.3: Similarity renormalization group transformation U of a big matrix of Hamiltonian matrix elements with very large cutoff (on the left) to the band diagonal matrix (in the center). White regions represent zero Hamiltonian matrix elements. The band diagonal form of the matrix in the center allows one to pick a small window from it and diagonalize it numerically to give a good approximation to the eigenvalues of the whole matrix that fit into the window.

for coupling constants f for $l = 0, 1$ and 2 in a theory with $\alpha = 9/4$, which is the critical value of coupling constant for $l = 1$.

3.2 Renormalization by integrating out large changes of energy

3.2.1 Distinction between eliminations of large-energies and large energy changes

The renormalization group procedure based on Gaussian elimination of high-energy degrees of freedom works well in simple models like the one presented in Sec. 3.1. However, there are several problems that one has to face in a realistic theory, like QCD. The first problem is that the cutoff on high-energy degrees of freedom is not Lorentz invariant. The idea of Wilsonian procedure is to write the eigenvalue problem in a space so small that it can be solved numerically (which seems necessary in realistic theories with complicated interactions, like QCD). Therefore, the cutoff Λ would need to be rather small. However, that means that bound states have limited momenta – if they move too fast they will have energies larger than Λ. The other problem is that the Gaussian elimination introduces the eigenvalues that one wants to find into the effective Hamiltonians. We neglected them in Eq. (3.7) assuming that $\mathcal{E}$ is much smaller than any Λ that we would use. However, to make precise calculations in a realistic theory one would like to evolve effective Hamiltonians to a region where the cutoff is comparable with the eigenvalues that one seeks.

Głazek and Wilson introduced a different kind of procedure called similarity renormalization group [54]. The idea is based on the observation that problems like divergent energy corrections are caused by interactions between states from vastly different energy scales. For example, in the canonical Hamiltonian interaction term $H_1^{\rm can}$, Eq. (2.61), the invariant mass of quark-gluon pair 12 may be on the order of the mass of the Sun, yet, the interaction of that pair with quark 3 is nonzero (the situation is even worse, because the interaction strength actually grows with relative momentum of quarks 1 and 2). Using the picture of the Hamiltonian matrix elements like in Fig. (3.1), one can say that the problems are caused by nonzero far-off-diagonal matrix elements. Therefore, one can define an effective theory by means of similarity transformation of the Hamiltonian matrix in such a way that far-off-diagonal matrix elements are zero, hence making the matrix band diagonal, see Fig. 3.3. The cutoff may be kept very large, hence allowing for relativistic description, and at the same time one can diagonalize only small matrices taken out of the band diagonal effective Hamiltonian to obtain good approximations to the eigenvalues of the whole Hamiltonian. A procedure that is specifically designed to automatically preserve as much of the Lorentz symmetry as it is possible in the FF of Hamiltonian dynamics and which uses the kind of transformation like the one depicted in Fig. 3.3 is presented in the next section.

3.2.2 Renormalization Group Procedure for Effective Particles (RGPEP)

Renormalization group procedure for effective particles takes the idea of diagonalizing Hamiltonian matrices with the help of similarity transformation a step further than similarity renormalization group. Instead of transforming matrices, one can transform particles [4]. One introduces the effective creation and annihilation operators,

$$q_t \;=\; \mathcal{U}_t q_0 \mathcal{U}_t^\dagger \;, \tag{3.20}$$

where q_0 stands for any of the creation or annihilation operators of initial, bare particles, for example quark and gluon operators b_f, d_f, a and $b_f^\dagger$, $d_f^\dagger$, $a^\dagger$ in Eq. (2.60); q_t stands for the corresponding effective particle operator; and $\mathcal{U}_t$ is a unitary operator transforming the bare particles into the effective ones. The effective particles are labelled with parameter $t = s^4$, where s has dimension of distance and an interpretation of size of effective particles. This interpretation comes from the form factors that appear in interaction vertices of the effective theory and make the Hamiltonian matrix band diagonal, *cf.* Eq. (3.31). The states, whose matrix elements are depicted in Fig. (3.3), are ordered according to their invariant masses, where the mass increases as one goes up and left on the picture. The width of the band is $\sim \lambda = 1/s$ and it tells by how much the invariant mass of the particles involved in the interaction can change.

The effective particles' creation and annihilation operators of Eq. (3.20) are used as a new basis, which is used to rewrite the initial Hamiltonian. Thus obtained effective Hamiltonians H_t are parameterized with parameter t. Instead of defining the unitary operator $\mathcal{U}_t$ explicitly, it is more convenient to define the differential equation that effective Hamiltonians should fulfill, which is what I present below. Rewriting the Hamiltonian in a new basis means that,

$$\mathcal{H}_t(q_t) \;=\; \mathcal{H}_0(q_0) \;. \tag{3.21}$$

where $\mathcal{H}_0(q_0)$ is the Hamiltonian written in terms of bare particles q_0 with interaction coefficients of the initial Hamiltonian, while $\mathcal{H}_t(q_t)$ is the Hamiltonian written in terms of effective particles q_t with effective interaction coefficients. Because we are first interested in the effective interaction coefficients it is useful to define $\mathcal{H}_t \equiv \mathcal{H}_t(q_0)$, that is the Hamiltonian written in terms of the bare particles' creation and annihilation operators but with effective interaction coefficients,

$$\mathcal{H}_t \;=\; \sum_{n=2}^{\infty} \int_{i_1 \ldots i_n} c_t(i_1, i_2, \ldots, i_n) q_{0\,i_1}^\dagger \ldots q_{0\,i_n} \;, \tag{3.22}$$

where c_t are the interaction coefficients and depend on all of the quantum numbers of particles involved in the interaction, and the creation and annihilation operators are normal ordered. Due to FF restriction of plus component of momentum $p_{i_k}^+ > 0$ the first operator is always a creation operator and the last operator is always an annihilation operator. It is also useful to define the Hamiltonian of free particles,

$$\mathcal{H}_f \;=\; \sum_i \int_i p_i^- q_i^\dagger q_i \;, \tag{3.23}$$

where the sum over i means sum over all kinds of particles. Using $\mathcal{U}_t$ one can write,

$$\mathcal{H}_t \;=\; \mathcal{U}_t^\dagger \mathcal{H}_0 \mathcal{U}_t \;. \tag{3.24}$$

By differentiating Eq. (3.24) with respect to t one obtains,

$$\mathcal{H}_t' \;=\; [\mathcal{G}_t, \mathcal{H}_t] \;, \tag{3.25}$$

where prime means differentiation with respect to t and $\mathcal{G}_t = -\mathcal{U}_t^\dagger \mathcal{U}_t'$ is called the generator of RGPEP transformation. One can define different generators, an early version can be found in Ref. [55]. The generator used in this thesis was introduced in Ref. [4] and is,

$$\mathcal{G}_t \;=\; \left[\mathcal{H}_f, \tilde{\mathcal{H}}_t\right] \;, \tag{3.26}$$

where

$$\tilde{\mathcal{H}}_t \;=\; \sum_{n=2}^{\infty}\int_{i_1\ldots i_n} c_t(i_1,i_2,\ldots,i_n)\left(\frac{1}{2}\sum_{k=1}^{n}p^+_{i_k}\right)^2 q^\dagger_{0\,i_1}\ldots q_{0\,i_n}\;. \tag{3.27}$$

In other words, $\tilde{\mathcal{H}}_t$ differs from $\mathcal{H}_t$ by a factor of square of the total +-momentum of all incoming (or all outgoing) particles in the interaction vertex. The purpose of inserting this factor is that it guarantees that RGPEP Eq. (3.25) is boost invariant and interaction vertices in the renormalized theory, written in terms of effective creation and annihilation operators, depend on the relative momenta of the particles involved in the interaction. The generator, Eq. (3.26) implies,

$$\mathcal{U}_t \;=\; T\exp\left(-\int_0^t d\tau\left[\mathcal{H}_f,\tilde{\mathcal{H}}_\tau\right]\right)\;, \tag{3.28}$$

where T means ordering of operators in the order of increasing parameter t from left to right.

Equation (3.25) may be rewritten in the following form [4],

$$\mathcal{H}'_{t\,ab} \;=\; -ab^2\mathcal{H}_{It\,ab}+\sum_x(p_{ax}ax+p_{bx}bx)\mathcal{H}_{It\,ax}\mathcal{H}_{It\,xb}\;, \tag{3.29}$$

where prime denotes derivative with respect to t, symbols a, b and x denote configurations of particles, *i.e.*, collections of all quantum numbers that characterize fully the particles in the configuration. $\mathcal{H}_{t\,ab}$ denotes a coefficient that stands in the Hamiltonian $\mathcal{H}_t$ in front of the product of creation operators from configuration a and annihilation operators from configuration b, $\mathcal{H}_{It}=\mathcal{H}_t-\mathcal{H}_f$ and the sum over x means the sum over all quantum numbers of particles in configuration x. Symbol ax denotes the difference $\mathcal{M}^2_{ax}-\mathcal{M}^2_{xa}$, where $\mathcal{M}_{ax}$ denotes the invariant mass of the particles from configuration a that were involved (created) in the interaction $\mathcal{H}_{It\,ax}$, while $\mathcal{M}_{xa}$ denotes the invariant mass of the particles from configuration x that were involved (annihilated) in interaction $\mathcal{H}_{It\,ax}$. Spectators (particles not involved in the interaction) do not contribute to those invariant masses. Finally, p_{ax} denotes the total plus momentum of particles from configuration a that were involved in the interaction $\mathcal{H}_{It\,ax}$. Analogous definitions are assumed for symbols ab, bx, p_{ax} and p_{bx}. An important feature of Eq. (3.29) is that its solutions have so-called RGPEP form factors that appear due to the first term on the right hand side of Eq. (3.29). For example, in perturbation theory the interaction Hamiltonian $\mathcal{H}_{It}$ is of order g and in the first-order calculation one can neglect the second term in Eq. (3.29). The solution is then

$$\mathcal{H}_{t\,ab} \;=\; f_{ab}\mathcal{H}_{0\,ab}\;, \tag{3.30}$$

where the RGPEP form factor $f_{a.b}$ is,

$$f_{ab} \;=\; e^{-t\,ab^2}\;. \tag{3.31}$$

Therefore, the interaction vertices cannot change invariant masses of states by more than $\lambda=t^{-1/4}$.

3.3 Renormalized Hamiltonian of QCD in orders first and second

The renormalized Hamiltonian is obtained as a solution of RGPEP Eq. (3.25), and it is expanded in powers of effective coupling constant g_t,

$$H_t \;=\; H_{t\,0}+g_tH_{t\,1}+g_t^2H_{t\,2}\;. \tag{3.32}$$

The first term is the free-propagation term of quarks, antiquarks and gluons. The rest of the terms contain interactions and all necessary counterterms. The fact that effective coupling constant depends on the scale parameter t becomes apparent only in a calculation that involves terms of order at least third [3], but I use this fact here to include implicitly some of the effects of the third- and higher-order terms.

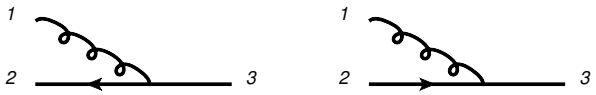

Figure 3.4: Gluon emission terms of the renormalized Hamiltonian in the first order in coupling constant, Eq. (3.34). The Hermitian conjugated terms correspond to gluon absorption diagrams with gluon coming from the right.

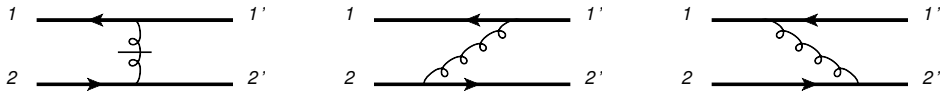

Figure 3.5: Second order terms of the renormalized Hamiltonian acting between a quark and an antiquark. The left figure represents the instantaneous interaction term $H_{t\,Q\bar{Q}\,\mathrm{inst}}$. The other two represent different contributions ($q^+ > 0$ and $q^+ < 0$) to $H_{t\,Q\bar{Q}\,\mathrm{exch}}$.

3.3.1 Zeroth order

The free part of the renormalized Hamiltonian is the same as the free part of canonical Hamiltonian, except creation and annihilation operators of bare particles are replaced with creation and annihilation operators of effective particles.

$$H_{t\,0} \;=\; \sum_{f=b,c} \int_1 p_1^- \left(b^\dagger_{t\,f\,1} b_{t\,f\,1} + d^\dagger_{t\,f\,1} d_{t\,f\,1} \right) + \int_1 p_1^- a^\dagger_{t\,1} a_{t\,1} \;, \tag{3.33}$$

3.3.2 First order

In the first order in coupling constant Hamiltonian terms are the same as corresponding terms in the regularized Hamiltonian, Eq. (2.73), but with effective creation and annihilation operators instead of bare ones and additionally each term acquires a form factor $f_{21.3}$,

$$H_{t\,1} \;=\; \sum_{f=b,c} \int_{123} r_{21.3} f_{21.3} \left[B_{21.3}\; t^1_{23}\; b^\dagger_{t\,f\,2} a^\dagger_{t\,1} b_{t\,f\,3} + D_{21.3}\; t^1_{32}\; d^\dagger_{t\,f\,2} a^\dagger_{t\,1} d_{t\,f\,3} + \mathrm{H.c.} \right] \;. \tag{3.34}$$

The form factor is, *cf.* Eq. (3.31),

$$f_{21.3} \;=\; \exp\left[-t(\mathcal{M}^2_{21} - m_3^2)^2 \right] \;, \tag{3.35}$$

where $\mathcal{M}^2_{21}$ is the square of free invariant mass of particles 1 and 2, see Eq. (2.13), and m_3 is the mass of particle 3. Figure 3.4 gives a graphic representation of the first order Hamiltonian terms.

3.3.3 Second order

The second-order solution of Eq. (3.29) for the renormalized Hamiltonian in the second order is in general [4],

$$\mathcal{H}_{t2\,ab} \;=\; f_{ab} \mathcal{H}_{02\,ab} + f_{ab} \sum_x \frac{p_{ax} ax + p_{bx} bx}{ax^2 + bx^2 - ab^2} \left(1 - \frac{f_{ax} f_{xb}}{f_{ab}} \right) \mathcal{H}_{01\,ax} \mathcal{H}_{01\,xb} \;. \tag{3.36}$$

To obtain the Hamiltonian H_t, one has to replace in $\mathcal{H}_t$ the creation and annihilation operators from the bare ones to the effective ones with $t > 0$.

Vertex

There are two quark-antiquark interaction terms in $H_{t\,2}$. The first one corresponds to the first term on the right-hand side of Eq. (3.36) and is the same as the instantaneous interaction term

in the regularized Hamiltonian, except for the form factor and effective creation and annihilation operators:

$$H_{t\,Q\bar{Q}\,\mathrm{inst}} = -\sum_{f_1,f_2=b,c}\int_{121'2'} \tilde{\delta}_{12.1'2'}\; r_{C\,12.1'2'}\; f_{12.1'2'}\; \frac{j^{+}_{11'}\bar{j}^{+}_{2'2}}{(p^{+}_{1}-p^{+}_{1'})^2} \times \quad t^{a}_{11'}t^{a}_{2'2}\; b^{\dagger}_{f_11}d^{\dagger}_{f_22}d_{f_22'}b_{f_11'}\;, \tag{3.37}$$

where $r_{C\,12.1'2'}$ is the regularization function given in Eq. (2.77), and the RGPEP form factor is,

$$f_{12.1'2'} = \exp\left[-t(\mathcal{M}_{12}-\mathcal{M}_{1'2'})^2\right]\;. \tag{3.38}$$

The other term, which is explicitly given below, corresponds to the second term on the right-hand side of Eq. (3.36) and is later called the exchange term, because in perturbation theory it is produced by the product of two first-order Hamiltonian terms – one that emits a gluon and another that absorbs a gluon, see Fig. 3.5. There are two diagrams in Fig. 3.5 with exchange of a gluon, which correspond to two mutually exclusive situations – either quark emits the gluon or the antiquark emits the gluon. Gluon plus momentum p^{+}_{4} can be only positive and quark either loses or gains its plus momentum. To easily distinguish between the two possibilities I define the difference of on-mass-shell[1] quark momenta before and after interaction,

$$q^{\mu}_{1} = p^{\mu}_{1'}-p^{\mu}_{1}\;, \tag{3.39}$$

whose plus component $q^{+}_{1}=q^{+}$ can be either positive or negative. This equation applies also to the minus component, $q^{-}_{1}=p^{-}_{1'}-p^{-}_{1}$. I also define the difference of antiquark momenta after and before interaction,

$$q^{\mu}_{2} = p^{\mu}_{2}-p^{\mu}_{2'}\;. \tag{3.40}$$

The two momenta have the same plus and transverse components,

$$q^{+}_{1} = q^{+}_{2} = q^{+}\;, \tag{3.41}$$
$$q^{\perp}_{1} = q^{\perp}_{2} = q^{\perp}\;. \tag{3.42}$$

The minus components are in general different, $q^{-}_{1}\neq q^{-}_{2}$, and therefore, also the squares of the fourmomentum transfers are different, $q^{2}_{1}\neq q^{2}_{2}$. The interaction with $q^{-}_{1}=q^{-}_{2}$ is called on-energy-shell. Moreover, the gluon momentum as it stands in the Hamiltonian is

$$p^{+}_{4} = |q^{+}|\;, \tag{3.43}$$
$$p^{\perp}_{4} = \epsilon(q^{+})q^{\perp}\;, \tag{3.44}$$
$$p^{-}_{4} = \frac{(p^{\perp}_{4})^2}{p^{+}_{4}}\;, \tag{3.45}$$

where $\epsilon(q^{+})=1$ for $q^{+}>0$ and $\epsilon(q^{+})=-1$ for $q^{+}<0$. The gluon momentum, as for any other particle in the Hamiltonian, is on-mass-shell, which means $p^{2}_{4}=m^{2}_{4}$, which is zero for a gluon. To write the interaction terms, I use a compact notation that combines the two cases, $q^{+}>0$ and $q^{+}<0$, but differs from the notation used in Refs. [6, 7].

$$H_{t\,Q\bar{Q}\mathrm{exch}} = -\int_{121'2'} \tilde{\delta}_{12.1'2'}\; r_{C\,12.1'2'}\; f_{12.1'2'}\;\cdot\; F(12;1'2')\; d_{\mu\nu}(p_4)\; j^{\mu}_{11'}\bar{j}^{\nu}_{2'2} \times \quad t^{a}_{11'}t^{a}_{2'2}\; b^{\dagger}_{f_11}d^{\dagger}_{f_22}d_{f_22'}b_{f_11'}\;, \tag{3.46}$$

[1] The on-mass-chillness condition for quarks means that

$$p^{-}_{1'} = \frac{m^{2}_{1}+(p^{\perp}_{1'})^2}{p^{+}_{1'}}\;,\quad p^{-}_{1} = \frac{m^{2}_{1}+(p^{\perp}_{1})^2}{p^{+}_{1}}\;.$$

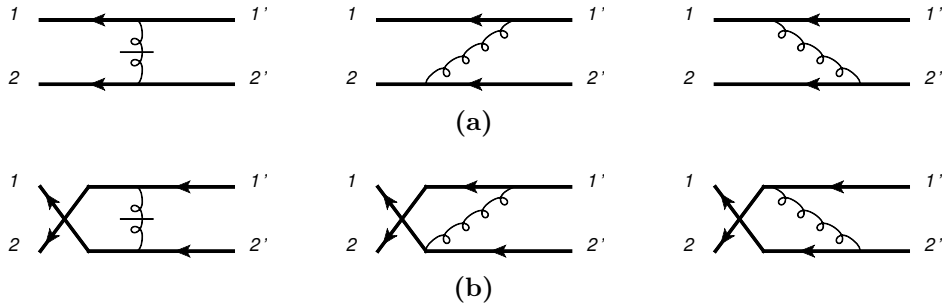

Figure 3.6: Second order terms of the renormalized Hamiltonian acting between a quark and an antiquark. The left diagram in both part (a) and part (b) represents the instantaneous interaction term $H_{t\,QQ\,\mathrm{inst}}$. The other two represent different contributions ($q^+ > 0$ and $q^+ < 0$) to $H_{t\,QQ\,\mathrm{exch}}$. If the two quarks have different flavors only diagrams from part (a) are present. If the two quarks are identical both part (a) and part (b) are necessary to perform antisymmetrization of interaction Hamiltonian, see Eqs. (3.52) and (3.53).

where

$$F(12;1'2') \;=\; \frac{\hat{x}_1^2 q_1^2 + \hat{x}_2^2 q_2^2}{\hat{x}_1^2 (q_1^2)^2 + \hat{x}_2^2 (q_2^2)^2 - (q_1^2 - q_2^2)^2} \left(1 - \frac{ff_{12.1'2'}}{f_{12.1'2'}}\right) \;, \tag{3.47}$$

and,

$$\hat{x}_1 \;=\; \max(x_1, x_{1'}) \;, \tag{3.48}$$

$$\hat{x}_2 \;=\; \max(x_2, x_{2'}) \;, \tag{3.49}$$

$$ff_{12.1'2'} \;=\; \theta(q^+)\; f_{14.1'} f_{2'4.2} + \theta(-q^+)\; f_{1'4.1} f_{24.2'} \;=\; \exp\left(-\,t\,\frac{\hat{x}_1^2 (q_1^2)^2 + \hat{x}_2^2 (q_2^2)^2}{x_4^2}\right) \;. \tag{3.50}$$

Moreover,

$$d_{\mu\nu}(p_4) \;=\; -g_{\mu\nu} + \frac{n_\mu p_{4\nu} + n_\nu p_{4\mu}}{p_4^+} \;, \tag{3.51}$$

where $n_+ = 1$, $n_- = n_1 = n_2 = 0$, arises as the sum of gluon polarization vectors over polarizations of the gluon, $d_{\mu\nu}(p_4) = \sum_{\sigma_4} \varepsilon_{4\mu} \varepsilon^*_{4\nu}$.

It is worth noting that on energy shell $q_1^2 = q_2^2 = q^2$, and the fraction in front of the round bracket in Eq. (3.47) simplifies to familiar $1/q^2$. There are several more steps to go from that statement to the demonstration that the renormalized Hamiltonian gives in the lowest order the same results for scattering of quarks as the Feynman diagrams do, but I want to emphasize that Eq. (3.47) is more complicated than just $1/q^2$ because the renormalized Hamiltonian is essentially off-energy-shell.

The interaction between quarks is given by the following Hamiltonian terms,

$$\begin{aligned} H_{t\,QQ\,\mathrm{inst}} \;&=\; \sum_{f=b,c} \frac{1}{2} \int_{121'2'} \tilde{\delta}_{12.1'2'}\; \mathrm{Asym}\Big\{\; r_{C\,12.1'2'}\; f_{12.1'2'}\; \frac{j^+_{11'} j^+_{22'}}{(p_1^+ - p_{1'}^+)^2}\; t^a_{11'} t^a_{22'} \Big\}\; b^\dagger_{f1} b^\dagger_{f2} b_{f2'} b_{f1'} \\ &+\; \int_{121'2'} \tilde{\delta}_{12.1'2'}\; r_{C\,12.1'2'}\; f_{12.1'2'}\; \frac{j^+_{11'} j^+_{22'}}{(p_1^+ - p_{1'}^+)^2}\; t^a_{11'} t^a_{22'}\; b^\dagger_{b1} b^\dagger_{c2} b_{c2'} b_{b1'} \;, \end{aligned} \tag{3.52}$$

$$\begin{aligned} H_{t\,QQ\,\mathrm{exch}} \;&=\; \sum_{f=b,c} \frac{1}{2} \int_{121'2'} \tilde{\delta}_{12.1'2'}\; \mathrm{Asym}\Big\{\; r_{C\,12.1'2'}\; f_{12.1'2'}\; \cdot\; F(12;1'2')\; d_{\mu\nu}(p_4)\; j^\mu_{11'} j^\nu_{22'} \\ &\times\; t^a_{11'} t^a_{22'} \Big\}\; b^\dagger_{f1} b^\dagger_{f2} b_{f2'} b_{f1'} \\ &+\; \int_{121'2'} \tilde{\delta}_{12.1'2'}\; r_{C\,12.1'2'}\; f_{12.1'2'}\; \cdot\; F(12;1'2')\; d_{\mu\nu}(p_4)\; j^\mu_{11'} j^\nu_{22'} \\ &\times\; t^a_{11'} t^a_{22'}\; b^\dagger_{b1} b^\dagger_{c2} b_{c2'} b_{b1'} \;, \end{aligned} \tag{3.53}$$

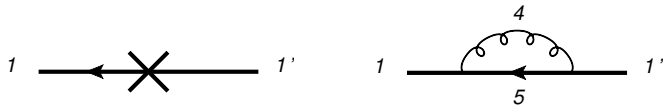

Figure 3.7: Second order self interaction terms for quark. Analogous diagrams can be drawn for antiquark.

The notable difference between quark-antiquark and quark-quark interaction is that quark-quark interactions may take place between two different quarks or two identical quarks. In the latter case an additional factor 1/2 appears and the interaction is antisymmetrized.

Finally, the quark and antiquark currents contracted with $d_{\mu\nu}$ are,

$$d_{\mu\nu}(p_4) j^{\mu}_{11'} \bar{j}^{\nu}_{2'2} = -g_{\mu\nu} j^{\mu}_{11'} \bar{j}^{\nu}_{2'2} - \frac{q_1^2 + q_2^2}{2(q^+)^2} j^{+}_{11'} \bar{j}^{+}_{2'2} \ , \tag{3.54}$$

$$d_{\mu\nu}(p_4) j^{\mu}_{11'} j^{\nu}_{22'} = -g_{\mu\nu} j^{\mu}_{11'} j^{\nu}_{22'} - \frac{q_1^2 + q_2^2}{2(q^+)^2} j^{+}_{11'} j^{+}_{22'} \ . \tag{3.55}$$

Mass terms

The mass terms are calculated from the same formula (3.36) that the vertex terms were calculated from. Here, one needs to supplement the canonical theory with a counterterm that removes divergences from matrix elements of the effective Hamiltonian H_t. The counterterm is *a priori* unknown. The condition that fixed its infinite part is that the matrix elements of $H_{t\,2}$ are finite when the ultraviolet cutoff $\Delta \to \infty$. I fix the notation for the renormalized Hamiltonian quark mass term in the following way,

$$H_{t\,2\,\delta m} = \sum_{f=b,c} \int_1 \frac{m^2_{f\,t\,2}}{p_1^+} \left(b^{\dagger}_{f\,1} b_{f\,1} + d^{\dagger}_{f\,1} d_{f\,1} \right) \ . \tag{3.56}$$

According to Eq. (3.36),

$$m^2_{f\,t\,2} = m^2_{f\,0\,2} - C_F \sum_{\sigma_5 \sigma_4} \int [x_{5/1} \kappa_{5/1}] \ r^2_{54.1} \ \frac{1}{\mathcal{M}^2_{54} - m_f^2} \left(1 - f^2_{54.1}\right) \bar{u}_1 \not{\epsilon}_4 u_5 \bar{u}_5 \not{\epsilon}^*_4 u_1 \ . \tag{3.57}$$

where $f^2_{54.1} = e^{-2t[\mathcal{M}^2_{54} - m_f^2]^2}$ and the integration measure $[x_{5/1}\kappa_{5/1}]$ is $dx_{5/1} d^2\kappa_{5/1}/[16\pi^3 x_{5/1}(1 - x_{5/1})]$, and $C_F = (N_c^2 - 1)/(2N_c)$, $N_c = 3$ is the number of colors. The two terms of the above equation are depicted in Fig. 3.7. For large transverse momenta the product of spinors and gluon polarization vectors behaves like $\mathcal{M}^2_{54}$. If I take the term with 1 in the parentheses in Eq. (3.57), then the integral diverges quadratically with the ultraviolet cutoff $\Delta \to \infty$. If I take the term with $f^2_{54.1}$ in the parentheses, it is finite with $\Delta \to \infty$. Therefore, to make $m^2_{f\,t\,2}$ finite I need to define $m^2_{f\,0\,2}$ in such a way that it cancels the divergent part of the integral. The easiest way to do it is the following

$$m^2_{f\,0\,2} = C_F \sum_{\sigma_5 \sigma_4} \int [x_{5/1} \kappa_{5/1}] \ r^2_{54.1} \ \frac{1}{\mathcal{M}^2_{54} - m_f^2} \bar{u}_1 \not{\epsilon}_4 u_5 \bar{u}_5 \not{\epsilon}^*_4 u_1 + \delta m^2_{f\,0\,2} \ , \tag{3.58}$$

where $\delta m^2_{f\,0\,2}$ is *a priori* unknown but finite when $\Delta \to \infty$. The finite parts of the counterterms cannot be determined without appeal to some observables and experiment. For the quark-mass term the ideal (because simplest) observable would be the physical mass of a quark. However, in QCD single-quark states cannot appear as asymptotic states, and one cannot speak of physical masses of quarks. Nevertheless, in the orders first and second in the coupling constant QCD is very similar to QED – the nonabelian effects manifest themselves explicitly only in the third order. Therefore, I will set the quark mass counterterm the same way I would set the electron

mass counterterm in QED. I write eigenvalue problem for a single quark. I perturbatively reduce this eigenvalue problem to one sector that contains a single quark (the reduction procedure is described in Sec. 4.3.1). It turns out that the mass squared of such "physical" single quark state is $m_f^2 + g_t^2 \delta m_{f\,0\,2}^2$. The "physical" mass of the quark should not depend on the renormalization group parameter t, therefore, $\delta m_{f\,0\,2}^2 = 0$. This way of fixing the finite part of the counterterm may turn out to be insufficient, but to check it one needs to calculate the effective Hamiltonian to higher orders than the second and to use hadronic observables. Moreover, nonperturbative determination of mass counterterms may, and probably should, due to chiral symmetry breaking, be different from the perturbative one, although for the heavy quarks perturbative calculations may be reliable. Finally, the renormalized quark mass term is,

$$m_{f\,t\,2}^2 \;=\; C_F \sum_{\sigma_5 \sigma_4} \int [x_{5/1} \kappa_{5/1}]\; r_{54.1}^2\; \frac{e^{-2t[\mathcal{M}_{54}^2 - m_f^2]^2}}{\mathcal{M}_{54}^2 - m_f^2} \bar{u}_1 \not{\epsilon}_4 u_5 \bar{u}_5 \not{\epsilon}_4^* u_1 \; . \tag{3.59}$$

It is important to notice that the renormalized mass term in Eq. (3.59) is finite in the limit $\Delta \to \infty$, but is divergent in the limit $\delta \to 0$. In other words, it is small-x divergent. The divergence cannot be removed by any counterterm inserted in the initial theory because the leading term in the limit $\delta \to 0$ is,

$$m_{f\,t\,2}^2 \;\sim\; \sqrt{\frac{2\pi}{t}} \log \frac{\Delta}{\delta} \; . \tag{3.60}$$

The divergent logarithm is multiplied by a function of t. The counterterm adds or subtracts terms, but they cannot depend on t, because the counterterm is inserted in the initial theory with $t = 0$. It may seem that a divergence that cannot be removed from the theory is a bad feature of the theory. However, in QCD such divergences may be the source for confinement. For example, color-singlet states may be free from divergences while color-nonsinglet states may have masses and energies that diverge due to small-x dynamics. This hypothesis is appealing but the mechanism behind the confinement probably has to be nonperturbative in nature, because similar kind of divergences is present also in QED. Since QED is well-defined in perturbation theory and charged states are physically admissible the small-x divergences have to have a way to cancel with each other in observables in perturbation theory. For the original treatment of infrared divergences in the theory of electron coupled with electromagnetic field see Ref. [56].

Chapter 4

Approximate Hamiltonians for mesons and baryons in heavy-flavor QCD

In this chapter I present derivation of the effective Hamiltonians for mesons and baryons in heavy-flavor QCD, which will be later used to find the first approximation for hadron masses, form factors and structure functions. The eigenvalue equation for renormalized Hamiltonian acts in the whole Fock space of states. I formulate gluon mass ansatz, which is nonperturbative in nature, to reduce the eigenvalue problem to only two sectors of the Fock space. Once this is done I use tools of Wilsonian renormalization group procedure to reduce perturbatively the eigenvalue problem to just one sector. The result is a Schrödinger-like equation in the space of $Q\bar{Q}$ for mesons or QQQ for baryons. The result of the calculation is that effective quarks interact with each other through Coulomb-like forces and harmonic oscillator potentials. This chapter is based on two papers written in collaboration with María Gómez-Rocha, Jai More and Stanisław Głazek [6, 7].

4.1 Motivation for studying the heavy-flavor theory

Hadrons are supposed to be bound states of quarks in QCD, but since interactions can change the particle content of a state the true bound states, or eigenvectors of the Hamiltonian are superpositions of states from different sectors of the Fock space. In principle, all states that have the same quantum numbers as the hadron of interest can contribute. For mesons the Fock sector with the minimal number of particles is the sector with a quark and an antiquark, but sectors with additional particles are also allowed. A general state of a meson is,

$$|\Psi_M\rangle \;=\; \big|Q_t\bar{Q}'_t\big\rangle + \big|Q_t\bar{Q}'_tG_t\big\rangle + \big|Q_t\bar{Q}'_tG_tG_t\big\rangle + \big|Q_t\bar{Q}'_tQ_t\bar{Q}_t\big\rangle + \dots \;, \tag{4.1}$$

where Q_t and $\bar{Q}'_t$ denote an effective quark and an effective antiquark of size $s = t^{1/4}$ and possibly of different flavors, while G_t denotes an effective gluon. The minimal particle content for a baryon state is three quarks, and a general state is,

$$|\Psi_B\rangle \;=\; \big|Q_tQ_tQ'_t\big\rangle + \big|Q_tQ_tQ'_tG_t\big\rangle + \big|Q_tQ_tQ'_tG_tG_t\big\rangle + \big|Q_tQ_tQ'_tQ_t\bar{Q}_t\big\rangle + \dots \;. \tag{4.2}$$

A priori, the number of sectors that contribute is infinite, especially, when one takes into account that interactions in local quantum field theories are divergent. However, using effective particles of RGPEP, as I did in Eqs. (4.1) and (4.2) only a restricted subset of all possible Fock sectors is expected to contribute. Take, for example, t such that $\lambda = t^{-1/4}$ is,

$$\Lambda_{\rm QCD} \ll \lambda \ll m_Q \;, \tag{4.3}$$

where m_Q is the mass a heavy quark. Remembering that light quarks are excluded from the theory, states with extra effective quark-antiquark pairs, like the fourth term in Eq. (4.1) and

the fourth term in Eq. (4.2), will contribute very little to the eigenvectors $|\Psi_M\rangle$ and $|\Psi_B\rangle$. The reason is that the renormalized Hamiltonian suppresses exponentially interactions that change invariant mass of a state by more than λ, *cf.* Eq. (3.30). For an interaction to connect, *e.g.*, $\left|Q_t\bar{Q}_t\right\rangle$ with $\left|Q_t\bar{Q}_t\ Q_t\bar{Q}_t\right\rangle$ the invariant mass would need to change by an amount of order $2m_Q$, which is much more than λ due to Eq. (4.3). Therefore, sectors with extra quark-antiquark pairs may be safely omitted. Sectors with gluons cannot *a priori* be omitted because gluons in QCD are massless. I address this issue in the next section. Equation (4.3) implies also that H_t can be calculated in perturbation theory, because for $\lambda \gg \Lambda_{\rm QCD}$ the effective coupling constant is small due to asymptotic freedom [3]. Smallness of the coupling constant is also related to small velocity of heavy quarks inside the hadron, hence, allowing one to use nonrelativistic approximations.[1] Equation (4.3) can be satisfied in QCD only for heavy quarks, which is the main motivation for the choice of heavy-flavor QCD in this thesis.

4.2 Eigenvalue problem in Fock space and gluon-mass ansatz

The eigenvalue equation for bound states in QCD is,

$$H_t|\Psi\rangle \;=\; P^-|\Psi\rangle\ , \tag{4.4}$$

where $P^- = [M^2 + (P^\perp)^2]/P^+$ and $P^{+,\perp}$ are the total longitudinal and transverse momenta of the bound state. The eigenvector $|\Psi\rangle$ is of the form given in Eq. (4.1) or Eq. (4.2). An important thing is that the exact form of H_t and $|\Psi\rangle$ depends on t, however, the eigenvalue P^- does not depend on t, because operation $\mathcal{U}_t$ is unitary. Using the perturbative expansion of the Hamiltonian, Eq. (3.32), the eigenvalue problem may be written in the following form,

$$\begin{bmatrix} \cdot & \cdot & \cdot \\ \cdot & H_{t\,0} + g_t^2 H_{t\,2} & g_t H_{t\,1} \\ \cdot & g_t H_{t\,1} & H_{t\,0} + g_t^2 H_{t\,2} \end{bmatrix} \begin{bmatrix} \cdot \\ |h\rangle \\ |l\rangle \end{bmatrix} \;=\; P^- \begin{bmatrix} \cdot \\ |h\rangle \\ |l\rangle \end{bmatrix}\ , \tag{4.5}$$

where $|l\rangle$ and $|h\rangle$ denote "lower" and "higher" sector of the Fock space and dots denote other Fock sectors that are not explicitly written. The lower sector is the sector with the minimal particle content necessary to have a state with desired quantum numbers. For mesons the lower sector is composed of quark and antiquark: $|l\rangle = |c\bar{c}\rangle$ for charmonium, $|l\rangle = \left|b\bar{b}\right\rangle$ for bottomonium, and $|l\rangle = \left|c\bar{b}\right\rangle$ for B_c^+. I omitted the subscript t, but these quarks are the effective quarks at the RGPEP scale t. For baryons the lower sector is composed of three quarks of proper flavors: $|l\rangle = |QQQ\rangle$ with $Q = b$ or c for Ω_{bbb} and Ω_{ccc}; $|l\rangle = |QQQ'\rangle$ with $Q = b$, $Q' = c$ for Ω_{bbc}, and $Q = c$, $Q' = b$ for Ω_{ccb}. The higher sector contains the particles that constitute the lower one and a gluon, $|h\rangle = |lG\rangle$. Equation (4.5) is written in the form that is supposed to resemble the matrix equations like the one depicted in Fig. 3.1. Hence, the elements of the matrix represent in fact matrix elements of the Hamiltonian between states from the appropriate sectors of the Fock space. For example, $H_{t\,1}$ in the upper right element of Eq. (4.5) represents in fact matrix elements $\langle h|H_{t\,1}|l\rangle$.

Even though extra quark-antiquark pairs from Eqs. (4.1) and (4.2) may be safely omitted, one cannot omit the sectors with gluons. The problem is that eigenvectors of H_t may contain significant contributions from many of them. *A priori* infinitely many of them could contribute. *A priori* it is also possible that nonperturbative solutions of RGPEP Eq. (3.25) contain large gluon masses that disallow for infinitely many gluons to contribute, and only small number of Fock sectors with effective gluons has to be taken into account. In the present, such considerations in the framework of RGPEP have a status of speculations, however, other theoretical approaches aimed at solving QCD arrive at a conclusion that gluons should indeed, acquire mass, see, *e.g.*, Ref. [57]. To deal with the problem of massless gluons, and to study what are implications of gluon mass in Hamiltonian formulation of QCD, I assume,

[1] Nonrelativistic approximations are applied only to relative momenta. The momentum of the hadron as a whole is arbitrary in the FF of Hamiltonian dynamics.

Ansatz: *All effects of sectors with more than one gluon can be included in the two-sector eigenproblem at the expense of introducing a gluon mass term in the higher sector:*

$$\begin{bmatrix} H_{t\,0}+\mu_t^2 & g_t H_{t\,1} \\ g_t H_{t\,1} & H_{t\,0}+g_t^2 H_{t\,2} \end{bmatrix} \begin{bmatrix} |h\rangle \\ |l\rangle \end{bmatrix} \;=\; P^- \begin{bmatrix} |h\rangle \\ |l\rangle \end{bmatrix} \;, \tag{4.6}$$

where μ_t^2 represents the gluon mass term that may (and in fact has to) depend on the gluon momentum with respect to the quarks in the higher sector. The gluon mass is supposed to be a nonperturbative effect of the order of $g_t^0 = 1$, and probably of nonabelian origin.

4.3 Effective Hamiltonians

4.3.1 Perturbative reduction of the eigenvalue equation

Eigenproblem with only two sectors is tractable as opposed to the problem with infinitely many of them. Therefore, one could try to solve it using some nonperturbative computational method, *e.g.*, defining some finite set of basis states in the two-sector space, writing the matrix of Hamiltonian matrix elements constructed using the basis states and diagonalize the matrix of the Hamiltonian [35]. However, one can apply a different, though approximate, approach. One can partially solve Eq. (4.6) using Gaussian-elimination-type of procedure. Such a procedure was used by Wilson [42] in his original work. The procedure, which I call "operation R," is defined perturbatively, and consists of integrating out a subspace of states. The whole space of states is divided into subspace P that is kept, which in my calculation consists of the lower sector, and space Q that is integrated out, which for my purposes consists of the higher sector. In general, the eigenstates of the Hamiltonian that one is interested in have components in space P as well as components in space Q. Due to gluon mass ansatz, I assume that the higher sector contributes relatively little to the the ground states of heavy hadrons and their low excitations. If this assumption is correct the perturbative reduction described here can indeed be performed. The key object of the procedure is operator R that acts from space P to space Q, and which, when provided with the P-space component of an eigenstate, yields the Q-space component of that eigenstate,

$$|h\rangle \;=\; R\,|l\rangle \;. \tag{4.7}$$

Using the operator R one can write an effective eigenvalue equation, in which only vectors entirely in space P appear, and has the same eigenvalues as the initial equation.[2] At the same time one retains information about, and possibility of reconstructing the Q-space component of any eigenstate of the effective eigenvalue problem.

The effective eigenvalue equation,

$$H_{\rm eff}|l_{\rm eff}\rangle \;=\; P^-|l_{\rm eff}\rangle \;, \tag{4.8}$$

is written in terms of the effective Hamiltonian,

$$H_{\rm eff} \;=\; \frac{1}{\sqrt{P+R^\dagger R}}\big(P+R^\dagger\big)H_t\big(P+R\big)\frac{1}{\sqrt{P+R^\dagger R}} \;, \tag{4.9}$$

where P is the projection operator on space P. The effective state $|l_{\rm eff}\rangle$ is not the same as $|l\rangle$ because if it were it would, for example, have a different norm than the full initial state $|l\rangle + |h\rangle$. The relation, which can be used to reconstruct eigenstates in the full space, is,

$$|l\rangle \;=\; \frac{1}{\sqrt{1+R^\dagger R}}\,|l_{\rm eff}\rangle \;. \tag{4.10}$$

[2] The smaller equation has fewer eigenvalues. The agreement applies only to those eigenvalues that fit into the small equation, the others are absent.

Therefore, the higher component is,

$$|h\rangle \;=\; R\frac{1}{\sqrt{1+R^\dagger R}}\,|l_{\rm eff}\rangle\ . \tag{4.11}$$

It is important to note that the relation between $|l\rangle$ and $|l_{\rm eff}\rangle$ is not a simple change in normalization constant. In general, $|l_{\rm eff}\rangle$ is reorganized so that it yields the same eigenvalue in the effective eigenproblem. Therefore, even though, both $|l\rangle$ and $|l_{\rm eff}\rangle$ are expressed in terms of the same effective particles (in the sense of creation and annihilation operators defined using RGPEP), they are different states and one is only a component of a bigger Fock state, while the other is constituent-like effective state.

In perturbative expansion around $g_t = 0$ the operator R contains terms of order g_t and higher, and the formulas for effective Hamiltonian and states can be expanded as well. The result for perturbative reduction of Eq. (4.6) is,

$$\begin{aligned}\langle l_{\rm eff}|H_{\rm eff}|l'_{\rm eff}\rangle \;&=\; \langle l_{\rm eff}|\big(H_{t\,0}+g_t^2 H_{t\,2}\big)|l'_{\rm eff}\rangle \\ &+\; \langle l_{\rm eff}|\frac{1}{2}g_t\,H_{t\,1}\left(\frac{1}{E_l-H_{t\,0}-\mu_t^2}+\frac{1}{E_{l'}-H_{t\,0}-\mu_t^2}\right)g_t\,H_{t\,1}|l'_{\rm eff}\rangle\ ,\end{aligned} \tag{4.12}$$

and in general,

$$|l\rangle \;=\; \left(1-\frac{1}{2}R^\dagger R\right)|l_{\rm eff}\rangle\ , \tag{4.13}$$

$$|h\rangle \;=\; R\,|l_{\rm eff}\rangle\ , \tag{4.14}$$

where only terms up to order g_t^2 are kept.

Effective Hamiltonians for mesons

For mesons the eigenvalue problems for a flavor-singlet system, $Q\bar{Q}$, and for a mixed-flavor system, $Q\bar{Q}'$, are virtually the same, with the only difference being that different flavors of quarks have different masses. Therefore, I will write down the most general form of the effective Hamiltonian for a quark of one flavor and an antiquark of a different flavor.

Arbitrary state in the $Q\bar{Q}'$ sector with a fixed total momentum P^+ and $P^\perp$ has the form,

$$|l_{\rm eff}\rangle \;=\; \int_{12} P^+\tilde{\delta}_{12.P}\ \frac{\delta_{c_1c_2}}{\sqrt{N_c}}\ \psi_{tQ\bar{Q}\,\sigma_1\sigma_2}(x_1,\kappa_1)\ b^\dagger_{t\,f_1\,1}\,d^\dagger_{t\,f_2\,2}|0\rangle\ , \tag{4.15}$$

where $\frac{\delta_{c_1c_2}}{\sqrt{N_c}}$ is the quark-antiquark color-singlet wave function with $N_c = 3$. The spin-momentum wave function $\psi_{tQ\bar{Q}}$ depends on spin of the quark σ_1, spin of the antiquark σ_2, and quark relative to antiquark momentum κ_1 as well as quark +-momentum fraction x_1.

The effective eigenvalue equation is

$$\begin{aligned}&\left(\frac{\mathcal{M}^2_{1,\,t}+(p_1^\perp)^2}{p_1^+}+\frac{\mathcal{M}^2_{2,\,t}+(p_2^\perp)^2}{p_2^+}\right)\ \psi_{tQ\bar{Q}}(12)\\ &+\,g_t^2\sum_{\sigma_{1'}\sigma_{2'}}\int[1'2']\ \tilde{\delta}_{1'2'.P}\ U_{Q\bar{Q}}(12;1'2')\ \psi_{tQ\bar{Q}}(1'2')\;=\;\frac{M^2+(P^\perp)^2}{P^+}\ \psi_{tQ\bar{Q}}(12)\ ,\end{aligned} \tag{4.16}$$

where $\psi_{tQ\bar{Q}}(12) = \psi_{tQ\bar{Q}\,\sigma_1\sigma_2}(x_1,\kappa_1)$. Transverse part of the eigenvalue $(P^\perp)^2/P^+$ cancels with part of the kinetic energy term on the left-hand side. The rest of the kinetic energy term contains terms with relative momentum $\kappa_1^\perp$ squared and divided by p_1^+ for quark (or p_2^+ for antiquark). After these simplifications, and after multiplying both sides by P^+, I obtain,

$$\begin{aligned}&\left(\frac{\mathcal{M}^2_{1,\,t}+(\kappa_1^\perp)^2}{x_1}+\frac{\mathcal{M}^2_{2,\,t}+(\kappa_1^\perp)^2}{x_2}\right)\ \psi_{tQ\bar{Q}}(12)\\ &+\,g_t^2\sum_{\sigma_{1'}\sigma_{2'}}\int[1'2']\ P^+\tilde{\delta}_{1'2'.P}\ U_{Q\bar{Q}}(12;1'2')\ \psi_{tQ\bar{Q}}(1'2')\;=\;M^2\ \psi_{tQ\bar{Q}}(12)\ .\end{aligned} \tag{4.17}$$

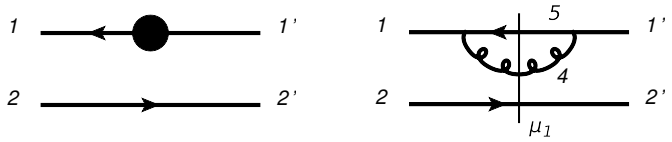

(a)

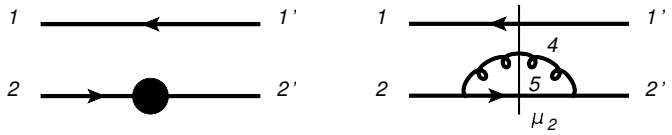

(b)

Figure 4.1: Second order quark (a) and antiquark (b) self-interaction terms in the effective Hamiltonian in the $Q\bar{Q}$ eigenvalue problem.

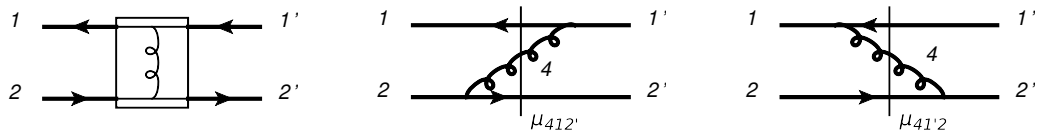

Figure 4.2: Second order gluon-exchange quark-antiquark interaction terms in the effective Hamiltonian in the $Q\bar{Q}$ eigenvalue problem. The left diagram corresponds to the matrix element $\langle l_{\rm eff}|(H_{t\,Q\bar{Q}\rm inst}+H_{t\,Q\bar{Q}\rm exch})|l'_{\rm eff}\rangle$ depicted in Fig. 3.5. The other two diagrams represent terms obtained from the product of two $H_{t\,1}$ in Eq. (4.12).

Integration measure $[1'2']$ with $P^+\tilde{\delta}_{1'2'.P}$ leads to integration over relative momenta $x_{1'}$ and $\kappa_{1'}$ without any trace of total momentum P^+ or $P^\perp$. $\mathcal{M}^2_{i,\,t}$ and $U_{Q\bar{Q}}(12;1'2')$ also depend only on relative momenta. Wave function $\psi_{tQ\bar{Q}}$ depends on relative momenta by assumption, which now turns out to be fully justified, because no matter what is the total momentum of the quarks, the equation and, hence, wave functions are the same. It is worth mentioning that the regulating functions also depend on relative momenta. On the way the role of eigenvalue was passed from P^-, which depends on total momentum, to mass squared M^2, which does not depend on the total momentum. The effective mass term is,

$$\mathcal{M}^2_{i,\,t} \;=\; m_i^2 + C_F g^2 \int \frac{dx d^2\kappa}{16\pi^3 x(1-x)}\; r^2_{54.i} \frac{e^{-2t\mathcal{S}^2_{54}}}{\mathcal{S}_{54}\mathcal{S}_{54\,\mu_i}} \frac{\mu_i^2}{x} \left[2\left(\frac{2}{x}-2+x\right)\mathcal{S}_{54} - 4m_i^2\right] \;, \quad (4.18)$$

where $x = p_4^+/p_i^+$, $\mathcal{S}_{45} = \mathcal{M}^2_{45} - m_i^2$, $\mathcal{S}_{45\,\mu_i} = \mathcal{S}_{45} + \mu_i^2/x$. The mass ansatz μ^2 is allowed to be a function of the gluon relative momentum with respect to the quark-antiquark pair, and $\mu_1^2 = \mu^2(p_4, p_5, p_2)$, $\mu_2^2 = \mu^2(p_4, p_1, p_5)$, see Fig. 4.1.

The effective interaction may be divided into two parts: one corresponding to the instantaneous interaction between quark and antiquark and the "exchange" part that collects both RGPEP effective vertex and effective interactions induced by operation R, see Fig. 4.2

$$U_{Q\bar{Q}} \;=\; U_{Q\bar{Q}\rm inst} + U_{Q\bar{Q}\rm exch} \;, \quad (4.19)$$

where

$$U_{Q\bar{Q}\rm inst}(12;1'2') \;=\; -C_F\; r_{C\,12.1'2'}\; f_{12.1'2'}\; \frac{j^+_{11'}\bar{j}^+_{2'2}}{(p_4^+)^2} \;, \quad (4.20)$$

$$U_{Q\bar{Q}\rm exch}(12;1'2') \;=\; -C_F\; r_{C\,12.1'2'}\; \mathcal{F}(12;1'2')\; d_{\mu\nu}(p_4)\; j^\mu_{11'}\bar{j}^\nu_{2'2} \;, \quad (4.21)$$

where

$$\mathcal{F}(12;1'2') \;=\; f_{12.1'2'}\; F(12;1'2') + ff_{12.1'2'}\; \mathcal{R}(12;1'2') \;, \quad (4.22)$$

$$\mathcal{R}(12;1'2') \;=\; \frac{1}{2}\left(\frac{1}{q_1^2-\mu^2} + \frac{1}{q_2^2-\mu^2}\right) \;. \quad (4.23)$$

The gluon mass function, which I write as a function of momenta of all particles in the intermediate state:

$$\mu^2 \;=\; \theta(q^+)\;\mu^2(p_4,p_1,p_{2'}) + \theta(-q^+)\;\mu^2(p_4,p_{1'},p_2)\;, \tag{4.24}$$

depends in fact only on the relative momentum of the gluon with respect to the quarks, $x_4 = p_4^+/P^+$ and $\kappa_4^\perp = p_4^\perp - x_4 P^\perp$. Without this assumption the gluon mass ansatz would be inconsistent with the relativistic invariance of FF wave functions.

Effective Hamiltonians for baryons

For baryons there are two cases that I investigate – baryons composed of three identical quarks, and baryons composed of two identical quarks and one different. For three identical quarks of flavor f,

$$|l_{\rm eff}\rangle \;=\; \int_{123} P^+\tilde\delta_{P.123}\,\frac{\epsilon^{c_1c_2c_3}}{\sqrt{6}}\,\psi_{tQQQ\sigma_1\sigma_2\sigma_3}(x_{1/12},\kappa_{1/12},x_3,\kappa_3)\;\frac{1}{\sqrt{3!}} b^\dagger_{t\,f\,1}b^\dagger_{t\,f\,2}b^\dagger_{t\,f\,3}|0\rangle\;. \tag{4.25}$$

where $\epsilon^{c_1c_2c_3}/\sqrt{6}$ is the color wave function for three quarks in the color-singlet state. The spin-momentum wave function depends only on relative momentum of quark 1 with respect to 2 in 12 subsystem, through $x_{1/12}$ and $\kappa_{1/12}$, and on relative momentum of quark 3 with respect to 12, through x_3 and κ_3. Since the entire wave function has to be antisymmetric with respect to permutations of the three quarks and color wave function is already fully antisymmetric, the spin-momentum part has to be fully symmetric. Factor $1/\sqrt{3!}$ is added due to indistinguishability of quarks. For two identical quarks of flavor f_1 and one of flavor f_3 the baryon state is

$$|l_{\rm eff}\rangle \;=\; \int_{123} P^+\tilde\delta_{P.123}\,\frac{\epsilon^{c_1c_2c_3}}{\sqrt{6}}\,\psi_{tQQQ\sigma_1\sigma_2\sigma_3}(x_{1/12},\kappa_{1/12},x_3,\kappa_3)\;\frac{1}{\sqrt{2!}} b^\dagger_{t\,f_1\,1}b^\dagger_{t\,f_1\,2}b^\dagger_{t\,f_3\,3}|0\rangle\;. \tag{4.26}$$

Because only the two first quarks are now indistinguishable, the spin-momentum wave function has to be symmetric only with respect to exchange of quarks 1 and 2. To make the notation shorter I will later use $\psi_{tQQQ}(123) = \psi_{tQQQ\sigma_1\sigma_2\sigma_3}(x_{1/12},\kappa_{1/12},x_3,\kappa_3)$. The factor $1/\sqrt{2!}$ in Eq. (4.26) and factor $1/\sqrt{3!}$ in Eq. (4.25) ensure that scalar products of states of type QQQ and those of type QQQ' look the same, regardless of how many quarks are identical:

$$\langle l_{\rm eff}|l'_{\rm eff}\rangle \;=\; P^+\tilde\delta_{P'.P}\sum_{\sigma_1\sigma_2\sigma_3}\int [123]P^+\tilde\delta_{123.P}\;\psi^*_{tQQQ\sigma_1\sigma_2\sigma_3}\,\psi'_{tQQQ\sigma_1\sigma_2\sigma_3}\;, \tag{4.27}$$

where $|l_{\rm eff}\rangle$ is a state with momentum P, while $|l'_{\rm eff}\rangle$ is a state with momentum P'.

The effective eigenvalue equation for the spin-momentum wave function is obtained in the form,

$$\begin{aligned}
&\left(\frac{\mathcal{M}^2_{1,\,t}+(\kappa_1^\perp)^2}{x_1}+\frac{\mathcal{M}^2_{2,\,t}+(\kappa_2^\perp)^2}{x_2}+\frac{\mathcal{M}^2_{3,\,t}+(\kappa_3^\perp)^2}{x_3}\right)\psi_{tQQQ}(123)\\
&+g^2\sum_{\sigma_{1'}\sigma_{2'}}\int[1'2']\;P^+_{12}\tilde\delta_{1'2'.12}\frac{1}{x_1+x_2}\;U_{QQ}(12;1'2')\;\psi_{tQQQ}(1'2'3)\\
&+g^2\sum_{\sigma_{3'}\sigma_{1'}}\int[3'1']\;P^+_{31}\tilde\delta_{31.3'1'}\frac{1}{x_3+x_1}\;U_{QQ}(31;3'1')\;\psi_{tQQQ}(1'23')\\
&+g^2\sum_{\sigma_{2'}\sigma_{3'}}\int[2'3']\;P^+_{23}\tilde\delta_{23.2'3'}\frac{1}{x_2+x_3}\;U_{QQ}(23;2'3')\;\psi_{tQQQ}(12'3')\\
&=M^2\;\psi_{tQQQ}(123)\;,
\end{aligned} \tag{4.28}$$

where $P^+_{ij} = p_i^+ + p_j^+$. The effective mass terms $\mathcal{M}^2_{i,\,t}$ are almost the same as those for quark-antiquark eigenvalue Eq. (4.18) except μ_i^2 depends here on different momenta: $\mu_1^2 = \mu^2(p_4,p_5,p_2,p_3)$,

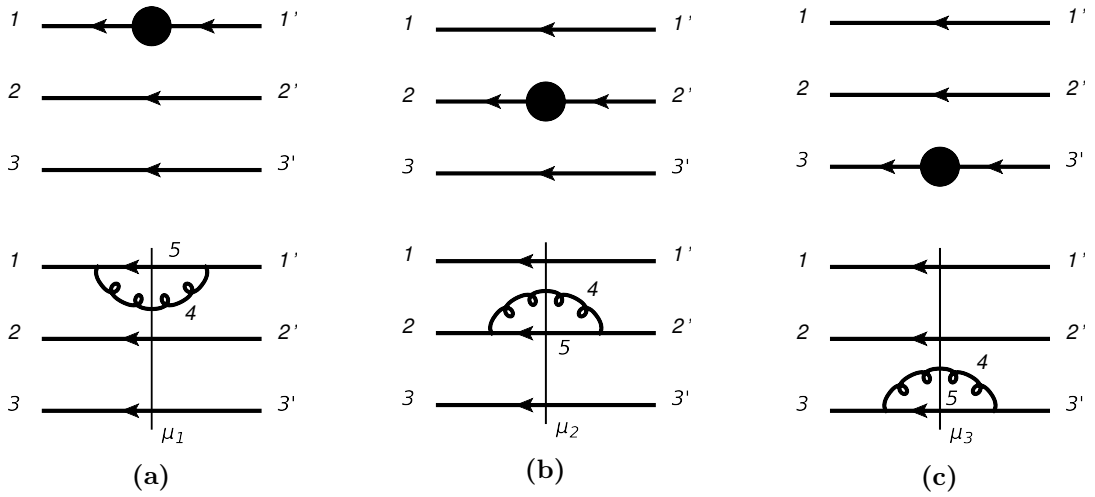

Figure 4.3: Second order quark self-interaction terms in the effective Hamiltonian in the QQQ eigenvalue problem. Parts (a), (b) and (c) depict contributions to $\mathcal{M}^2_{1,\,t}$, $\mathcal{M}^2_{2,\,t}$ and $\mathcal{M}^2_{3,\,t}$, respectively. The upper diagrams are terms of matrix element $\langle l_{\rm eff}|H_{t\,2}|l'_{\rm eff}\rangle$, *cf.* Fig. 3.7; the lower diagrams are terms obtained from the product of two $H_{t\,1}$ in Eq. (4.12).

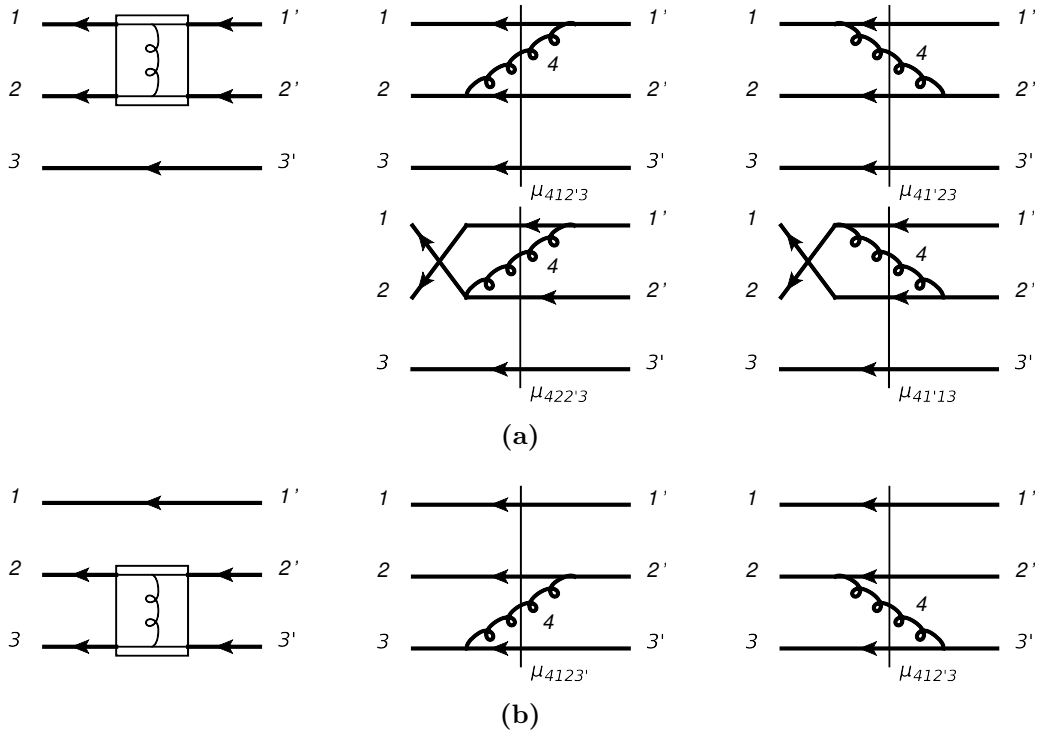

Figure 4.4: Second order gluon-exchange quark-quark interaction terms in the effective Hamiltonian in the QQQ eigenvalue problem. Part (a) represents interaction of quarks 1 and 2, which are identical, hence, the interaction terms should be symmetrized. Part (b) represents interaction of quarks 2 and 3, which may have different flavors, in which case there are no symmetrization diagrams. The most left diagrams in parts (a) and (b) are terms of the matrix element $\langle l_{\rm eff}|(H_{t\,QQ{\rm inst}} + H_{t\,QQ{\rm exch}})|l'_{\rm eff}\rangle$ depicted in Fig. 3.6. The other diagrams represent terms obtained from the product of two $H_{t\,1}$ in Eq. (4.12).

$\mu_2^2 = \mu^2(p_4, p_5, p_3, p_1)$ and $\mu_3^2 = \mu^2(p_4, p_5, p_1, p_2)$, see Fig. 4.3. Although I wrote momenta of all quarks, the gluon mass in fact depends only on the relative momentum of a gluon *with respect to three quarks*.

The gluon-exchange interactions again include instantaneous and exchange terms, see Fig. 4.4,

$$U_{QQ} \;=\; U_{QQ\mathrm{inst}} + U_{QQ\mathrm{exch}} \;, \tag{4.29}$$

where for pair 12 of quarks,

$$U_{QQ\mathrm{inst}}(12;1'2') \;=\; \mathrm{Sym}\left\{ -\frac{C_F}{N_c-1}\; r_{C\,12.1'2'}\; f_{t\,12.1'2'} \frac{j^+_{11'} j^+_{22'}}{(p_4^+)^2} \right\} \;, \tag{4.30}$$

$$U_{QQ\mathrm{exch}}(12;1'2') \;=\; \mathrm{Sym}\left\{ -\frac{C_F}{N_c-1}\; r_{C\,12.1'2'}\; \mathcal{F}(12;1'2')\; d_{\mu\nu}(p_4)\; j^\mu_{11'} j^\nu_{22'} \right\} \;. \tag{4.31}$$

Symbol Sym denotes symmetrization, and needs to be done because quarks 1 and 2 are always identical. Note that the color part of the interaction is already evaluated and the effect of it is the factor $C_F/(N_c-1)$. The color wave function was antisymmetric, hence to obtain antisymmetry of the whole function one needs to symmetrize the spin-momentum part of the interaction terms. For pairs 31 and 23 the symmetrization is required only if flavor of quark 3 is the same as that of quarks 1 and 2. In that case, the other two interaction terms, $U_{QQ}(31;3'1')$ and $U_{QQ}(23;2'3')$, are obtained by cyclic permutations of 1, 2, 3 and $1'$, $2'$, $3'$ in the formulas for $U_{QQ}(12;1'2')$. Note also that in baryons the gluon mass ansatz in $\mathcal{R}(12;1'2')$, given in Eq. (4.23) depends on relative momentum of the gluon with respect to three quarks.

However, for *bbc* and *ccb* systems symmetrization of pairs 31 and 23 should not be performed and,

$$U_{QQ\mathrm{inst}}(23;2'3') \;=\; -\frac{C_F}{N_c-1}\; r_{C\,23.2'3'}\; f_{t\,23.2'3'} \frac{j^+_{22'} j^+_{33'}}{(p_4^+)^2} \;, \tag{4.32}$$

$$U_{QQ\mathrm{exch}}(23;2'3') \;=\; -\frac{C_F}{N_c-1}\; r_{C\,23.2'3'}\; \mathcal{F}(23;2'3')\; d_{\mu\nu}(p_4)\; j^\mu_{22'} j^\nu_{33'} \;, \tag{4.33}$$

and analogous expressions hold for $U_{QQ\mathrm{inst}}(31;3'1')$ and $U_{QQ\mathrm{exch}}(31;3'1')$, but with 3 replaced with 1 and 2 replaced with 3.

4.3.2 Small-x divergences

Using Eqs. (4.20)–(4.23), (3.47) and (3.54) I rewrite $U_{Q\bar{Q}}$ in the following form,

$$\begin{aligned} U_{Q\bar{Q}}(12;1'2') \;&=\; C_F\; r_{C\,12.1'2'}\; g_{\mu\nu} j^\mu_{11'} \bar{j}^\nu_{2'2} \left[f_{12.1'2'}\; F(12;1'2') + ff_{12.1'2'}\; \mathcal{R}(12;1'2') \right] \\ &+\; C_F\; r_{C\,12.1'2'}\; \frac{j^+_{11'} \bar{j}^+_{2'2}}{(q^+)^2} \left[f_{12.1'2'}\; I_1 + ff_{12.1'2'}\; I_2 \right] \;, \end{aligned} \tag{4.34}$$

where

$$I_1 \;=\; \frac{\hat{x}_1^2 q_1^2 + \hat{x}_2^2 q_2^2}{\hat{x}_1^2 (q_1^2)^2 + \hat{x}_2^2 (q_2^2)^2 - (q_1^2 - q_2^2)^2} \frac{q_1^2 + q_2^2}{2} - 1 \;, \tag{4.35}$$

$$I_2 \;=\; \frac{q_1^2 + q_2^2}{2} \left[\frac{1}{2} \left(\frac{1}{q_1^2 - \mu^2} + \frac{1}{q_2^2 - \mu^2} \right) - \frac{\hat{x}_1^2 q_1^2 + \hat{x}_2^2 q_2^2}{\hat{x}_1^2 (q_1^2)^2 + \hat{x}_2^2 (q_2^2)^2 - (q_1^2 - q_2^2)^2} \right] \;. \tag{4.36}$$

$(q^+)^2$ in the denominator in the second line of Eq. (4.34) may produce small-x divergence, therefore, the first thing to investigate is whether any such divergence appears. If the interaction was on-energy-shell, $q_1^2 = q_2^2 = q^2$, and μ^2 were zero, both I_1 and I_2 would be zero. However, interactions in bound states are essentially off-energy-shell. I need to check how the interactions behave in

the vicinity of $q^+ = 0$. From definition $\hat{x}_1 = x_1 + \theta(q^+)q^+/P^+$ and $\hat{x}_2 = x_2 - \theta(-q^+)q^+/P^+$. Moreover,

$$q_2^2 \;=\; q_1^2 + q^+ \frac{\mathcal{M}_{12}^2 - \mathcal{M}_{1'2'}^2}{P^+} \;. \tag{4.37}$$

Off shell, $\mathcal{M}_{12}^2 - \mathcal{M}_{1'2'}^2$ is nonzero but finite because effective interactions cannot change invariant masses by too much. I expand I_1 in powers of q^+,

$$I_1 \;=\; \frac{1}{2q_1^2}\frac{x_1 - x_2}{x_1^2 + x_2^2}\frac{\mathcal{M}_{12}^2 - \mathcal{M}_{1'2'}^2}{P^+}\; q^+ + O\left[(q^+)^2\right] \;. \tag{4.38}$$

The leading term is of order q^+, therefore, when divided in Eq. (4.34) by $(q^+)^2$ produces $1/q^+$, which by itself is not integrable. However, the interaction term contains also regularization factor $r_{C\,12.1'2'}$, which makes the integrals finite, and the limit $\delta \to 0$ is well defined – it corresponds to taking the Cauchy principal value of the integral.

The term with I_2 needs a different analysis. $ff_{12.1'2'}$ regulates the interaction for any fixed q_1^2 and q_2^2 by going exponentially to zero when $q^+ \to 0$. However, it does not regulate interactions when both $q^+ \to 0$ and q_1^2 and q_2^2 go to zero. For small $x_4 = |q^+|/P^+$ one has $q_1^2 \approx q_2^2 \approx -\kappa_4^2$. Therefore, for small x_4,

$$ff_{12.1'2'} \;\approx\; e^{-t(x_1^2+x_2^2)\frac{\kappa_4^4}{x_4^2}} \;=\; e^{-t(x_1^2+x_2^2)a^2} \;, \tag{4.39}$$

where $a^\perp = \sqrt{x_4}\kappa_4^\perp$. Hence, if x_4 goes to zero in such a way that $a^\perp$ is constant, then $ff_{12.1'2'}$ does not go to zero and does not regulate the interaction. To check if the interaction leads to small-x divergences one has to analyze the integral in Eq. (4.17). The part that is necessary here is,

$$\int dx_{1'} d^2\kappa_{1'} \frac{1}{x_4^2} ff_{12.1'2'}\; I_2 \;, \tag{4.40}$$

where factor $1/x_4^2$ comes from $1/(q^+)^2$ in Eq. (4.34) and I omitted numerical factors, $j^+_{11'}\bar{j}^+_{2'2}$, the wave function, which is irrelevant in the analysis (it may be approximated by a constant), and also the regularization function $r_{C\,12.1'2'}$. Now, I change integration variables. Transverse momentum $\kappa_{1'}^\perp$ is equal to $\kappa_1^\perp - \kappa_4^\perp$ for $q^+ > 0$ and to $\kappa_1^\perp + \kappa_4^\perp$ for $q^+ < 0$. In both cases I change the integration variables from $\kappa_{1'}^\perp$ to $\kappa_4^\perp$, and in both cases the modulus of Jacobian is one. Then I change the integration variables from $\kappa_4^\perp$ to $a^\perp = \sqrt{x_4}\kappa_4^\perp$. Therefore, $d^2\kappa_4 = x_4 d^2a$. The integration over $x_{1'}$ is changed to integration over x_4,

$$\int_0^1 dx_{1'} \;=\; \int_0^{x_1} dx_{1'}\theta(q^+) + \int_{x_1}^1 dx_{1'}\theta(-q^+) \;=\; \int_0^{x_1} dx_4\theta(q^+) + \int_0^{1-x_1} dx_4\theta(-q^+) \;, \tag{4.41}$$

where for $q^+ > 0$, I used $x_{1'} = x_1 - x_4$ and for $q^+ < 0$, I used $x_{1'} = x_1 + x_4$. Therefore, the integral (4.40) becomes,

$$\int_0^{\cdot} dx_4 \int d^2a \frac{1}{x_4} e^{-t(x_1^2+x_2^2)a^2}\; I_2 \;, \tag{4.42}$$

which represents both integrals from Eq. (4.41). The integral over x_4 ranges from 0 to x_1 or $1 - x_1$ but only the lower limit is important. Note, that here the factor that is problematic is $1/x_4$ which is always positive and not $1/q^+$, which may be positive or negative. Therefore, the principal value prescription does not work here and I_2 has to vanish when $x_4 \to 0$ (and $a^\perp$ is kept fixed), because otherwise the integral is divergent and the eigenvalue equation ill-defined. The leading term of I_2 in expansion around $x_4 = 0$ is,

$$I_2 \;\approx\; -\frac{\mu^2/x_4}{a^2 + \mu^2/x_4} \;. \tag{4.43}$$

The behavior of I_2 and, hence, the well-definiteness of Eq. (4.17), depend on the behavior of the gluon mass ansatz μ^2 when $x_4 \to 0$. First of all, if μ^2 were zero, then I_2 would also be zero in the limit $x_4 \to 0$. When μ^2 is introduced it cannot be a constant, but if it behaves like $\mu^2 \sim x_4^{1+\delta_\mu}$ with $\delta_\mu > 0$ for small x_4, then it regulates small-x region of dynamics. Another example of acceptable behavior near zero x_4 is $\mu^2 \sim x_4^{\delta_\mu}\kappa_4^2 = x_4^{1+\delta_\mu}a^2$. The parameter δ_μ may be regarded as a phenomenological parameter, however, the oscillator potentials that are implied by the gluon mass ansatz, see below, do not depend on the details of the gluon mass ansatz. To be sure that eigenvalue Eq. (4.17) is free from small-x divergences when μ^2 vanishes properly with x_4 one needs to check also $\mathcal{M}^2_{i,t}$. The analysis is even simpler than for the exchange interaction kernel $U_{Q\bar{Q}}(12;1'2')$. It turns out that the same behavior of gluon mass ansatz near $x_4 = 0$ that regulates the gluon exchange interaction, regulates also the self interaction terms $\mathcal{M}^2_{i,t}$.

For baryons, it is also possible to choose the behavior of gluon mass ansatz that regulates small-x divergent factors in both interaction term and self-energy terms. In baryon, the gluon mass ansatz can depend on the gluon momentum relative to all three quarks $\kappa_4^\perp$. Examples of behavior of gluon mass ansatz near $x_4 = 0$ are again $\mu^2 \sim x_4^{1+\delta_\mu}$ and $\mu^2 \sim x_4^{\delta_\mu}\kappa_4^2$. The notation is the same as for quarkonia but the definition of κ_4 and x_4 in baryons is different than the definition of κ_4 and x_4 in quarkonia. For example, in baryons, $x_4 = p_4^+/(p_1^+ + p_2^+ + p_3^+)$, while in quarkonia $x_4 = p_4^+/(p_1^+ + p_2^+)$. However, $\mu^2 \sim x_4^{\delta_\mu}\kappa_4^2$ implies that $\mu^2 \sim x_{4/12}^{\delta_\mu}\kappa_{4/12}^2$ near $x_{4/12} = 0$, where $x_{4/12}$ and $\kappa_{4/12}^\perp$ are relative momenta in pair 12. The kernel in Eq. (4.31) depends on $x_{4/12}$ and $\kappa_{4/12}^\perp$ in the same way as the interaction kernel Eq. (4.21) depends on κ_4 and x_4 in quarkonia. Therefore, the analysis I presented for quarkonia applies also for baryons.

4.3.3 Coulomb potential and harmonic oscillator

Definition of the nonrelativistic limit

In the previous sections I presented the effective eigenvalue equations for mesons and baryons and showed that they do not posses small-x divergences if the gluon mass ansatz vanishes properly when gluon +-momentum fraction goes to zero. In order to estimate solutions to these well-defined equations, one can take advantage of the fact that quarks are heavy to simplify these equations even more. Large masses of quarks in Eqs. (4.17) and (4.28), formally much larger than λ, imply that the quark-antiquark or three-quark system is nonrelativistic, which means that the relative momenta of particles are small compared with masses. Term "relative momenta" needs a precise definition because +-momentum fraction x of a particle is not usually used in the nonrelativistic quantum mechanics. In meson systems I use the following nonrelativistic momentum of the quark relative to the antiquark [58],

$$k_{12}^\perp = \sqrt{\frac{\beta_1\beta_2}{x_1x_2}}\kappa_1^\perp \ , \tag{4.44}$$

$$k_{12}^z = \sqrt{\frac{\beta_1\beta_2}{x_1x_2}}(m_1+m_2)(x_1-\beta_1) \ , \tag{4.45}$$

where $\perp = x, y$ and $\beta_i = m_i/(m_1+m_2)$. It is convenient to write $\vec{k}_{12} = (k_{12}^x, k_{12}^y, k_{12}^z)$. The nonrelativistic limit is defined as,

$$\frac{\vec{k}_{12}}{m_1+m_2} \to 0 \ . \tag{4.46}$$

In that limit

$$\kappa_1^\perp = k_{12}^\perp \ , \tag{4.47}$$

$$x_1 = \beta_1 + \frac{k_{12}^z}{m_1+m_2} \ . \tag{4.48}$$

In baryon systems I distinguish pair 12 and define the nonrelativistic momentum of quark 1 with respect to quark 2 [58],

$$K_{12}^{\perp} = \sqrt{\frac{\beta_1\beta_2(1-x_3)}{x_1x_2(1-\beta_3)}}\kappa_{1/12}^{\perp} , \tag{4.49}$$

$$K_{12}^{z} = \sqrt{\frac{\beta_1\beta_2(1-x_3)}{x_1x_2(1-\beta_3)}}(m_1+m_2)\left(x_{1/12}-\beta_{1/12}\right) , \tag{4.50}$$

where $\beta_i = m_i/(m_1+m_2+m_3)$, $x_{1/12} = x_1/(x_1+x_2)$ and $\beta_{1/12} = \beta_1/(\beta_1+\beta_2)$. Moreover, the nonrelativistic momentum of quark 3 with respect to pair 12 is,

$$Q_3^{\perp} = \sqrt{\frac{\beta_3(1-\beta_3)}{x_3(1-x_3)}}\kappa_3^{\perp} , \tag{4.51}$$

$$Q_3^{z} = \sqrt{\frac{\beta_3(1-\beta_3)}{x_3(1-x_3)}}(m_1+m_2+m_3)(x_3-\beta_3) . \tag{4.52}$$

It is convenient to write $\vec{K}_{12} = (K_{12}^x, K_{12}^y, K_{12}^z)$, $\vec{Q}_3 = (Q_3^x, Q_3^y, Q_3^z)$. The nonrelativistic limit is defined as,

$$\frac{\vec{K}_{12}}{m_1+m_2+m_3} \to 0 , \quad \frac{\vec{Q}_3}{m_1+m_2+m_3} \to 0 . \tag{4.53}$$

In the nonrelativistic limit

$$\kappa_{1/12}^{\perp} = K_{12}^{\perp} , \tag{4.54}$$

$$x_1 = \beta_1 + \frac{K_{12}^z - \beta_{1/12}Q_3^z}{m_1+m_2+m_3} , \tag{4.55}$$

$$\kappa_3^{\perp} = Q_3^{\perp} , \tag{4.56}$$

$$x_3 = \beta_3 + \frac{Q_3^z}{m_1+m_2+m_3} . \tag{4.57}$$

Schrödinger equation for mesons

Having introduced suitable variables I can now present the eigenvalue equations for masses and states of mesons and baryons. To write the interaction kernel, Eq. (4.34), one needs to know that in the nonrelativistic limit,

$$q_1^2 = -\vec{q}^{\,2} , \tag{4.58}$$

$$q_2^2 = -\vec{q}^{\,2} , \tag{4.59}$$

where $\vec{q} = \vec{k}_{12} - \vec{k}_{1'2'}$. Therefore,

$$F(12;1'2') = -\frac{1}{\vec{q}^{\,2}}\left(1 - \frac{ff_{12.1'2'}}{f_{12.1'2'}}\right) , \tag{4.60}$$

$$\mathcal{R}(12;1'2') = -\frac{1}{\mu^2+\vec{q}^{\,2}} , \tag{4.61}$$

$$I_1 = 0 , \tag{4.62}$$

$$I_2 = -\frac{\mu^2}{\mu^2+\vec{q}^{\,2}} . \tag{4.63}$$

Additionally,

$$g_{\mu\nu}j_{11'}^{\mu}\bar{j}_{2'2}^{\nu} = 4m_1m_2\delta_{\sigma_1\sigma_{1'}}\delta_{\sigma_2\sigma_{2'}} . \tag{4.64}$$

These give,

$$U_{Q\bar{Q}}(12;1'2') \;=\; C_F\; 4m_1m_2\;\delta_{\sigma_1\sigma_{1'}}\delta_{\sigma_2\sigma_{2'}}\left\{-\frac{f_{12.1'2'}}{\vec{q}^{\,2}} - ff_{12.1'2'}\left[\frac{1}{(q^z)^2}-\frac{1}{\vec{q}^{\,2}}\right]\frac{\mu^2}{\mu^2+\vec{q}^{\,2}}\right\}\;, \tag{4.65}$$

where

$$f_{12.1'2'} \;=\; \exp\left[-t\frac{(\vec{k}_{12}^{\,2}-\vec{k}_{1'2'}^{\,2})^2}{\beta_1^2\beta_2^2}\right]\;, \tag{4.66}$$

$$ff_{12.1'2'} \;=\; \exp\left[-t(m_1^2+m_2^2)\left(\frac{\vec{q}^{\,2}}{q^z}\right)^2\right]\;. \tag{4.67}$$

The effective self-interaction terms are

$$\mathcal{M}_{1,t}^2 \;=\; m_1^2 + m_1 g_t^2 C_F\int\frac{d^3q}{(2\pi)^3}\;\left[\frac{1}{(q^z)^2}-\frac{1}{\vec{q}^{\,2}}\right]\frac{\mu^2}{\mu^2+\vec{q}^{\,2}}\exp\left[-2tm_1^2\left(\frac{\vec{q}^{\,2}}{q^z}\right)^2\right]\;, \tag{4.68}$$

$$\mathcal{M}_{2,t}^2 \;=\; m_2^2 + m_2 g_t^2 C_F\int\frac{d^3q}{(2\pi)^3}\;\left[\frac{1}{(q^z)^2}-\frac{1}{\vec{q}^{\,2}}\right]\frac{\mu^2}{\mu^2+\vec{q}^{\,2}}\exp\left[-2tm_2^2\left(\frac{\vec{q}^{\,2}}{q^z}\right)^2\right]\;, \tag{4.69}$$

where $\vec{q}$ is the nonrelativistic momentum of the gluon and is defined differently than $\vec{q}$ from quark-antiquark interaction. Here, $q^\perp = \kappa^\perp$ and $q^z = xm_1$. Moreover, the integration measure in the nonrelativistic limit is,

$$\int[1'2']\;P^+\tilde{\delta}_{1'2'.P} \;=\; \int\frac{d^3k_{1'2'}}{(2\pi)^3}\;\frac{1}{2\mu_{12}}\;, \tag{4.70}$$

where $\mu_{12} = m_1m_2/(m_1+m_2)$ is the reduced mass in the quark pair 12

After division by $2(m_1+m_2)$ Eq. (4.17) in the nonrelativistic limit is,

$$\begin{aligned}&\left[\frac{k_{12}^2}{2\mu_{12}} + C_F\int\frac{d^3q}{(2\pi)^3}\frac{W_{11}(\vec{q})+W_{22}(\vec{q})}{2}\right]\psi(\vec{k}_{12})\\ &- C_F\int\frac{d^3q}{(2\pi)^3}\left[\frac{g_t^2}{\vec{q}^{\,2}}f_{12.1'2'}+W_{12}(\vec{q})\right]\psi(\vec{k}_{12}-\vec{q}) \;=\; E\;\psi(\vec{k}_{12})\;,\end{aligned} \tag{4.71}$$

where,

$$W_{ij}(\vec{q}) \;=\; g_t^2\left[\frac{1}{(q^z)^2}-\frac{1}{\vec{q}^{\,2}}\right]\frac{\mu^2}{\mu^2+\vec{q}^{\,2}}\exp\left[-t(m_i^2+m_j^2)\left(\frac{\vec{q}^{\,2}}{q^z}\right)^2\right]\;, \tag{4.72}$$

and the eigenvalue E of Eq. (4.71) is related to the eigenvalue M of Eq. (4.17) in the following way,

$$E \;=\; \frac{M^2-(m_1+m_2)^2}{2(m_1+m_2)}\;. \tag{4.73}$$

Furthermore,

$$\psi(\vec{k}_{12}-\vec{q}) \;=\; \psi(\vec{k}_{12}) - q^i\frac{\partial}{\partial k_{12}^i}\psi(\vec{k}_{12}) + \frac{1}{2}q^iq^j\frac{\partial^2}{\partial k_{12}^i\partial k_{12}^j}\psi(\vec{k}_{12}) + \dots\;, \tag{4.74}$$

where $i,j = x,y,z$. The first term combines with the self-interaction terms. The term linear in $\vec{q}$ integrates to zero. Term quadratic in $\vec{q}$ is nonzero for $i=j$ and produces harmonic oscillator

force. Assuming that higher-order terms in expansion into powers of relative momentum are small, I omit them. The term in Eq. (4.71) that comes from the third term in Eq. (4.74) is,

$$-C_F \int \frac{d^3q}{(2\pi)^3} W_{12}(\vec{q}) \frac{1}{2} (q^i)^2 \frac{\partial^2}{\partial k_{12}^{i\,2}} \psi(\vec{k}_{12}) \ . \tag{4.75}$$

I can approximate W_{12} by assuming $\mu^2/(\mu^2 + \vec{q}^{\,2}) \approx 1$, because $|\vec{q}| \sim \alpha\mu_{12} \ll \mu$ in the dominant region of integration. Moreover, this assumption implies that the coefficient in front of derivatives in each direction is the same, which is not guaranteed by general form of W_{12} in Eq. (4.72). Therefore, Eq. (4.71) becomes,

$$\left[\Sigma + \frac{k_{12}^2}{2\mu_{12}} - \frac{\mu_{12}\omega_{12}^2 \Delta_k}{2}\right] \psi(\vec{k}_{12}) - C_F \int \frac{d^3q}{(2\pi)^3} \frac{g_t^2}{\vec{q}^{\,2}} f_{12.1'2'} \ \psi(\vec{k}_{12} - \vec{q}) \ = \ E \ \psi(\vec{k}_{12}) \ , \tag{4.76}$$

where Δ_k is the Laplacian in momentum space, which corresponds to harmonic oscillator potential in position space.[3] The frequency of the harmonic oscillator potential is,

$$\omega_{12} \ = \ \sqrt{\frac{\alpha}{18\sqrt{\pi}\,\mu_{12}} \left(\frac{\lambda^2}{\sqrt{m_1^2 + m_2^2}}\right)^3} \ , \tag{4.77}$$

where $\alpha = g_t^2/(4\pi)$, depends rather strongly on the RGPEP scale λ. Note, that Coulomb potential $1/\vec{q}^{\,2}$ is multiplied by the RGPEP form factor $f_{12.1'2'}$, see Eq. (4.66), which makes the interaction nonlocal. The relativistic expression for the mass of a bound state in terms of the eigenvalue E implied by Eq. (4.73) has the form,

$$M \ = \ (m_1 + m_2)\sqrt{1 + \frac{2E}{m_1 + m_2}} \ , \tag{4.78}$$

which in the nonrelativistic limit is $M \approx m_1 + m_2 + E$. However, since Eq. (4.76) is derived from the FF Hamiltonian of QCD I use Eq. (4.78).

The universal shift Σ of masses of eigenstates of Eq. (4.76),

$$\Sigma \ = \ \frac{C_F}{2} g_t^2 \int \frac{d^3q}{(2\pi)^3} \left[\frac{1}{(q^z)^2} - \frac{1}{\vec{q}^{\,2}}\right] \frac{\mu^2}{\mu^2 + \vec{q}^{\,2}} \left[e^{-tm_1^2\left(\frac{\vec{q}^{\,2}}{q^z}\right)^2} - e^{-tm_2^2\left(\frac{\vec{q}^{\,2}}{q^z}\right)^2}\right]^2 \ , \tag{4.79}$$

comes from the difference between self-interaction terms $\mathcal{M}_{i,\,t}^2$ and the gluon-exchange interaction term, in which wave function is approximated by a constant, see the first term in Eq. (4.74). It is zero if $m_1 = m_2$. However, if $m_1 \neq m_2$, then Σ depends on precise form of μ^2, because in Eq. (4.79) one cannot approximate $\mu^2/(\mu^2 + \vec{q}^{\,2}) \approx 1$ – that would make the integral divergent. Assumed behavior of μ^2 for $|\vec{q}| \sim 0$ guarantees that Σ is finite but depends on δ_μ. It is possible to make Σ smaller than the harmonic oscillator frequency ω_{12} or even on the order of splittings introduced by spin-dependent interactions (which I neglect in this thesis). But Σ can be on the order of ω_{12} or even much bigger than ω_{12}. That would imply large shifts of energies of B_c mesons. Because for charmonia and bottomonia $\Sigma = 0$, in Chapter 5 I calculated spectrum of B_c assuming that $\Sigma = 0$ also in this case and the results agree well with experimental data. That fact together with strong dependence of Σ on the gluon mass ansatz suggests that this term will be substantially corrected in a study that uses the renormalized Hamiltonian H_t calculated up to terms of order g_t^4. On the other hand, formally, no dependence of ω_{12} on the gluon mass ansatz suggests that harmonic oscillator potential with frequency ω_{12} is a result that will also appear in the future calculations.

[3] Position here is defined as a variable conjugate to relative momentum $\vec{k}$.

Schrödinger equation for baryons

For baryons the derivation of the Schrödinger equation is analogous to the derivation for mesons. Quark-quark gluon-exchange interaction between quarks i and j can be most easily written in terms of nonrelativistic momentum of one quark relative to the other. Therefore, in addition to Eqs. (4.49)–(4.52) I define two new sets of momenta: $\vec{K}_{23}$, $\vec{Q}_1$ and $\vec{K}_{31}$, $\vec{Q}_2$. Appropriate formulas can be obtained by using Eqs. (4.49) and (4.52) as a template and changing every index in a consistent way, *e.g.*, $1 \to 2$, $2 \to 3$, $3 \to 1$. Relations between different sets in the nonrelativistic limit are,

$$\vec{K}_{23} = -\frac{\beta_3}{\beta_2+\beta_3}\vec{K}_{12} - \frac{\beta_2}{(\beta_2+\beta_3)(\beta_1+\beta_2)}\vec{Q}_3 \ , \tag{4.80}$$

$$\vec{Q}_1 = \vec{K}_{12} - \frac{\beta_1}{\beta_1+\beta_2}\vec{Q}_3 \ , \tag{4.81}$$

and

$$\vec{K}_{31} = -\frac{\beta_3}{\beta_3+\beta_1}\vec{K}_{12} + \frac{\beta_1}{(\beta_3+\beta_1)(\beta_1+\beta_2)}\vec{Q}_3 \ , \tag{4.82}$$

$$\vec{Q}_2 = -\vec{K}_{12} - \frac{\beta_2}{\beta_1+\beta_2}\vec{Q}_3 \ . \tag{4.83}$$

The formulas for various objects in the nonrelativistic limit are almost the same as for mesons, but one has to change $\vec{q}$ in favor of $\Delta\vec{K}_{ij} = \vec{K}_{ij} - \vec{K}_{i'j'}$. Hence, the interaction kernels are,

$$\begin{aligned} U_{QQ}(ij;i'j') &= \frac{C_F}{N_c-1}\ 4m_i m_j\ \delta_{\sigma_i\sigma_{i'}}\delta_{\sigma_j\sigma_{j'}} \\ &\times \left\{ -\frac{f_{ij.i'j'}}{\Delta\vec{K}_{ij}^2} - ff_{ij.i'j'}\left[\frac{1}{(\Delta K_{ij}^z)^2} - \frac{1}{\Delta\vec{K}_{ij}^2}\right]\frac{\mu^2}{\mu^2+\Delta\vec{K}_{ij}^2}\right\} \ , \end{aligned} \tag{4.84}$$

where,

$$f_{ij.i'j'} = \exp\left[-t\frac{(\vec{K}_{ij}^{\,2} - \vec{K}_{i'j'}^{\,2})^2}{\beta_i^2\beta_j^2}\right] \ , \tag{4.85}$$

$$ff_{ij.i'j'} = \exp\left[-t(m_i^2+m_j^2)\left(\frac{\Delta\vec{K}_{ij}{}^2}{\Delta K_{ij}^z}\right)^2\right] \ . \tag{4.86}$$

The effective self-interaction terms are given by formulas exactly like Eq. (4.68), but with proper quark mass and with formally different definition of the gluon mass ansatz. The integration measure in the nonrelativistic limit is,

$$\int [i'j']\ P_{ij}^+\tilde{\delta}_{i'j'.ij} = \int \frac{d^3K_{i'j'}}{(2\pi)^3}\ \frac{1}{2\mu_{ij}} \ . \tag{4.87}$$

After division by $2(m_1+m_2+m_3)$ Eq. (4.28) in the nonrelativistic limit is,

$$\begin{aligned} &\left[\frac{K_{12}^2}{2\mu_{12}} + \frac{Q_3^2}{2\mu_{3(12)}} + C_F\int\frac{d^3q}{(2\pi)^3}\frac{W_{11}(\vec{q})+W_{22}(\vec{q})+W_{33}(\vec{q})}{2}\right]\psi(123) \\ &-\frac{C_F}{2}\int\frac{d^3K_{1'2'}}{(2\pi)^3}\left[\frac{g^2}{|\Delta\vec{K}_{12}|^2}f_{12.1'2'} + W_{12}(\Delta\vec{K}_{12})\right]\psi(1'2'3) \\ &-\frac{C_F}{2}\int\frac{d^3K_{2'3'}}{(2\pi)^3}\left[\frac{g^2}{|\Delta\vec{K}_{23}|^2}f_{23.2'3'} + W_{23}(\Delta\vec{K}_{23})\right]\psi(1'23') \\ &-\frac{C_F}{2}\int\frac{d^3K_{3'1'}}{(2\pi)^3}\left[\frac{g^2}{|\Delta\vec{K}_{31}|^2}f_{31.3'1'} + W_{31}(\Delta\vec{K}_{31})\right]\psi(12'3') = E\ \psi(123) \ , \end{aligned} \tag{4.88}$$

where I put $N_c = 3$, $\mu_{3(12)} = (2m_1)m_3/(2m_1 + m_3)$ is the reduced mass of quark 3 with respect to pair 12 and the arguments of wave functions in interaction terms are written in a simplified way. The eigenvalue E of Eq. (4.88) is related to the eigenvalue M of Eq. (4.28) in the following way,

$$E = \frac{M^2 - (m_1 + m_2 + m_3)^2}{2(m_1 + m_2 + m_3)} . \tag{4.89}$$

Expansion of the wave function in the interaction term where quarks 1 and 2 interact is,

$$\begin{aligned} \psi(\vec{K}_{1'2'}, \vec{Q}_3) &= \psi(\vec{K}_{1'2'}, \vec{Q}_3) - \Delta K_{12}^i \frac{\partial}{\partial K_{12}^i} \psi(\vec{K}_{1'2'}, \vec{Q}_3) \\ &+ \frac{1}{2} \Delta K_{12}^i \Delta K_{12}^j \frac{\partial^2}{\partial K_{12}^i \partial K_{12}^j} \psi(\vec{K}_{1'2'}, \vec{Q}_3) + \dots , \end{aligned} \tag{4.90}$$

where $i, j = x, y, z$. Like for mesons the first term combines with the self-interaction terms, the term linear in $\Delta\vec{K}_{12}$ integrates to zero, and the term quadratic in $\Delta\vec{K}_{12}$ produces harmonic oscillator force. Assuming $\mu^2/(\mu^2 + \Delta\vec{K}_{12}{}^2) \approx 1$, I obtain, three harmonic oscillator potentials between quarks of each pair. The terms in Eq. (4.88) that correspond to those harmonic oscillators are,

$$-\frac{1}{4} \left[w_{12} \left(\frac{\partial}{\partial \vec{K}_{12}} \right)^2 + w_{23} \left(\frac{\partial}{\partial \vec{K}_{23}} \right)^2 + w_{31} \left(\frac{\partial}{\partial \vec{K}_{31}} \right)^2 \right] \psi(\vec{K}_{12}, \vec{Q}_3) , \tag{4.91}$$

where

$$w_{ij} = \frac{\alpha\lambda^3}{18\sqrt{\pi}} \left(\frac{\lambda^2}{m_i^2 + m_j^2} \right)^{3/2} , \tag{4.92}$$

Using $w_{31} = w_{23}$ and relations between $\vec{K}_{23}$, $\vec{K}_{31}$ and $\vec{K}_{12}$, $\vec{Q}_3$ I rewrite Eq. (4.91) to the following form,

$$= -\frac{1}{4} \left[\left(w_{12} + \frac{1}{2} w_{23} \right) \left(\frac{\partial}{\partial \vec{K}_{12}} \right)^2 + 2 w_{23} \left(\frac{\partial}{\partial \vec{Q}_3} \right)^2 \right] \psi(\vec{K}_{12}, \vec{Q}_3) . \tag{4.93}$$

Therefore, the three oscillators between quarks in each pair of quarks can be written as two oscillators: one oscillator between quarks 1 and 2, and the second one between quark 3 and pair 12. The eigenvalue Eq. (4.88) becomes,

$$\begin{aligned} &\left[\Sigma + \frac{K_{12}^2}{2\mu_{12}} + \frac{Q_3^2}{2\mu_{3(12)}} - \frac{\mu_{12}\omega_{12}^2 \Delta_K}{2} - \frac{\mu_{3(12)}\omega_{3(12)}^2 \Delta_Q}{2} \right] \psi\left(\vec{K}_{12}, \vec{Q}_3\right) \\ &- \frac{C_F}{2} \int \frac{d^3q}{(2\pi)^3} \frac{g_t^2}{|\vec{q}|^2} f_{12.1'2'} \, \psi\left(\vec{K}_{12} - \vec{q}, \vec{Q}_3\right) \\ &- \frac{C_F}{2} \int \frac{d^3q}{(2\pi)^3} \frac{g_t^2}{|\vec{q}|^2} f_{23.2'3'} \, \psi\left(\vec{K}_{12} + \frac{1}{2}\vec{q}, \vec{Q}_3 + \vec{q}\right) \\ &- \frac{C_F}{2} \int \frac{d^3q}{(2\pi)^3} \frac{g_t^2}{|\vec{q}|^2} f_{31.3'1'} \, \psi\left(\vec{K}_{12} + \frac{1}{2}\vec{q}, \vec{Q}_3 - \vec{q}\right) = E \, \psi\left(\vec{K}_{12}, \vec{Q}_3\right) , \end{aligned} \tag{4.94}$$

where the frequencies of the harmonic oscillators are,

$$\omega_{12} = \frac{2w_{12} + w_{13}}{4\mu_{12}} , \tag{4.95}$$

$$\omega_{3(12)} = \frac{w_{13}}{\mu_{3(12)}} . \tag{4.96}$$

In case of the equal masses of quarks,

$$\omega_{12} = \omega_{3(12)} = \omega = \frac{\sqrt{3}}{2}\sqrt{\frac{\alpha}{18\sqrt{2\pi}}}\frac{\lambda^3}{m^2} . \tag{4.97}$$

The relativistic expression for the mass of a bound state in terms of the eigenvalue E has the form,

$$M = (m_1 + m_2 + m_3)\sqrt{1 + \frac{2E}{m_1 + m_2 + m_3}} . \tag{4.98}$$

The mass shift term Σ is zero for baryons with equal masses of all quarks. For baryons with two different kinds of quarks and $m_1 = m_2 \neq m_3$ it is given by the same Eq. (4.79) but with m_2 replaced with m_3. Therefore, as for mesons, this term is likely to be an artifact of the gluon mass ansatz and I omit it when I compute the spectra of heavy baryons built from quarks of different flavors. Further discussion of this term is in Chapter 5.

Chapter 5

Spectra of heavy mesons and baryons

Derivation of the approximate Hamiltonians for mesons and baryons in the previous chapter relies on the assumption that in heavy-flavor QCD the dynamics of the effective gluons inside ground states and lowest excited states of heavy hadrons can be approximated by including only one such gluon but supplied with an ansatz for its mass, which is a function of relative momentum of gluon with respect to quarks. The simplest test of the ansatz is the calculation of masses of doubly-heavy mesons and triply-heavy baryons. The obtained mass spectra do not include any spin effects other than those due to antisymmetrization of wave functions in identical quarks. Therefore, the purpose of this calculation is to check if the spectra are qualitatively acceptable rather than to compute precisely the masses. Hence, we make crude approximations. Nevertheless, the same approximations are made for baryons and quarkonia. Therefore, fitting masses of quarkonia to experimental values fixes free parameters of the theory, and the masses of baryons that we arrive at can be treated as rough estimates of yet to be observed heavy baryons. The results for ground states and low-lying excited states are consistent with estimates produced by other known methods. Especially interesting and encouraging is qualitative agreement between our results and Lattice QCD simulations for ground states and excited states spectrum of Ω_{ccc} and Ω_{bbb} baryons.

5.1 Introduction

If we could solve QCD exactly then no calculated quantity would depend on the renormalization group parameter λ, and there would be no point in introducing the family of effective Hamiltonians H_t, because only one renormalized Hamiltonian would suffice. In an approximate calculation one can and should choose λ that has value related to characteristic scales involved in the problem. The frequencies of the oscillators obtained in Chapter 4 depend quite strongly on renormalization group parameter λ. Therefore, the masses of bound states can be accurately described using our approximations and assumptions only in a limited window of values of λ [59, 60]. The basic assumption that we make about λ is that the best choice for its value scales with the characteristic mass of the system m and coupling constant α as $\lambda \sim \sqrt{\alpha} m$. We make this choice because it implies that the frequencies of the harmonic oscillators scale as α^2, which means that the characteristic momentum of the harmonic oscillator $p \sim \sqrt{m\omega}$ scales as α. The characteristic momentum in the Coulomb potential (Bohr momentum) also scales as α. Hence, all terms: kinetic energy, Coulomb potential (neglecting the form factors) and the harmonic oscillator potential scale with the coupling constant as α^2. Therefore, the binding energy also scales as α^2. Moreover, the RGPEP form factors that multiply the Coulomb potential formally do not differ much from 1 because their arguments being momentum over λ to the forth power scale as α^2, hence, are formally small. Therefore, I omit the RGPEP form factors in approximate calculations of masses of heavy hadrons. The exact formula for λ that we use to calculate masses of heavy mesons is,

$$\lambda_{Q\bar{Q}} \;=\; \sqrt{\alpha}\left(a\,\bar{m}_{Q\bar{Q}} + b\right)\;, \tag{5.1}$$

where $\bar{m}_{Q\bar{Q}}$ is the average mass of the quark and the antiquark. The analogous formula for baryons is,

$$\lambda_{3Q} = \sqrt{\alpha}\,(a\,\bar{m}_{3Q} + b)\ , \tag{5.2}$$

where $\bar{m}_{3Q}$ is the average mass of the three quarks. The coupling constant α is assumed to be known and running [3],

$$\alpha = \frac{1}{\beta_0 \log(\lambda^2/\Lambda^2_{\rm QCD})}\ , \tag{5.3}$$

where $\beta_0 = (33 - 2n_f)/(12\pi)$. We fix the number of quark flavors to $n_f = 2$, and $\alpha = 0.1181$ for $\lambda = M_Z = 91.1876$ GeV [21]. That means $\Lambda_{\rm QCD} = 371$ MeV. Variation in the number of flavors does not change significantly the mass spectra. The quark masses are assumed to be independent of λ, because their dependence on the scale can be first studied using the renormalized Hamiltonian H_t computed up to the fourth order in perturbation theory.

The unknown masses of quarks m_b and m_c and constants a and b have to be fitted to experimental data [21]. We use masses of charmonium states J/ψ, $\psi(2S)$ and $\chi_{c1}(1P)$ to get the best values of $\lambda_{c\bar{c}}$ and m_c. And we use bottomonium states $\Upsilon(1S)$, $\Upsilon(2S)$ and $\chi_{b1}(1P)$ to get the best values of $\lambda_{b\bar{b}}$ and m_b. Using Eq. (5.1), we necessarily obtain the only possible values of constants a and b and we compute $\lambda_{b\bar{c}}$ that is used to for the calculation of masses of $B_c(1S)$ and $B_c(2S)$ states.

A comment is due about the method of estimating solutions of the eigenvalue Eqs. (4.76) and (4.94). For the purpose of estimation of the mass spectra of heavy hadrons it appears sufficient to account for the Coulomb potential in perturbation theory. We assume that the "unperturbed" parts of the approximate Hamiltonians for mesons and baryons consist of kinetic energy and harmonic oscillator potentials, while the Coulomb potential constitutes a "perturbation" and is treated in the first order perturbation theory. My check of the quality of that calculation for zero-angular-momentum states in *bbb* and *ccc* systems is in App. B. A more accurate calculation gives mass of the *bbb* ground state that is shifted by less than 50 MeV from the result of the first order perturbation theory. The analogous shift for ground state of *ccc* is about 30 MeV. Shifts of excited states are smaller, as expected, because Coulomb potential is strongest in the center and the ground state has the biggest values of the wave function in the vicinity of the center. Shifts of this magnitude or even larger are already expected to come from spin interactions that we neglect. Therefore, treating Coulomb potential in the first order of perturbation theory appears justified.

5.2 Mass spectrum of mesons

Using the basis of eigenstates of the harmonic oscillator one can classify states according to its excitations. If there is one oscillator, *i.e.*, for mesons, the successive excitations are denoted $1S$, $1P$, $2S$, $1D$, and so on, where $1S$ is the ground state, $1P$ is the p-wave excitation (the first orbital excitation), $2S$ is the first radial excitation and $1D$ denotes the lowest-energy d-wave state. Wave functions of s-wave states are denoted ψ_{1S}, ψ_{2S}, and so on. P-wave states come in multiplets of different projections of the orbital angular momentum on z axis, $\psi_{1P_{-1}}$, ψ_{1P_0}, $\psi_{1P_{+1}}$. The general oscillator eigenstate with definite angular momentum and its projection on z-axis is,

$$\psi_{kl_m}(\vec{p}) = N_{kl}\ e^{-\nu p^2}\ L_k^{(l+1/2)}(2\nu p^2)\ p^l Y_{lm}(\hat{p})\ , \tag{5.4}$$

where k is the radial excitation number, l is the orbital angular momentum number, m is the projection of the angular momentum on the z axis, $\nu = 1/(2\mu\omega)$, Y_{lm} are spherical harmonics and $L_k^a(x)$ are generalized Laguerre polynomials. The first two polynomials are $L_0^a(x) = 1$, $L_1^a(x) = 1 + a - x$. The normalization factors are

$$N_{kl} = \sqrt{\sqrt{\frac{2\nu^3}{\pi}}\frac{2^{k+2l+3}k!\nu^l}{(2k+2l+1)!!}}(2\pi)^{3/2}\ , \tag{5.5}$$

so that

$$\int \frac{d^3p}{(2\pi)^3}\psi^*_{kl_m}\psi_{k'l'_{m'}} = \delta_{kk'}\delta_{ll'}\delta_{mm'} \ . \tag{5.6}$$

The energy of an eigenstate is

$$E = \omega\left(2k + l + \frac{3}{2}\right) \ . \tag{5.7}$$

The ground state has $E = 3\omega/2$, $1P$ states constitute so-called first band of the harmonic oscillator with energy ω above the ground state, while $2S$ and $1D$ states are degenerated and constitute the second band with excitation energy 2ω. Combination of momentum wave functions with spin wave functions is simple when spin-dependent interactions are absent. Quark and antiquark may form only spin-0 singlet or spin-1 triplet. Then the orbital and spin angular momenta are added using well-known Clebsch-Gordan coefficients tabulated for example in Ref. [21]. In Chapter 6, where I calculate electromagnetic form factors, I need to include also leading relativistic corrections to wave functions induced by motion of particles with spin to obtain satisfactory results for magnetic properties of hadrons.

The binding energies E of mesons, including first order Coulomb corrections to the harmonic oscillator levels are,

$$E_{1S} = \frac{3}{2}\omega - \frac{4}{3}\alpha\sqrt{\frac{2}{\pi\nu}} \ , \tag{5.8}$$

$$E_{1P} = \frac{5}{2}\omega - \frac{8}{9}\alpha\sqrt{\frac{2}{\pi\nu}} \ , \tag{5.9}$$

$$E_{2S} = \frac{7}{2}\omega - \frac{10}{9}\alpha\sqrt{\frac{2}{\pi\nu}} \ . \tag{5.10}$$

In App. C there are listed binding energies of other states that also appear in Fig. 5.1. The masses are given by Eq. (4.78). For bottomonium we fit m_b quark mass and $\lambda_{b\bar{b}}$ to obtain the best agreement between masses computed using E_{1S}, E_{2S}, E_{1P} and the experimental masses of $\Upsilon(1S)$, $\Upsilon(2S)$, $\chi_{b1}(1P)$. The best fit is,

$$m_b = 4698 \text{ MeV} \quad \text{and} \quad \lambda_{b\bar{b}} = 4258 \text{ MeV} \ . \tag{5.11}$$

Using the above $\lambda_{b\bar{b}}$ and Eq. (5.3) we have $\alpha(\lambda_{b\bar{b}}) = 0.2664$. The harmonic oscillator frequency is $\omega_{b\bar{b}} = 268.8$ MeV. The best agreement between masses of states computed using E_{1S}, E_{2S}, E_{1P} and experimental masses of J/ψ, $\psi(2S)$ and $\chi_{c1}(1P)$ is,

$$m_c = 1460 \text{ MeV} \quad \text{and} \quad \lambda_{c\bar{c}} = 1944 \text{ MeV} \ . \tag{5.12}$$

$\lambda_{c\bar{c}}$ and m_c imply $\alpha(\lambda_{c\bar{c}}) = 0.3926$ and $\omega_{c\bar{c}} = 321.6$ MeV. Knowing the values of $\lambda_{b\bar{b}}$, $\lambda_{c\bar{c}}$, m_b, and m_c we can calculate the coefficients a and b from Eq. (5.1),

$$a = 1.589 \ , \tag{5.13}$$

$$b = 783 \text{ MeV} \ . \tag{5.14}$$

Using again Eq. (5.1), this time for $b\bar{c}$ system, we have,

$$\lambda_{bc} = 3134 \text{ MeV} \ . \tag{5.15}$$

Using Eq. (5.3) and the values of m_b, m_c and λ_{bc}, we have $\alpha(\lambda_{bc}) = 0.3047$ and $\omega_{bc} = 261.1$ MeV.

Figure 5.1, presents spectra of all three systems, $b\bar{b}$, $c\bar{b}$ and $c\bar{c}$. The states that were used for fitting free parameters are close to the experimental data. Also $1D$ states of charmonium and bottomonium agree well with experiment. States of the third and fourth band of harmonic

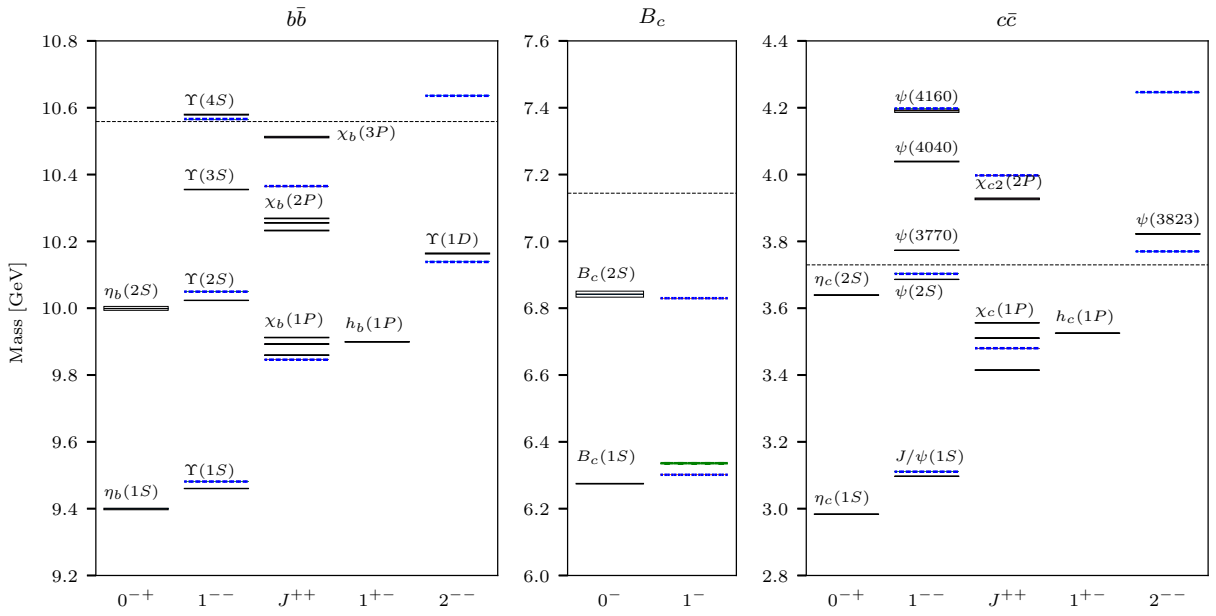

Figure 5.1: Results of our fit to $b\bar{b}$ and $c\bar{c}$ low-mass states, are shown by dotted blue lines on the background of data for heavy quarkonia and B_c mesons. The dashed green line represents an average of various predictions for B_c^* mass [61]. Dashed lines across a panel represent thresholds. We include the states $3S$ that appear at the level of observed states that are interpreted as $4S$. Such highly excited states may contain an important component with effective gluons, not properly accounted for by the perturbative calculation in our pilot study. (Plot and caption first published in Ref. [7])

oscillator are too high, *e.g.*, our $\Upsilon(3S)$ has the mass of the state experimentally presented as $\Upsilon(4S)$. The discrepancy may be explained by the fact that we include gluonic degrees of freedom implicitly by using perturbative reduction to the quark-antiquark Fock sector. For highly excited states the perturbative reduction probably breaks down because Fock sectors with gluons are likely to provide important contributions to such quarkonium states. In that case an eigenvalue equation like Eq. (4.6), with at least two Fock sectors instead of just one, should be solved to obtain reliable results. The standard quark model of charmonium and bottomonium [24] reproduces $\Upsilon(3S)$ well because it employs the linear confining potential instead of the harmonic one. There is a correspondence between linear potential in the instant form and the quadratic potential in the FF of Hamiltonian dynamics [30]. In Eq. (4.78) for large E compared to $m_1 + m_2$ the mass M behaves like a square root of E, hence, gives smaller values for masses than $m_1 + m_2 + E$ would give. However, this effect is too small for bottomonium or charmonium to shift masses of $\Upsilon(3S)$ or $\psi(3S)$ down enough. The problem with proper description of $\Upsilon(3S)$ and quite good agreement of our estimates with other, low-lying states suggests an interesting conclusion that already $\Upsilon(3S)$ contains an important gluonic component and that, maybe, the usual linearly rising confining potential between constituent quarks can be derived from QCD in a calculation that properly includes gluons in the dynamics of the system.

Comparison of experimental masses of B_c and $B_c(2S)$ with our estimates also shows quite good agreement if the Σ term of Eq. (4.79) is neglected.

5.3 Mass spectrum of baryons

In baryons there are two oscillators: between quarks 1 and 2, and between quark 3 and pair 12. The basic building blocks to construct the eigenstates of the system are tensor products of wave functions of the two oscillators. The notation is to write the excitation state of both harmonic

States	$L \otimes S$	J
1S1S	$0 \otimes \frac{3}{2}$	$\frac{3}{2}^+$
	$0 \otimes \left(\frac{1}{2}\right)_S$	$\frac{1}{2}^+$
1P1S	$1 \otimes \left(\frac{1}{2}\right)_A$	$\frac{3}{2}^- \oplus \frac{1}{2}^-$
1S1P	$1 \otimes \frac{3}{2}$	$\frac{5}{2}^- \oplus \frac{3}{2}^- \oplus \frac{1}{2}^-$
	$1 \otimes \left(\frac{1}{2}\right)_S$	$\frac{3}{2}^- \oplus \frac{1}{2}^-$
1D1S	$2 \otimes \frac{3}{2}$	$\frac{7}{2}^+ \oplus \frac{5}{2}^+ \oplus \frac{3}{2}^+ \oplus \frac{1}{2}^+$
	$2 \otimes \left(\frac{1}{2}\right)_S$	$\frac{5}{2}^+ \oplus \frac{3}{2}^+$
1S1D	$2 \otimes \frac{3}{2}$	$\frac{7}{2}^+ \oplus \frac{5}{2}^+ \oplus \frac{3}{2}^+ \oplus \frac{1}{2}^+$
	$2 \otimes \left(\frac{1}{2}\right)_S$	$\frac{5}{2}^+ \oplus \frac{3}{2}^+$
1P1P	$2 \otimes \left(\frac{1}{2}\right)_A$	$\frac{5}{2}^+ \oplus \frac{3}{2}^+$
	$1 \otimes \left(\frac{1}{2}\right)_A$	$\frac{3}{2}^+ \oplus \frac{1}{2}^+$
	$0 \otimes \left(\frac{1}{2}\right)_A$	$\frac{1}{2}^+$

Table 5.1: Summary of oscillator basis states for systems *ccb* and *bbc* [7].

oscillators: first the oscillator 12, then the oscillator 3(12). For example,

$$\psi_{1P_{+1}1S}(\vec{K}_{12}, \vec{Q}_3) \;=\; \psi_{1P_{+1}}(\vec{K}_{12})\psi_{1S}(\vec{Q}_3) \;, \tag{5.16}$$

where in $\psi_{1P_{+1}}(\vec{K}_{12})$ the parameter $\nu = \nu_{12} = 1/(2\nu_{12}\omega_{12})$, while in $\psi_{1S}(\vec{Q}_3)$ the parameter $\nu = \nu_{3(12)} = 1/(2\nu_{3(12)}\omega_{3(12)})$. I am interested only in states that can be built from the ground state $1S1S$, the first band $1P1S$, $1S1P$, and the second band $2S1S$, $1S2S$, $1D1S$, $1S1D$, $1P1P$.[1] Because the Coulomb potential is central it conserves the total orbital angular momentum and its projection on z axis. Therefore, it is advantageous to work with states that have these quantum numbers definite. The only states of interest that do not have definite orbital angular momentum are $1P1P$ states. The appropriate combinations of $1P$ states can be constructed using Clebsch-Gordan tables [21] and are denoted $1P1P_{L=0}$, $1P1P_{L=1}$ and $1P1P_{L=2}$. To produce states of physical particles orbital angular momentum has to be coupled with spin. Spins of three quarks combine to spin-3/2 quadruplet that is symmetric in all three quarks,

$$\left|+\frac{3}{2}\right\rangle \;=\; |\uparrow\uparrow\uparrow\rangle \;, \quad \left|+\frac{1}{2}\right\rangle = \ldots \;, \tag{5.17}$$

spin-1/2 doublet, called $(1/2)_S$, that is symmetric in the first two quarks,

$$\left|+\frac{1}{2}S\right\rangle \;=\; \sqrt{\frac{1}{6}}\,(\;\; 2|\uparrow\uparrow\downarrow\rangle - |\uparrow\downarrow\uparrow\rangle - |\downarrow\uparrow\uparrow\rangle) \;, \tag{5.18}$$

$$\left|-\frac{1}{2}S\right\rangle \;=\; \sqrt{\frac{1}{6}}\,(-2|\downarrow\downarrow\uparrow\rangle + |\downarrow\uparrow\downarrow\rangle + |\uparrow\downarrow\downarrow\rangle) \;, \tag{5.19}$$

and spin-1/2 doublet, called $(1/2)_A$, that is antisymmetric in the first two quarks,

$$\left|+\frac{1}{2}A\right\rangle \;=\; \sqrt{\frac{1}{2}}\,(|\uparrow\downarrow\uparrow\rangle - |\downarrow\uparrow\uparrow\rangle) \;, \tag{5.20}$$

$$\left|-\frac{1}{2}A\right\rangle \;=\; \sqrt{\frac{1}{2}}\,(|\uparrow\downarrow\downarrow\rangle - |\downarrow\uparrow\downarrow\rangle) \;. \tag{5.21}$$

The symmetry of the spin wave functions is important because for *bbc* and *ccb* systems the first two quarks are identical and combined spin-momentum wave function has to be symmetric in

[1] The term "band" makes sense only if $\omega_{12} = \omega_{3(12)}$, because then, *e.g.*, $1P1S$ and $1S1P$ states are degenerated and indeed form one "band."

States	Wave functions	Baryons
0ω	$1S1S \otimes \frac{3}{2}$	$\frac{3}{2}^+$
1ω	$1P1S \otimes \left(\frac{1}{2}\right)_A - 1S1P \otimes \left(\frac{1}{2}\right)_S$	$\frac{3}{2}^- \oplus \frac{1}{2}^-$
A	$2S1S_+ \otimes \frac{3}{2}$	$\frac{3}{2}^+$
B	$2S1S_- \otimes \left(\frac{1}{2}\right)_S - 1P1P_{L=0} \otimes \left(\frac{1}{2}\right)_A$	$\frac{1}{2}^+$
C	$1D1S_+ \otimes \frac{3}{2}$	$\frac{7}{2}^+ \oplus \frac{5}{2}^+ \oplus \frac{3}{2}^+ \oplus \frac{1}{2}^+$
D	$1D1S_- \otimes \left(\frac{1}{2}\right)_S - 1P1P_{L=2} \otimes \left(\frac{1}{2}\right)_A$	$\frac{5}{2}^+ \oplus \frac{3}{2}^+$

Table 5.2: Summary of states for systems *ccc* and *bbb* [7]. For example, $1D1S_- \otimes \left(\frac{1}{2}\right)_S$ means that we use $|1D_m1S\rangle_-$ states and $(1/2)_S$ spin states to obtain one of $J = 5/2$ or $J = 3/2$ states according to the rules of adding angular momenta, *i.e.*, using the Clebsch-Gordan coefficients. $1P1P_{L=2} \otimes \left(\frac{1}{2}\right)_A$ means that we combine $1P1P_{L=2}$ states and $(1/2)_A$ spin states to obtain a state with the same quantum numbers. We then subtract the latter from the former, as indicated in the table, and normalize the result to obtain the final expression, such as in Eqs. (A.10) or (A.11), where the states with $J = 5/2$, $J_z = +5/2$ and $J = 3/2$, $J_z = +3/2$ are written explicitly.

the first two quarks (because the color wave function is antisymmetric in the first two quarks). For example, $1P1S$ is antisymmetric in $\vec{K}_{12}$ and therefore can be combined only with $(1/2)_A$ to produce a 12-symmetric function. The complete list of states is provided in Table 5.1.

Baryons with three identical quarks require some extra care, because combined spin-momentum wave functions need to be completely symmetric with respect to permutations of quarks (the color wave function is completely antisymmetric). The problem is how to combine wave functions with different symmetry properties (symmetric and of mixed symmetry) to form a completely symmetric spin-momentum wave function [62]. The prescriptions for appropriate combinations of the wave functions are listed in Table 5.2. These prescriptions differ in sign from the prescriptions given, *e.g.*, in Refs. [63, 26], because our momentum $\vec{Q}_3$ is a momentum of quark 3 with respect to pair 12, instead of pair 12 with respect to quark 3. Table 5.2 uses also the following combinations of momentum wave functions (written in ket notation),

$$|2S1S\rangle_\pm = \frac{|2S1S\rangle \pm |2S1S\rangle}{\sqrt{2}} , \tag{5.22}$$

$$|1D_m1S\rangle_\pm = \frac{|1D_m1S\rangle \pm |1D_m1S\rangle}{\sqrt{2}} . \tag{5.23}$$

The symmetric baryon wave functions listed in Table 5.2 are given in App. A.

The masses of all baryons in our approximation scheme are already determined, because quark masses are fitted to reproduce quarkonia states, Eqs. (5.11) and (5.12), and we use the interpolating formula Eq. (5.2) that fixes the values of λ for each baryon and, hence, also the frequencies of harmonic oscillators in baryons. The analytic formulas for masses are given in App. C. Here, I present the resulting mass spectra of *bbb* and *ccc* bound states in Fig. 5.2, and mass spectra of *bbc* and *ccb* bound states in Fig. 5.3, assuming that $\Sigma = 0$. The collective plot of excitation spectra of all four systems is presented in Fig. 5.4.

Although experimentally triply-heavy baryons are difficult to produce and detect over the years there have been quite a few theoretical calculations we can compare with. Masses of *bbb* and *ccc* baryons agree rather well with model calculations [64, 65, 66, 67, 68, 69, 70, 71], quark-diquark [72] and hypercentral approximations [73, 74], bag models [75, 76, 77], Regge phenomenology [78, 79], sum rules [80, 81, 82, 83], pNRQCD [84], Dyson-Schwinger approach [85, 86] and lattice studies [87, 88, 89, 90, 91, 92, 93], where comparison is available. Especially interesting seems comparison with lattice calculations. Different lattice calculations report the *ccc* ground state mass from 4733 MeV to 4796 MeV, with mean value of 4768 MeV. Our result, 4797 MeV, differs by 29 MeV from the mean. The lattice results for the *bbb* ground state mass are 14366 MeV in Ref. [87], and 14371 MeV

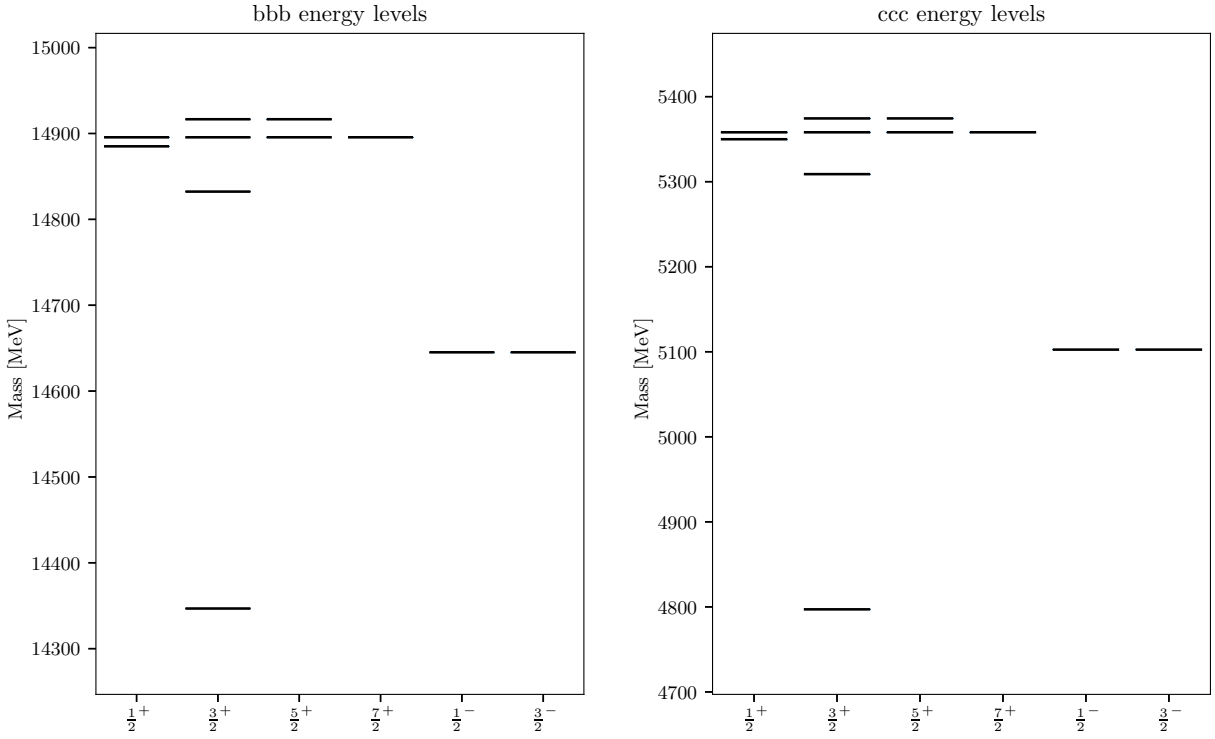

Figure 5.2: Single-flavor-baryon mass spectra

in Ref. [88], with uncertainties bigger than the difference between the two results. The simple mean is 14369 MeV and our result, 14346 MeV, differs by only 23 MeV from the mean. The splittings between the excited states and the ground state that we arrive at are generally smaller than the same lattice splittings, however, for *bbb* the difference is on the order of 10 %, while for *ccc* it is not greater than 20 %. It is worth noting that in a more accurate calculation that goes beyond first order of perturbation theory, which is presented in App. B the splittings between the ground and excited states grow – the splitting between state A and the ground state grows by about 7 % for *bbb* and by about 4 % for *ccc*. The most surprising result is a qualitative agreement between the splittings among A, B, C, D states and analogous states on the lattice. It is true that in the first order of perturbation theory the energies of the states that form the second band of harmonic oscillators in baryons split in a fixed ratio that is independent of the perturbing potential [63]. The energy differences $E_D - E_C$, $E_C - E_B$ and $E_B - E_A$ are in ratio $2:1:5$. Interestingly the author of Ref. [88] presents the results for these splittings with spin interactions switched off, and the ratio $2:1:5$ turns out to be a property of the spectrum computed in such a way (up to theoretical uncertainties). All of the above, suggests that RGPEP with gluon mass ansatz works very well for the single-flavor baryons, and encourages to perform more precise calculations.

For the mixed-flavor baryons the situation is a bit different than for single-flavor baryons. Here, the lattice results are limited to the ground states only. Assuming $\Sigma = 0$, see Eq. (4.79), the ground state of *bbc*, 11218 MeV, is very close to the lattice result 11229 MeV [87]. For this comparison I used the lattice result for the mass of Ω^*_{bbc}, which is a $3/2^+$ state, because its spin structure, $|\uparrow\uparrow\uparrow\rangle$, is similar to the spins structures of J/ψ and $\Upsilon(1S)$, $|\uparrow\uparrow\rangle$, which were used to fit free parameters of our calculation. Even if $\Sigma = 0$, the ground state of *ccb* is about 300 MeV higher than the lattice result. This may be due to large frequency of the oscillator between quarks 1 and 2 (between c quarks), which implies large zero-point energy. Such large frequency follows from large ratio λ_{ccb}/m_c and suggests that c quarks form a diquark, because it is hard to excite them in motion with respect to each other.

The situation is somewhat reversed for *bbc*, where ratio λ_{bbc}/m_b is small and the frequency ω_{12} is small. That would suggest a configuration in which c quark is between b quarks. The presence

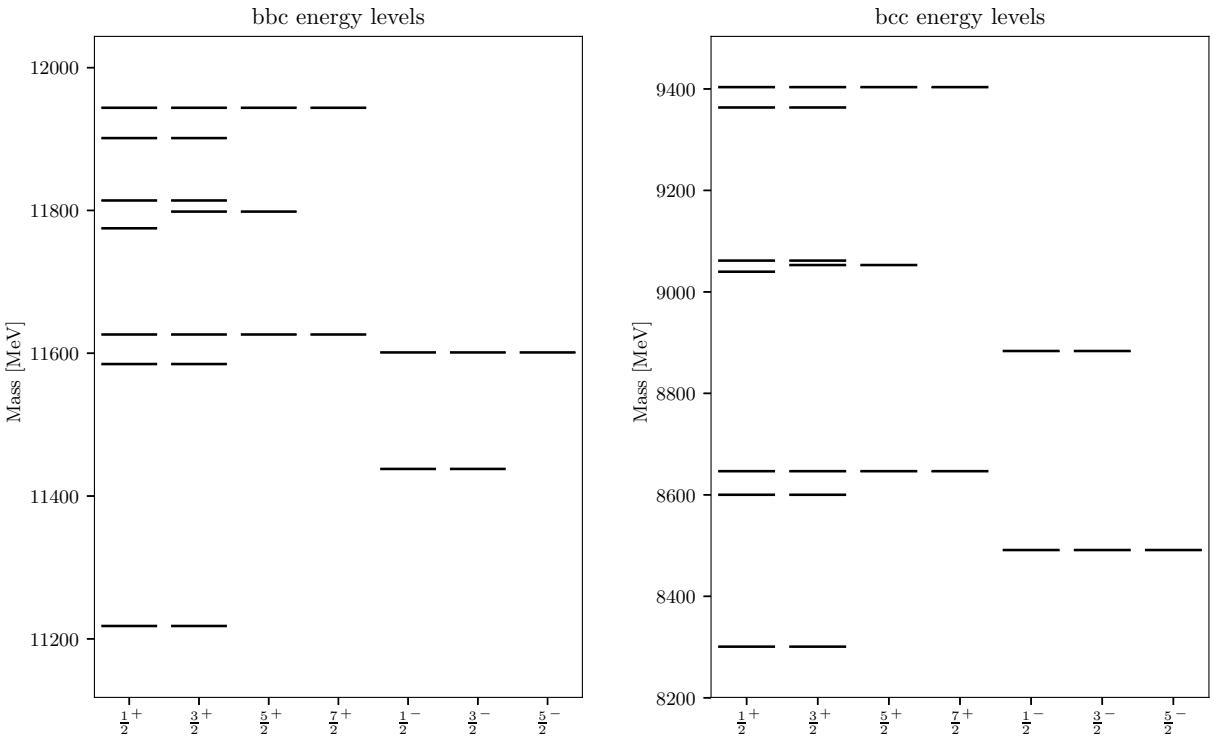

Figure 5.3: Mixed-flavor-baryon mass spectra

of the Σ term in the baryon eigenvalue equation also presents a problem because, it could shift the *bbc* ground state too high and it would make the *ccb* ground state even more distant from the lattice calculations.

The appearance of the Σ term may be due to insufficiency of the gluon mass ansatz. Apart from the gluon mass term, a lot of other terms may appear in Eq. (4.6) as a result of elimination of sectors with two and more gluons, and we do not know which of them may be important. The Σ-term may also be caused by the presence of two different scales in the problem, m_b and m_c with the bottom quark more than three times heavier than the charm quark. In such systems choosing only one λ may be not enough for the leading approximation of the Hamiltonian to correctly grasp the physics. For example, interactions in the Hamiltonian related to one quark might be best approximated by an interaction vertex that has λ_1, while interactions related to the other quark may be better approximated with $\lambda_2 \neq \lambda_1$. To resolve the problem more precise calculations of the effective Hamiltonian are needed, and are certainly encouraged by the results of *bbb* and *ccc* spectra. Note that the term Σ that in our approximate calculation differs form zero only when quarks differ in mass, could instead vanish in that case also if the RGPEP vertex form factor arguments in Eq. (4.79) obtained corrections that would scale t inversely to the mass squared. Such corrections may also change the harmonic oscillator frequencies, which depend on the form of interaction form factors. Therefore, the spectra of *ccb* and *bbc* systems should be treated with caution.

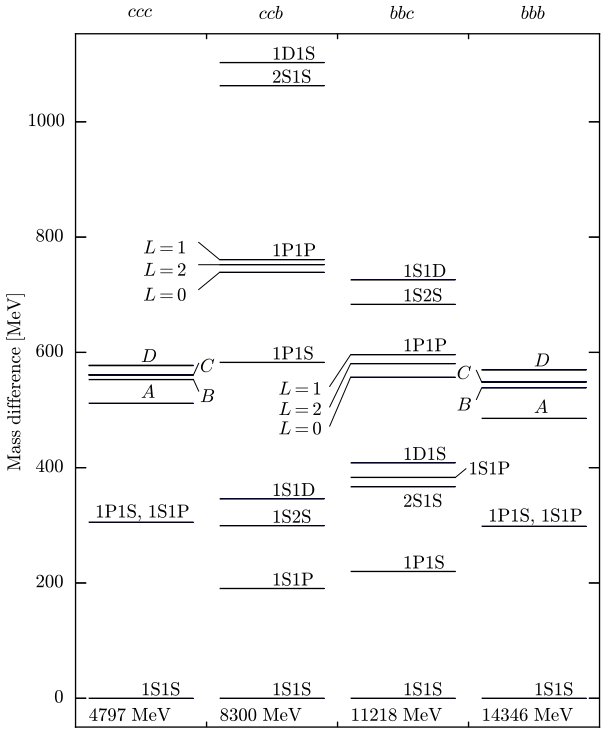

Figure 5.4: Qualitative picture of triply heavy baryon mass spectrum implied by the second-order RGPEP in heavy-flavor QCD and our gluon mass ansatz [7]. The figure shows excitations above the ground states $1S1S$, whose absolute masses are written at the bottom of each column. The *ccb* spectrum displays extraordinarily large mass excitation for states $1P1S$, $2S1S$ and $1D1S$. Such high excitations are associated with formation of *cc*-diquarks, bound by a harmonic force that is strong because the charmed quarks are much lighter than the bottom quarks. Much less pronounced splittings appear in the *bbc* baryons. See the text for further discussion.

Chapter 6

Form factors

6.1 Introduction

One of the nice features of studying hadrons in the FF of Hamiltonian dynamics is that as a result one obtains wave functions, which may be then used to compute various observables that in the instant form of Hamiltonian dynamics are hard to obtain because they require preservation of Lorentz symmetry. In this chapter I compute electromagnetic form factors of the mesons and baryons with spins equal one or smaller whose states have been approximately calculated in the previous chapters. Electromagnetic form factors of a hadron are defined as some scalar functions that parametrize relativistic scattering amplitude, *e.g.*, of an electron off that hadron. Because the scattering amplitude factorizes in the leading (one photon exchange) approximation into a part that depends only on the properties of the hadron and the rest, the form factors carry information about the electromagnetic properties of the hadron. For a scalar particle, the most important small-momentum-transfer quantities that characterize it are the charge and so-called mean square charge radius. For a spin-1/2 particle one can also define magnetic dipole moment, and for a particle of spin 1 there is also the electric quadrupole moment. In hadronic physics measurement of form factors is possible only for long-lived particles, like proton and neutron, or particles that are experimentally abundant, like pions. Form factors of heavy mesons and triply-heavy baryons that have not been observed yet may still be of interest because they provide intuition and estimates about the properties of these particles sizes that may be important,*e.g.*, in complex systems like dense hadronic matter.

From the theoretical point of view, FF calculation of form factors constitutes a challenge because it is sensitive to the direction distinguished by the the front. Due to nonrelativistic approximation for the relative motion of quarks only results for $Q \ll M$, where Q is the momentum transfer from electron to the hadron of mass M, may give reliable estimates for the form factors. Charge radii are defined in the limit $Q \to 0$, therefore, the estimates for hadron radii should be reliable. The construction of fully relativistic scattering amplitudes of bound states is a difficult task that has to account for the dynamics of the binding mechanism, and the issue has no definite solution that would apply in the case of QCD [94]. The results that I obtain here confirm that conviction, because the matrix elements that I compute do not have the expected, relativistic form. But the deviations I obtain are small. They are of the order of the binding energy divided by the mass of the hadron. At the level of approximations and assumptions we used in the previous chapter, one should expect violation of rotational symmetry. The smallness of obtained violation is an important result, because more accurate calculations using the same method, *i.e.*, including higher order terms in the RGPEP evolution and more Fock sectors in the bound state equations, may nearly restore rotational symmetry.

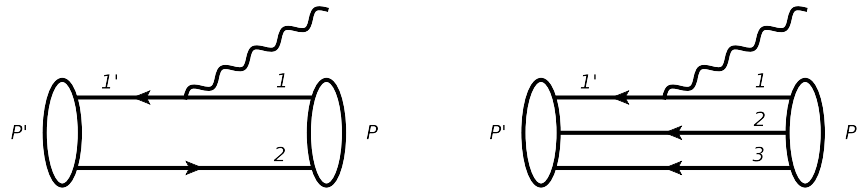

Figure 6.1: Illustration of the $J_{\sigma'\sigma}(P',P)$ matrix element for a quarkonium and a baryon.

6.2 Hadronic matrix elements of the electromagnetic current operator

Calculation of form factors starts with the computation of matrix elements of the electromagnetic current between states of a hadron with different momenta and, in general, in different spin states. I define,

$$J^\mu_{\sigma'\sigma}(P',P) \;\equiv\; \left\langle P',\sigma'\right|\, \hat{J}^\mu(0)\, \left|P,\sigma\right\rangle \;, \tag{6.1}$$

where the electromagnetic current operator at $x^\nu = 0$ is,

$$\hat{J}^\mu(0) \;=\; \sum_{f=b,c} Q_f \int_{1'1}\; j^\mu_{1'1}\; \delta_{c_1c_{1'}} b^\dagger_{f\,1'} b_{f\,1} + \sum_{f=b,c} Q_{\bar{f}} \int_{2'2}\; \bar{j}^\mu_{22'}\; \delta_{c_2c_{2'}} d^\dagger_{f\,2'} d_{f\,2} \;, \tag{6.2}$$

where Q_f is the electric charge of a quark of flavor f and $Q_{\bar{f}}$ is the electric charge of an antiquark of flavor f. For b and c quarks, $Q_b = -Q_{\bar{b}} = -1/3$ and $Q_c = -Q_{\bar{c}} = 2/3$. $|P,\sigma\rangle$ denotes a state of a hadron with momentum P and FF spin σ. One defines,

$$q^\mu \;=\; P'^\mu - P^\mu \;, \tag{6.3}$$

which to some extent may be interpreted as the momentum of the virtual photon exchanged between the electron and the hadron. It is advantageous to compute matrix elements with $q^+ = 0$ because then the calculations simplify. Since particles have positive plus component of the momentum, creation of pairs by the exchanged photon is impossible.

According to Eqs. (4.13) and (4.14),

$$|P,\sigma\rangle \;\approx\; \left(1 - \frac{1}{2}R^\dagger R\right)|l_{\rm eff}\rangle + R\,|l_{\rm eff}\rangle \;, \tag{6.4}$$

where R is order g_t. Similarly $|l'_{\rm eff}\rangle$ denotes the effective state in the lower sector with momentum P' and spin σ'. Therefore, up to terms order g_t^2,

$$J^\mu_{\sigma'\sigma}(P',P) \;=\; \langle l'_{\rm eff}|\left(\hat{J}^\mu + R^\dagger \hat{J}^\mu R - \frac{1}{2}R^\dagger R \hat{J}^\mu - \frac{1}{2}\hat{J}^\mu R^\dagger R\right)|l_{\rm eff}\rangle \;. \tag{6.5}$$

The terms that involve R cancel each other in the nonrelativistic limit, which one can verify by explicit calculation in the case of states η_b and η_c. Therefore, in the following I calculate only the leading term in Eq. (6.5), where only $\hat{J}^\mu$ is kept.

Formulas for quarkonia

The effective state $|l_{\rm eff}\rangle$ for quarkonium is given in Eq. (4.15). Here, I need to change a bit the notation: instead of $\psi_{tQ\bar{Q}\,\sigma_1\sigma_2}$ I write $\psi^\sigma_{\sigma_1\sigma_2}$, where σ is the spin projection of the hadron on z-axis. The electric charge of the quark is Q_q and the electric charge of the antiquark is $Q_{\bar{q}}$. Assuming that only quark is active (that $Q_{\bar{q}} = 0$),

$$J^\mu_{\sigma'\sigma}(P',P) \;=\; Q_q \sum_{\sigma_1\sigma_2\sigma_{1'}} \int [12] P^+ \tilde{\delta}_{12.P}\; \psi^{\sigma'}_{\sigma_{1'}\sigma_2}(x_1,\kappa_{1'/P'})^*\; \frac{j^\mu_{1'1}}{x_1}\; \psi^\sigma_{\sigma_1\sigma_2}(x_1,\kappa_{1/P}) \tag{6.6}$$

$$\;=\; Q_q \sum_{\sigma_1\sigma_2\sigma_{1'}} \int \frac{dx_1 d^2\kappa_1}{16\pi^3 x_1(1-x_1)}\; \psi^{\sigma'}_{\sigma_{1'}\sigma_2}(x_1,\kappa_{1'})^*\; \frac{j^\mu_{1'1}}{x_1}\; \psi^\sigma_{\sigma_1\sigma_2}(x_1,\kappa_1) \;, \tag{6.7}$$

where in the first line I explicitly indicated that for $\kappa_{1'}$ the parent momentum is P' and for $\kappa_{1'}$ the parent momentum is P. Longitudinal momenta do not change, $P'^+ = P^+$ and $p_{1'}^+ = p_1^+$ because $q^+ = 0$. The relative transverse momenta are related,

$$\kappa_{1'}^\perp = \kappa_1^\perp + (1-x_1)\, q^\perp \,. \tag{6.8}$$

In the nonrelativistic limit,

$$J^\mu_{\sigma'\sigma}(P',P) = Q_q \sum_{\sigma_1\sigma_2\sigma_{1'}} \int \frac{d^3k_{12}}{(2\pi)^3}\, \psi^{\sigma'}_{\sigma_{1'}\sigma_2}\left(\vec{k}_{1'2}\right)^* \, \frac{j^\mu_{1'1}}{\beta_1}\, \psi^{\sigma}_{\sigma_1\sigma_2}\left(\vec{k}_{12}\right) \,, \tag{6.9}$$

where

$$\vec{k}_{1'2} = \vec{k}_{12} + (1-\beta_1)\vec{q}\,, \tag{6.10}$$

$\vec{q} = (q^\perp, 0)$, and ψ is normalized according to Eq. (5.6). Including also the antiquark the current matrix element is,

$$\begin{aligned} J^\mu_{\sigma'\sigma}(P',P) &= Q_q \sum_{\sigma_1\sigma_2\sigma_{1'}} \int \frac{d^3k_{12}}{(2\pi)^3}\, \psi^{\sigma'}_{\sigma_{1'}\sigma_2}(\vec{k}_{1'2})^* \, \frac{j^\mu_{1'1}}{\beta_1}\, \psi^{\sigma}_{\sigma_1\sigma_2}(\vec{k}_{12}) \\ &+ Q_{\bar q} \sum_{\sigma_1\sigma_2\sigma_{1'}} \int \frac{d^3k_{12}}{(2\pi)^3}\, \psi^{\sigma'}_{\sigma_1\sigma_{2'}}(\vec{k}_{12'})^* \, \frac{\bar{j}^\mu_{22'}}{\beta_2}\, \psi^{\sigma}_{\sigma_1\sigma_2}(\vec{k}_{12}) \,, \end{aligned} \tag{6.11}$$

where

$$\vec{k}_{12'} = \vec{k}_{12} - (1-\beta_2)\vec{q}\,. \tag{6.12}$$

It is convenient to express the current as a matrix whose components are enumerated by spin indices, and to combine wave functions into a similar matrix (this way of writing current matrix elements is especially convenient for baryons, see below). The current matrix elements then take the form:

$$J^\mu_{\sigma'\sigma}(P',P) = Q_q \int \frac{d^3k}{(2\pi)^3}\, \frac{1}{\beta_1} \mathrm{Tr}(\rho_{1\sigma'\sigma}\, \mathbf{j}^\mu) + Q_{\bar q} \int \frac{d^3k}{(2\pi)^3}\, \frac{1}{\beta_2} \mathrm{Tr}(\rho_{2\sigma'\sigma}\, \bar{\mathbf{j}}^\mu) \,, \tag{6.13}$$

where

$$\mathbf{j}^+ = \begin{pmatrix} 2p_1^+ & 0 \\ 0 & 2p_1^+ \end{pmatrix} \,, \tag{6.14}$$

$$\mathbf{j}^1 = \begin{pmatrix} p_1^1 + p_{1'}^1 - iq^2 & 0 \\ 0 & p_1^1 + p_{1'}^1 + iq^2 \end{pmatrix} \,, \tag{6.15}$$

$$\mathbf{j}^2 = \begin{pmatrix} p_2^2 + p_{2'}^2 + iq^1 & 0 \\ 0 & p_2^2 + p_{2'}^2 - iq^1 \end{pmatrix} \,, \tag{6.16}$$

and

$$[\rho_{1\sigma'\sigma}]_{\sigma_1\sigma_{1'}} = \sum_{\sigma_2} \psi^{\sigma}_{\sigma_1\sigma_2}(\vec{k}_{12}) \psi^{\sigma'*}_{\sigma_{1'}\sigma_2}(\vec{k}_{1'2}) \,, \tag{6.17}$$

$$[\rho_{2\sigma'\sigma}]_{\sigma_2\sigma_{2'}} = \sum_{\sigma_1} \psi^{\sigma}_{\sigma_1\sigma_2}(\vec{k}_{12}) \psi^{\sigma'*}_{\sigma_1\sigma_{2'}}(\vec{k}_{12'}) \,. \tag{6.18}$$

Formulas for baryons

For QQQ' baryons the effective states are given in Eq. (4.26). I change notation: instead of $\psi_{tQQQ\sigma_1\sigma_2\sigma_3}$ I write $\psi^{\sigma}_{\sigma_1\sigma_2\sigma_3}$, where σ is the spin projection of the baryon on z-axis. The electric charges of the quarks Q and Q' are Q_q and $Q_{q'}$, respectively. The current matrix element is the sum of three terms – one for interaction with each of the three quarks. The first two quarks are indistinguishable, therefore, two terms are identical,

$$\begin{aligned} J^{\mu}_{\sigma'\sigma}(P',P) &= 2Q_q \sum_{\sigma_1\sigma_2\sigma_3\sigma_{1'}} \int [123]\ P^+\tilde{\delta}_{123.P}\ \psi^{\sigma'*}_{\sigma_{1'}\sigma_2\sigma_3}(1'23)\ \frac{j^{\mu}_{1'1}}{x_1}\ \psi^{\sigma}_{\sigma_1\sigma_2\sigma_3}(123) \\ &+ Q_{q'} \sum_{\sigma_1\sigma_2\sigma_3\sigma_{3'}} \int [123]\ P^+\tilde{\delta}_{123.P}\ \psi^{\sigma'*}_{\sigma_1\sigma_2\sigma_{3'}}(123')\ \frac{j^{\mu}_{3'3}}{x_3}\ \psi^{\sigma}_{\sigma_1\sigma_2\sigma_3}(123)\ , \end{aligned} \tag{6.19}$$

where

$$\kappa^{\perp}_{1'} = \kappa^{\perp}_1 + (1-x_1)\ q^{\perp}\ , \tag{6.20}$$

$$\kappa^{\perp}_{3'} = \kappa^{\perp}_3 + (1-x_3)\ q^{\perp}\ . \tag{6.21}$$

In the nonrelativistic limit,

$$\begin{aligned} J^{\mu}_{\sigma'\sigma}(P',P) &= 2Q_q \sum_{\sigma_1\sigma_2\sigma_3\sigma_{1'}} \int \frac{d^3K_{12}}{(2\pi)^3}\frac{d^3Q_3}{(2\pi)^3}\ \psi^{\sigma'*}_{\sigma_{1'}\sigma_2\sigma_3}(\vec{K}_{1'2},\vec{Q}'_3)\ \frac{j^{\mu}_{1'1}}{\beta_1}\ \psi^{\sigma}_{\sigma_1\sigma_2\sigma_3}(\vec{K}_{12},\vec{Q}_3) \\ &+ Q_{q'} \sum_{\sigma_1\sigma_2\sigma_3\sigma_{3'}} \int \frac{d^3K_{12}}{(2\pi)^3}\frac{d^3Q_3}{(2\pi)^3}\ \psi^{\sigma'*}_{\sigma_1\sigma_2\sigma_{3'}}(\vec{K}_{12},\vec{Q}_{3'})\ \frac{j^{\mu}_{3'3}}{\beta_3}\ \psi^{\sigma}_{\sigma_1\sigma_2\sigma_3}(\vec{K}_{12},\vec{Q}_3)\ , \end{aligned} \tag{6.22}$$

where

$$\vec{K}_{1'2} = \vec{K}_{12} + \frac{1}{2}\vec{q}\ , \tag{6.23}$$

$$\vec{Q}'_3 = \vec{Q}_3 - \beta_3\vec{q}\ , \tag{6.24}$$

$$\vec{Q}_{3'} = \vec{Q}_3 + (1-\beta_3)\vec{q}\ , \tag{6.25}$$

$\vec{q}=(q^{\perp},0)$, and ψ is normalized in such a way that $\int \frac{d^3K_{12}}{(2\pi)^3}\frac{d^3Q_3}{(2\pi)^3}\ \psi^{\sigma*}_{\sigma_1\sigma_2\sigma_3}\ \psi^{\sigma}_{\sigma_1\sigma_2\sigma_3} = 1$.

Equation (6.22) contains a lot of spin indices. To write it in a simple form I write currents $j^{\mu}_{1'1}$ and $j^{\mu}_{3'3}$ as matrices $\mathbf{j^{\mu}_1}$ and $\mathbf{j^{\mu}_3}$ whose components are enumerated with spin indices. I define similar matrices $\rho_{1\sigma'\sigma}$ and $\rho_{3\sigma'\sigma}$ constructed from the wave functions.

$$J^{\mu}_{\sigma'\sigma}(P',P) = 2Q_q \int \frac{d^3k}{(2\pi)^3}\ \frac{1}{\beta_1}\mathrm{Tr}\ \rho_{1\sigma'\sigma}\ \mathbf{j}^{\mu}_1 + Q_{q'}\int \frac{d^3k}{(2\pi)^3}\ \frac{1}{\beta_3}\mathrm{Tr}\ \rho_{3\sigma'\sigma}\ \mathbf{j}^{\mu}_3\ , \tag{6.26}$$

where

$$[\rho_{1\sigma'\sigma}]_{\sigma_1\sigma_{1'}} = \sum_{\sigma_2\sigma_3} \psi^{\sigma}_{\sigma_1\sigma_2\sigma_3}(\vec{K}_{12},\vec{Q}_3)\psi^{\sigma'*}_{\sigma_{1'}\sigma_2\sigma_3}(\vec{K}_{1'2},\vec{Q}'_3)\ , \tag{6.27}$$

$$[\rho_{3\sigma'\sigma}]_{\sigma_3\sigma_{3'}} = \sum_{\sigma_1\sigma_2} \psi^{\sigma}_{\sigma_1\sigma_2\sigma_3}(K_{12},\vec{Q}_3)\psi^{\sigma'*}_{\sigma_1\sigma_2\sigma_{3'}}(\vec{K}_{12},\vec{Q}_{3'})\ , \tag{6.28}$$

and

$$\mathbf{j}^{+}_1 = \begin{pmatrix} 2p^+_1 & 0 \\ 0 & 2p^+_1 \end{pmatrix}\ , \tag{6.29}$$

$$\mathbf{j}^{1}_1 = \begin{pmatrix} p^1_1 + p^1_{1'} - iq^2 & 0 \\ 0 & p^1_1 + p^1_{1'} + iq^2 \end{pmatrix}\ , \tag{6.30}$$

$$\mathbf{j}^{2}_1 = \begin{pmatrix} p^2_1 + p^2_{1'} + iq^1 & 0 \\ 0 & p^2_1 + p^2_{1'} - iq^1 \end{pmatrix}\ , \tag{6.31}$$

$$\mathbf{j}_3^+ = \begin{pmatrix} 2p_3^+ & 0 \\ 0 & 2p_3^+ \end{pmatrix} , \tag{6.32}$$

$$\mathbf{j}_3^1 = \begin{pmatrix} p_3^1 + p_{3'}^1 - iq^2 & 0 \\ 0 & p_3^1 + p_{3'}^1 + iq^2 \end{pmatrix} , \tag{6.33}$$

$$\mathbf{j}_3^2 = \begin{pmatrix} p_3^2 + p_{3'}^2 + iq^1 & 0 \\ 0 & p_3^2 + p_{3'}^2 - iq^1 \end{pmatrix} . \tag{6.34}$$

For baryons composed of three identical quarks Eq. (6.26) is valid, however, since the quarks are indistinguishable, instead of two terms it is easier to compute just the second one and multiply the result by three.

6.3 Definitions of form factors, charge radii and momenta

6.3.1 Spin 0

For a spinless particle the situation is most simple. There is only one current matrix element (with $\sigma' = \sigma = 0$), whose form expected from relativistic covariance is,

$$J^\mu(P', P) = (P^\mu + P'^\mu)\, F(Q^2) , \tag{6.35}$$

where spins σ' and σ are omitted from the notation. The sole form factor F depends on the square of the transferred four-momentum,

$$Q^2 = -q^\mu q_\mu = (q^\perp)^2 , \tag{6.36}$$

where the second equality follows from $q^+ = 0$. The form factor is normalized to the charge of the particle, $F(0) = Q_{q\bar{q}}$, and is used to define mean charge radius squared,

$$r^2 = -\frac{1}{Q_{q\bar{q}}} 6 \frac{dF}{dQ^2}(0) . \tag{6.37}$$

That definition, however, does not apply to charmonia and bottomonia because they have zero charge. Moreover, the form factors computed using Eq. (6.13) are zero, because the contribution from the quark is cancelled by the contribution from the antiquark. Therefore, it is customary to separate contributions from the quark and from the antiquark,

$$F(Q^2) = Q_{f_1} F^{(1)}(Q^2) + Q_{\bar{f}_2} F^{(2)}(Q^2) , \tag{6.38}$$

where 1 and 2 denote the quark and the antiquark, *cf.* Fig. 6.1. These new form factors are normalized to unity, $F^{(1)}(0) = F^{(2)}(0) = 1$ and I define mean radius squared related to the constituent i,

$$r_i^2 = -6 \frac{dF^{(i)}}{dQ^2}(0) . \tag{6.39}$$

6.3.2 Spin $\frac{1}{2}$

Spin-$\frac{1}{2}$ particle possesses two form factors, F_1 called the Dirac form factor and F_2 called the Pauli form factor, that are related to the current matrix elements in the following way,

$$J^\mu_{\sigma'\sigma} = \bar{u}_{\sigma'}(P') \left[\gamma^\mu F_1(Q^2) + \frac{i\sigma^{\mu\nu} q_\nu}{2M} F_2(Q^2) \right] u_\sigma(P) , \tag{6.40}$$

where M is the mass of the particle. Special combinations of these form factors are called Sachs electric, G_E, and magnetic, G_M, form factors, and are defined as follows,

$$G_E(Q^2) = F_1(Q^2) - \tau F_2(Q^2) , \tag{6.41}$$

$$G_M(Q^2) = F_1(Q^2) + F_2(Q^2) , \tag{6.42}$$

where

$$\tau = \frac{Q^2}{4M^2} . \tag{6.43}$$

The normalizations of these form factors are,

$$G_E(0) = F_1(0) = Q_{qqq} , \tag{6.44}$$
$$G_M(0) = \mu_{qqq} , \tag{6.45}$$

where Q_{qqq} is the charge of the particle (baryon in my case) and μ_{qqq} is the magnetic moment of the particle. Moreover, the charge radius is,

$$r^2 = -\frac{6}{G_E(0)}\frac{dG_E}{dQ^2}(0) . \tag{6.46}$$

Similarly as for the scalar particles it is convenient to separate contributions from each of the quarks,

$$F_i = 2Q_{f_1}F_i^{(1)} + Q_{f_3}F_i^{(3)} , \tag{6.47}$$
$$G_I = 2Q_{f_1}G_I^{(1)} + Q_{f_3}G_I^{(3)} , \tag{6.48}$$

where $i = 1, 2$ and $I = E, M$. The terms on the right hand side represent contributions from the quark 1 (multiplied by two, because quark 2 is identical with 1) and from the quark 3. The normalization is $F_1^{(1)}(0) = F_1^{(3)}(0) = 1$. The charge radii related to each of the quarks are,

$$r_1^2 = -6\frac{dG_E^{(1)}}{dQ^2}(0) , \tag{6.49}$$

$$r_3^2 = -6\frac{dG_E^{(3)}}{dQ^2}(0) . \tag{6.50}$$

I find it good for practical purposes to write the collection of $J^\mu_{\sigma'\sigma}$ matrix elements in a form of four 2×2 matrices for four values of μ where the elements of the matrices are,

$$J^\mu = \begin{bmatrix} J^\mu_{\uparrow\uparrow} & J^\mu_{\uparrow\downarrow} \\ J^\mu_{\downarrow\uparrow} & J^\mu_{\downarrow\downarrow} \end{bmatrix} . \tag{6.51}$$

For $q^+ = 0$ the form of these matrices expected from Eq. (6.40) is,

$$J^+ = 2P^+ \begin{bmatrix} F_1 & -\frac{q^{(-)}}{\sqrt{2}M}F_2 \\ -\frac{q^{(+)}}{\sqrt{2}M}F_2 & F_1 \end{bmatrix} , \tag{6.52}$$

$$J^1 = (P^1 + P'^1)\frac{J^+}{2P^+} - iq^2(F_1 + F_2)\begin{bmatrix} 1 & 0 \\ 0 & -1 \end{bmatrix} , \tag{6.53}$$

$$J^2 = (P^2 + P'^2)\frac{J^+}{2P^+} + iq^1(F_1 + F_2)\begin{bmatrix} 1 & 0 \\ 0 & -1 \end{bmatrix} , \tag{6.54}$$

where[1]

$$q^{(\pm)} = \frac{\mp q^1 - iq^2}{\sqrt{2}} . \tag{6.55}$$

[1]The idea for that particular definition of $q^{(\pm)}$ comes from the standard form of spherical harmonics, which for $l = 1$ may we written in the following form,

$$Y_{1,\pm1}(\hat{p}) = \sqrt{\frac{3}{4\pi}}\frac{p^{(\pm)}}{|\vec{p}|} , \quad Y_{1,0}(\hat{p}) = \sqrt{\frac{3}{4\pi}}\frac{p^3}{|\vec{p}|} .$$

The minus current matrix J^- is irrelevant, because the current operator $\hat{J}^-$ does not enter the Hamiltonian of QCD coupled to QED (due to the choice of gauge $A^+ = 0$). Again, it is convenient to separate quarks' contributions,

$$J^\mu = 2Q_{f_1} J_1^\mu + Q_{f_3} J_3^\mu \ . \tag{6.56}$$

6.3.3 Spin 1

For spin-1 particle there are three form factors that are related to the current matrix elements in the following way,

$$\begin{aligned} J^\mu_{\sigma'\sigma}(P',P) &= -(P^\mu + P'^\mu)(\varepsilon'^* \cdot \varepsilon) F_1(Q^2) \\ &+ \left[\varepsilon'^{\mu *}(\varepsilon \cdot q) - \varepsilon^\mu(\varepsilon'^* \cdot q)\right] F_2(Q^2) \\ &+ (P^\mu + P'^\mu)\frac{(\varepsilon \cdot q)(\varepsilon'^* \cdot q)}{2M^2} F_3(Q^2) \ , \end{aligned} \tag{6.57}$$

where $\varepsilon = \varepsilon_\sigma$ denotes the polarization vector of spin-1 particle with momentum P and spin σ, and $\varepsilon' = \varepsilon_{\sigma'}$ is the polarization vector of particle with momentum P' and spin σ'. The $\sigma = \pm 1$ polarization vectors are the same as those given in Eq. (2.58), while ε_0^μ may be obtained from the conditions, $\varepsilon_0 \cdot P = 0$, $\varepsilon_0 \cdot \varepsilon_{\pm 1} = 0$, $\varepsilon_0 \cdot \varepsilon_0 = -1$ and $\varepsilon_0^+ > 0$. One then defines charge, magnetic dipole and electric quadrupole form factors in the following way [95],

$$G_C(Q^2) = F_1(Q^2) + \frac{2}{3}\tau G_Q(Q^2) \ , \tag{6.58}$$

$$G_M(Q^2) = F_2(Q^2) \ , \tag{6.59}$$

$$G_Q(Q^2) = F_1(Q^2) - F_2(Q^2) + (1+\tau)F_3(Q^2) \ . \tag{6.60}$$

Charge radius squared, magnetic dipole moment, and electric quadrupole moment are,

$$r^2 = -\frac{6}{G_C(0)}\frac{dG_C}{dQ^2}(0) \ , \tag{6.61}$$

$$\mu = G_M(0) \ , \tag{6.62}$$

$$\mathcal{Q} = G_Q(0) \ . \tag{6.63}$$

The form factors and the mean charge radii squared are then separated according to the same pattern that was used for spin-0 and spin-1/2 particles. Spin-1 particles considered here are quark-antiquark bound states, hence,

$$F_i = Q_{f_1} F_i^{(1)} + Q_{\bar{f}_2} F_i^{(2)} \ , \tag{6.64}$$

$$G_I = Q_{f_1} G_I^{(1)} + Q_{\bar{f}_2} G_I^{(2)} \ , \tag{6.65}$$

$$r_j^2 = -6\frac{dG_C^{(j)}}{dQ^2}(0) \ , \tag{6.66}$$

where $i = 1,2,3$ and $I = C, M, Q$, $j = 1,2$ and the normalization is $F_1^{(1)}(0) = F_1^{(2)}(0) = 1$.

Similarly as for spin-$\frac{1}{2}$ I define matrices,

$$J^\mu = \begin{bmatrix} J_{++} & J_{+0} & J_{+-} \\ J_{0+} & J_{00} & J_{0-} \\ J_{-+} & J_{-0} & J_{--} \end{bmatrix} \ , \tag{6.67}$$

where $\pm$ means $\sigma = \pm 1$. The form that follows from Eq. (6.57 is,

$$J^+ = 2P^+ \begin{bmatrix} F_1+\tau F_3 & \frac{q^{(-)}}{2M}\widetilde{F} & -\frac{[q^{(-)}]^2}{2M^2}F_3 \\ \frac{q^{(+)}}{2M}\widetilde{F} & (1-2\tau)F_1+2\tau F_2-2\tau^2 F_3 & \frac{q^{(-)}}{2M}\widetilde{F} \\ -\frac{[q^{(+)}]^2}{2M^2}F_3 & \frac{q^{(+)}}{2M}\widetilde{F} & F_1+\tau F_3 \end{bmatrix} , \quad (6.68)$$

$$J^1 = (P^1+P'^1)\frac{J^+}{2P^+} - iq^2 F_2 \begin{bmatrix} 1 & \frac{q^{(-)}}{2M} & 0 \\ \frac{q^{(+)}}{2M} & 0 & -\frac{q^{(-)}}{2M} \\ 0 & -\frac{q^{(+)}}{2M} & -1 \end{bmatrix} , \quad (6.69)$$

$$J^2 = (P^2+P'^2)\frac{J^+}{2P^+} + iq^1 F_2 \begin{bmatrix} 1 & \frac{q^{(-)}}{2M} & 0 \\ \frac{q^{(+)}}{2M} & 0 & -\frac{q^{(-)}}{2M} \\ 0 & -\frac{q^{(+)}}{2M} & -1 \end{bmatrix} , \quad (6.70)$$

where $q^+ = 0$ is assumed and

$$\widetilde{F} = 2F_1 - F_2 + 2\tau F_3 . \quad (6.71)$$

The matrices separate into sum of quark and antiquark contributions,

$$J^\mu = Q_{f_1} J_1^\mu + Q_{\bar{f}_2} J_2^\mu . \quad (6.72)$$

6.4 Mesons

6.4.1 Wave functions

To compute the electromagnetic current matrix elements I need to use wave functions of the hadronic states. Wave functions of mesons that were discussed in Chapter 5 are constructed from harmonic oscillator eigenstates, Eq. 5.4, and spin wave functions added according to the rules of adding states with definite angular momenta to obtain spin-0 states η and χ_0 and spin-1 states Υ or ψ. Since we neglected spin-dependent interactions, the spin structure of a state did not influence the energy of the state. For the calculation of magnetic properties of particles, however, such approximation is insufficient. Note, for example, that for a slowly-moving electron, described using Dirac equation with an external magnetic field, one needs to take into account the small components of the spinor to obtain the magnetic dipole interaction term [96]. To obtain corrections necessary to fix the problem with magnetic observables it is desirable to perform more precise calculations that involve fourth order Hamiltonian terms in Eq. (3.32). However, for the purpose of illustration of the method and its capabilities, which is the intended purpose of this thesis, it is sufficient to estimate the corrections using free spinors. It is not very difficult to propose the form of corrections. They have to be written using relativistic objects, spinors defined in Eqs. (2.50) and (2.51), and the expressions should have the correct properties under action of discrete symmetries. Below, I list the wave functions of mesons that include the leading relativistic corrections.

For pseudoscalar quarkonia, $\eta(nS)$, the form of the wave function that includes relativistic corrections is,

$$\psi_{\sigma_1\sigma_2}(\vec{k}) = \mathcal{N}_{PS}\ \bar{u}_1\gamma^5 v_2\ \psi_{nS}(\vec{k}) = \left[\frac{|\uparrow\downarrow\rangle - |\downarrow\uparrow\rangle}{\sqrt{2}} - \frac{k^{(-)}}{2\mu_{12}}|\uparrow\uparrow\rangle + \frac{k^{(+)}}{2\mu_{12}}|\downarrow\downarrow\rangle\right]\ \psi_{nS}(\vec{k}) , \quad (6.73)$$

where $\mathcal{N}_{PS} = -1/\sqrt{8m_1m_2}$ is the proper normalization constant and, for example, $|\uparrow\downarrow\rangle$ means that $\sigma_1 = +1/2$ and $\sigma_2 = -1/2$. Neglecting the terms that are linear in momenta, $\psi_{\sigma_1\sigma_2}(\vec{k})$ reduces to spin singlet wave function times momentum wave function, as required. Moreover,

$$\rho_1 = \frac{1}{2}\begin{pmatrix} 1 & \frac{k^{(-)}-k'^{(-)}}{\sqrt{2}\mu_{12}} \\ \frac{k^{(+)}-k'^{(+)}}{\sqrt{2}\mu_{12}} & 1 \end{pmatrix} \psi_{nS}(\vec{k})\psi^*_{nS}(\vec{k'}) . \quad (6.74)$$

Only diagonal terms matter when one computes the trace in Eq. (6.13), hence from now on I will neglect off-diagonal terms in matrices ρ. The fact that the diagonal of ρ_1 is not corrected with terms linear in momenta means that the form factor F is also unaltered. It is not surprising because the purpose of correcting nonrelativistic wave functions was to properly describe magnetic effects, but spin-0 particles do not have magnetic moments.

For scalar quarkonium, $\chi_0(1P)$,

$$\psi^{\sigma}_{\sigma_1\sigma_2}(\vec{k}\,) \;=\; \mathcal{N}_S \bar{u}_1 v_2 \; e^{-\nu\vec{k}^2} \;=\; \frac{1}{\sqrt{3}}\left[|\uparrow\uparrow\rangle\;\psi_{1P_{-1}}(\vec{k}\,) - \frac{|\uparrow\downarrow\rangle + |\downarrow\uparrow\rangle}{\sqrt{2}}\;\psi_{1P_0}(\vec{k}\,) + |\downarrow\downarrow\rangle\;\psi_{1P_{+1}}(\vec{k}\,)\right] , \tag{6.75}$$

where $\mathcal{N}_S = -\sqrt{\beta_1\beta_2/(8\pi)}N_{01}$ and N_{01} is given in Eq. (5.5). The terms linear in momenta that come from $\bar{u}_1 v_2$ produce the desired momentum wave functions of fixed L and L^z, that is $\psi_{1P_{\pm1}}(\vec{k}\,)$ and $\psi_{1P_0}(\vec{k}\,)$. It is worth noting that Eq. (6.75) is exact, *i.e.*, has no corrections of higher powers of momentum, which is an effect of the choice of nonrelativistic momenta Eqs. (4.44) and (4.45). Using wave function of Eq. (6.75) I get,

$$\rho_1 \;=\; \frac{1}{3}\begin{pmatrix} \psi_{1P_{-1}}\psi^*_{1P_{-1}} + \frac{1}{2}\psi_{1P_0}\psi^*_{1P_0} & \cdot \\ \cdot & \psi_{1P_{+1}}\psi^*_{1P_{+1}} + \frac{1}{2}\psi_{1P_0}\psi^*_{1P_0} \end{pmatrix} , \tag{6.76}$$

where ψ_{1P_m} depend on $\vec{k}$ while $\psi^*_{1P_m}$ depend on $\vec{k}'$.

For vector bottomonium, $\Upsilon(nS)$, or vector charmonium, $\psi(nS)$, the wave function is,

$$\psi^{\sigma}_{\sigma_1\sigma_2}(\vec{k}\,) \;=\; \mathcal{N}_V \;\bar{u}_1\gamma^\mu v_2 \varepsilon_{\sigma\mu}\;\psi_{nS}(\vec{k}\,) , \tag{6.77}$$

where $\mathcal{N}_V = 1/\sqrt{8m_1m_2}$, and ε^μ_σ is the polarization vector of the hadron. The $\sigma = 0$ vector should have $\varepsilon^3_0 = 1$ in *the rest frame of the hadron* (where $P^+ = M$). It turns out that this leads to problems, because $\bar{u}_1\gamma^\mu v_2\varepsilon_{\sigma\mu}$ does not reduce to the expected spin-1 triplet wave function. To be more precise it reduces to spin-1 triplet only in the limit of hadron mass equaling the mass of the quarks, $M \to m_1 + m_2$, or in other words if the binding energy is vanishingly small. To solve this problem I use ε^μ_σ that has $\varepsilon^3_0 = 1$ in *the rest frame of the quarks* (where $P^+ = m_1 + m_2$). The other polarization vectors, $\varepsilon^\mu_{\pm1}$, are independent of the frame and present no problem. Therefore,

$$\psi^{+1}_{\sigma_1\sigma_2}(\vec{k}\,) \;=\; \psi_{nS}(\vec{k}\,)\left[|\uparrow\uparrow\rangle - \frac{k^{(+)}}{\sqrt{2}m_2}|\uparrow\downarrow\rangle + \frac{k^{(+)}}{\sqrt{2}m_1}|\downarrow\uparrow\rangle\right] , \tag{6.78}$$

$$\psi^{0}_{\sigma_1\sigma_2}(\vec{k}\,) \;=\; \psi_{nS}(\vec{k}\,)\left[\frac{|\uparrow\downarrow\rangle + |\downarrow\uparrow\rangle}{\sqrt{2}} + \left(\frac{k^{(-)}}{2m_1} - \frac{k^{(-)}}{2m_2}\right)|\uparrow\uparrow\rangle + \left(\frac{k^{(+)}}{2m_1} - \frac{k^{(+)}}{2m_2}\right)|\downarrow\downarrow\rangle\right] , \tag{6.79}$$

$$\psi^{-1}_{\sigma_1\sigma_2}(\vec{k}\,) \;=\; \psi_{nS}(\vec{k}\,)\left[|\downarrow\downarrow\rangle + \frac{k^{(-)}}{\sqrt{2}m_1}|\uparrow\downarrow\rangle - \frac{k^{(-)}}{\sqrt{2}m_2}|\downarrow\uparrow\rangle\right] . \tag{6.80}$$

There are nine ρ_1 matrices, one for each combination of σ' and σ:

$$\rho_{1,+1,+1} \;=\; \psi_{nS}(\vec{k})\psi^*_{nS}(\vec{k}')\begin{pmatrix} 1 & \cdot \\ \cdot & 0 \end{pmatrix} , \tag{6.81}$$

$$\rho_{1,+1,0} \;=\; \psi_{nS}(\vec{k})\psi^*_{nS}(\vec{k}')\begin{pmatrix} \frac{k^{(-)}}{2m_1} + \frac{k'^{(-)}-k^{(-)}}{2m_2} & \cdot \\ \cdot & -\frac{k'^{(-)}}{2m_1} \end{pmatrix} , \tag{6.82}$$

$$\rho_{1,+1,-1} \;=\; \psi_{nS}(\vec{k})\psi^*_{nS}(\vec{k}')\begin{pmatrix} 0 & \cdot \\ \cdot & 0 \end{pmatrix} , \tag{6.83}$$

$$\rho_{1,0,+1} \;=\; \psi_{nS}(\vec{k})\psi^*_{nS}(\vec{k}')\begin{pmatrix} -\frac{k'^{(+)}}{2m_1} + \frac{k'^{(+)}-k^{(+)}}{2m_2} & \cdot \\ \cdot & +\frac{k^{(+)}}{2m_1} \end{pmatrix} , \tag{6.84}$$

$$\rho_{1,0,0} \;=\; \psi_{nS}(\vec{k})\psi^*_{nS}(\vec{k}')\begin{pmatrix} \frac{1}{2} & \cdot \\ \cdot & \frac{1}{2} \end{pmatrix} , \tag{6.85}$$

$$\rho_{1,0,-1} = \psi_{nS}(\vec{k})\psi^*_{nS}(\vec{k}') \begin{pmatrix} \frac{k^{(-)}}{2m_1} & \cdot \\ \cdot & -\frac{k'^{(-)}}{2m_1} - \frac{k^{(-)}-k'^{(-)}}{2m_2} \end{pmatrix} , \quad (6.86)$$

$$\rho_{1,-1,+1} = \psi_{nS}(\vec{k})\psi^*_{nS}(\vec{k}') \begin{pmatrix} 0 & \cdot \\ \cdot & 0 \end{pmatrix} , \quad (6.87)$$

$$\rho_{1,-1,0} = \psi_{nS}(\vec{k})\psi^*_{nS}(\vec{k}') \begin{pmatrix} -\frac{k^{(+)}}{2m_1} & \cdot \\ \cdot & +\frac{k^{(+)}}{2m_1} + \frac{k'^{(+)}-k^{(+)}}{2m_2} \end{pmatrix} , \quad (6.88)$$

$$\rho_{1,-1,-1} = \psi_{nS}(\vec{k})\psi^*_{nS}(\vec{k}') \begin{pmatrix} 0 & \cdot \\ \cdot & 1 \end{pmatrix} . \quad (6.89)$$

6.4.2 Form factors

Using the formulas provided in Sec. 6.4.1 I compute the hadronic matrix elements given in Eq. (6.13) neglecting the contribution from the antiquark. Therefore, I present the results for form factors $F^{(1)}$ and $F_i^{(1)}$, and matrices J_1^μ, *cf.* Secs. 6.3.1 and 6.3.3. The contributions from the antiquark are easily obtained by replacing index 1 with index 2.

For pseudoscalar and scalar mesons the current matrix elements reproduce Eq. (6.35) with the following form factors,

$$\eta(1S): \quad F^{(1)}(Q^2) = e^{-\frac{1}{2}(1-\beta_1)^2\nu Q^2} , \quad (6.90)$$

$$\eta(2S): \quad F^{(1)}(Q^2) = \left[1 - \frac{2}{3}(1-\beta_1)^2\nu Q^2 + \frac{1}{6}(1-\beta_1)^4\nu^2 Q^4\right] e^{-\frac{1}{2}(1-\beta_1)^2\nu Q^2} , \quad (6.91)$$

$$\chi_0(1P): \quad F^{(1)}(Q^2) = \left[1 - \frac{1}{3}(1-\beta_1)^2\nu Q^2\right] e^{-\frac{1}{2}(1-\beta_1)^2\nu Q^2} , \quad (6.92)$$

where, for the record, $\nu = (2\mu_{12}\omega_{12})^{-1}$.

For the vector meson $\Upsilon(1S)$ (the results for J/ψ and B_c^* have the same form but with appropriate quark masses),

$$J_1^+ = 2P^+ \, e^{-\frac{1}{2}(1-\beta_1)^2\nu Q^2} \begin{bmatrix} 1 & \frac{q^{(-)}}{2M_{12}}\frac{m_1-m_2}{m_1} & 0 \\ \frac{q^{(+)}}{2M_{12}}\frac{m_1-m_2}{m_1} & 1 & \frac{q^{(-)}}{2M_{12}}\frac{m_1-m_2}{m_1} \\ 0 & \frac{q^{(+)}}{2M_{12}}\frac{m_1-m_2}{m_1} & 1 \end{bmatrix} , \quad (6.93)$$

$$J_1^1 = (P^1 + P'^1)\frac{J_1^+}{2P^+} - iq^2\frac{1}{\beta_1}e^{-\frac{1}{2}(1-\beta_1)^2\nu Q^2} \begin{bmatrix} 1 & \frac{q^{(-)}}{2M_{12}} & 0 \\ \frac{q^{(+)}}{2M_{12}} & 0 & -\frac{q^{(-)}}{2M_{12}} \\ 0 & -\frac{q^{(+)}}{2M_{12}} & -1 \end{bmatrix} , \quad (6.94)$$

$$J_1^2 = (P^2 + P'^2)\frac{J_1^+}{2P^+} + iq^1\frac{1}{\beta_1}e^{-\frac{1}{2}(1-\beta_1)^2\nu Q^2} \begin{bmatrix} 1 & \frac{q^{(-)}}{2M_{12}} & 0 \\ \frac{q^{(+)}}{2M_{12}} & 0 & -\frac{q^{(-)}}{2M_{12}} \\ 0 & -\frac{q^{(+)}}{2M_{12}} & -1 \end{bmatrix} , \quad (6.95)$$

where $M_{12} = m_1 + m_2$. For the vector meson $\Upsilon(2S)$ the results for $J_1^{+,\perp}$ are almost the same as those in Eqs. (6.93)–(6.95), except they are multiplied by a polynomial in Q^2:

$$J^{+,\perp}_{1,\Upsilon(2S)} = \left[1 - \frac{2}{3}\nu(1-\beta_1)^2 Q^2 + \frac{1}{6}\nu^2(1-\beta_1)^4 Q^4\right] J^{+,\perp}_{1,\Upsilon(1S)} . \quad (6.96)$$

Comparison of the computed $J_1^{+,\perp}$ matrices with Eqs. (6.68)–(6.70) reveals that their forms differ, even though I included corrections to the wave functions. This is a known problem that formulas for scattering amplitudes calculated in the FF of dynamics depend on the direction distinguished by the front [94]. Therefore, the extraction of form factors is ambiguous, because one has to decide which of the scattering amplitudes are computed correctly, and which depend on physics

not included in the calculation. For example, for spin-1 particles it is argued that J^+ current should be used but the matrix element J^+_{00} is sensitive to physics of zero-modes, hence should be ignored unless zero-modes are correctly accounted for [97]. One may also argue that since ε^μ_0 depends on dynamics, see discussion below Eq. (6.77), it is not to be trusted unless the binding mechanism is relativistically well described.

The form factors extracted from J^+_1 (ignoring J^+_{100}) are,

$$\begin{aligned}
\Upsilon(1S): \quad F_1^{(1)}(Q^2) &= e^{-\frac{1}{2}(1-\beta_1)^2\nu Q^2}\ , && (6.97)\\
F_2^{(1)}(Q^2) &= \left(\frac{M}{m_1}-2\frac{M-M_{12}}{M_{12}}\right)e^{-\frac{1}{2}(1-\beta_1)^2\nu Q^2}\ , && (6.98)\\
F_3^{(1)}(Q^2) &= 0\ , && (6.99)\\
\Upsilon(2S): \quad F_1^{(1)}(Q^2) &= \left[1-\frac{2}{3}\nu(1-\beta_1)^2Q^2+\frac{1}{6}\nu^2(1-\beta_1)^4Q^4\right]e^{-\frac{1}{2}(1-\beta_1)^2\nu Q^2}\ , && (6.100)\\
F_2^{(1)}(Q^2) &= \left(\frac{M}{m_1}-2\frac{M-M_{12}}{M_{12}}\right)F_1^{(1)}(Q^2)\ , && (6.101)\\
F_3^{(1)}(Q^2) &= 0\ . && (6.102)
\end{aligned}$$

Using the above form factors and Eq. (6.68) one would expect $J^+_{100}=1+aQ^2/M^2$, where a is of order one. From Eq. (6.93) $J^+_{100}=1$. Hence the two values do not match. However, the relative difference is of order Q^2/M^2 and is small for $Q\ll M$. Due to nonrelativistic approximations that I made this is an acceptable agreement. How about the perpendicular components of the electromagnetic current? For $J^\perp_1$ not only 00 but also $0\pm$ and ±0 components cause trouble. Ignoring them I obtain $F_3^{(1)}=0$, as before, $F_1^{(1)}$ that is the same as in Eqs. (6.97) and (6.100), and $F_2^{(1)}=(1/\beta_1)F_1^{(1)}$. The results obtained using the two ways of extracting the form factors differ only for $F_2^{(1)}$. The difference depends on $M-M_{12}$ and vanishes when $M=M_{12}$. Therefore, the extraction of the magnetic form factor $G_M=F_2$ is ambiguous and probably depends on proper inclusion of higher-order correction in the bound state problem.

6.5 Baryons

6.5.1 Wave functions

For the same reason that was given in the beginning of Sec. 6.4.1, the use of wave functions discussed in Sec. 5.3 and listed in App. A is not sufficient to properly describe the magnetic properties of baryons. To include appropriate corrections in the wave function I need an expression that is written using relativistic objects and has proper quantum numbers. I limit the discussion to the ground state of $\Omega_{ccb,\frac{1}{2}^+}$ and $\Omega_{bbc,\frac{1}{2}^+}$. I choose the following wave function [98] inspired by Ioffe currents [99] that includes the nonrelativistic wave function of Chapter 5 and relativistic corrections,

$$\psi^\sigma_{\sigma_1\sigma_2\sigma_3}(\vec{K}_{12},\vec{Q}_3) = \mathcal{N}\left(\bar{u}_1\gamma^\mu C\bar{u}_2^T\right)\ \bar{u}_3\gamma_\mu\gamma^5 u_{M_{123}}(P,\sigma)\ \psi_{1S1S}(\vec{K}_{12},\vec{Q}_3)\ , \qquad (6.103)$$

where the normalization constant $\mathcal{N}=-1/\sqrt{96m_1^2m_3M_{123}}$, $M_{123}=m_1+m_2+m_3$ and $C=-i\gamma^0\gamma^2$ is the charge conjugation matrix. For vector quarkonia I had to take polarization vector that was at rest in the rest frame of quarks, instead of at rest in the rest frame of the quarkonium.[2] Here, similarly, I take the spinor of the baryon, $u_{M_{123}}(P,\sigma)$, that is at rest in the rest frame of quarks, which means that the mass that is distinguished for the spinor is $m=M_{123}$, *cf.* Eq. (2.50).

[2]Rest frame of the baryon is defined as the frame in which the baryon has $P^\perp=0$ and $P^+=M$. Rest frame of quarks is defined as the frame in which quarks have $P^\perp=0$ and $P^+=\mathcal{M}_{123}\approx M_{123}$.

Expansion of $\psi^{\sigma}_{\sigma_1\sigma_2\sigma_3}$ up to terms linear in momentum gives,

$$\begin{aligned}
\psi^{\uparrow}(\vec{K}_{12},\vec{Q}_3) &= \frac{\psi_{1S1S}(\vec{K}_{12},\vec{Q}_3)}{\sqrt{6}}\left[2|\uparrow\uparrow\downarrow\rangle - |\uparrow\downarrow\uparrow\rangle - |\downarrow\uparrow\uparrow\rangle + \frac{\sqrt{2}\kappa_3^{(-)}}{\mu_{3(12)}}|\uparrow\uparrow\uparrow\rangle + \frac{\kappa_3^{(+)}}{\sqrt{2}m_1}|\downarrow\downarrow\uparrow\rangle\right. \\
&- \left.\sqrt{2}\left(\frac{\kappa_3^{(+)}}{2m_3} - \frac{\kappa_1^{(+)}}{m_1}\right)|\downarrow\uparrow\downarrow\rangle - \sqrt{2}\left(\frac{\kappa_3^{(+)}}{2m_3} - \frac{\kappa_2^{(+)}}{m_1}\right)|\uparrow\downarrow\downarrow\rangle\right] , \qquad (6.104)\\
\psi^{\downarrow}(\vec{K}_{12},\vec{Q}_3) &= \frac{\psi_{1S1S}(\vec{K}_{12},\vec{Q}_3)}{\sqrt{6}}\left[-2|\downarrow\downarrow\uparrow\rangle + |\downarrow\uparrow\downarrow\rangle + |\uparrow\downarrow\downarrow\rangle - \frac{\sqrt{2}\kappa_3^{(+)}}{\mu_{3(12)}}|\downarrow\downarrow\downarrow\rangle - \frac{\kappa_3^{(-)}}{\sqrt{2}m_1}|\uparrow\uparrow\downarrow\rangle\right. \\
&+ \left.\sqrt{2}\left(\frac{\kappa_3^{(-)}}{2m_3} - \frac{\kappa_1^{(-)}}{m_1}\right)|\uparrow\downarrow\uparrow\rangle + \sqrt{2}\left(\frac{\kappa_3^{(-)}}{2m_3} - \frac{\kappa_2^{(-)}}{m_1}\right)|\downarrow\uparrow\uparrow\rangle\right] , \qquad (6.105)
\end{aligned}$$

where

$$\begin{aligned}
\kappa_1^{\perp} &= \kappa_{1/12}^{\perp} - x_{1/12}\kappa_3^{\perp} \approx K_{12}^{\perp} - \frac{1}{2}Q_3^{\perp} , \qquad (6.106)\\
\kappa_2^{\perp} &= \kappa_{2/12}^{\perp} - x_{2/12}\kappa_3^{\perp} \approx -K_{12}^{\perp} - \frac{1}{2}Q_3^{\perp} , \qquad (6.107)\\
\kappa_3^{\perp} &= Q_3^{\perp} . \qquad (6.108)
\end{aligned}$$

The spin structure in the limit of zero relative momenta reduces to spin $(1/2)_S$ wave function, Eqs. (5.18) and (5.19), as required. The ρ matrices constructed from the baryon wave function up to terms linear in momentum are,

$$\begin{aligned}
\rho_{1\uparrow\uparrow} &= A_1\begin{pmatrix}\frac{5}{6} & \cdot\\ \cdot & \frac{1}{6}\end{pmatrix} , \qquad (6.109)\\
\rho_{1\uparrow\downarrow} &= A_1\begin{pmatrix}\frac{\kappa_1^{(-)}}{3m_1} + \frac{\kappa_2^{(-)}-\kappa_2'^{(-)}}{6m_1} - \frac{\kappa_3^{(-)}-\kappa_3'^{(-)}}{12m_3} & \cdot\\ \cdot & -\frac{\kappa_1'^{(-)}}{3m_1} + \frac{\kappa_2^{(-)}-\kappa_2'^{(-)}}{6m_1} - \frac{\kappa_3^{(-)}-\kappa_3'^{(-)}}{12m_3}\end{pmatrix} , \qquad (6.110)\\
\rho_{1\downarrow\uparrow} &= A_1\begin{pmatrix}-\frac{\kappa_1'^{(+)}}{3m_1} + \frac{\kappa_2^{(+)}-\kappa_2'^{(+)}}{6m_1} - \frac{\kappa_3^{(+)}-\kappa_3'^{(+)}}{12m_3} & \cdot\\ \cdot & \frac{\kappa_1^{(+)}}{3m_1} + \frac{\kappa_2^{(+)}-\kappa_2'^{(+)}}{6m_1} - \frac{\kappa_3^{(+)}-\kappa_3'^{(+)}}{12m_3}\end{pmatrix} , \qquad (6.111)\\
\rho_{1\downarrow\downarrow} &= A_1\begin{pmatrix}\frac{1}{6} & \cdot\\ \cdot & \frac{5}{6}\end{pmatrix} , \qquad (6.112)\\
\rho_{3\uparrow\uparrow} &= A_3\begin{pmatrix}\frac{1}{3} & \cdot\\ \cdot & \frac{2}{3}\end{pmatrix} , \qquad (6.113)\\
\rho_{3\uparrow\downarrow} &= A_3\begin{pmatrix}-\frac{\kappa_3^{(-)}}{6m_3} + \frac{\kappa_1^{(-)}-\kappa_1'^{(-)}}{6m_1} + \frac{\kappa_2^{(-)}-\kappa_2'^{(-)}}{6m_1} & \cdot\\ \cdot & \frac{\kappa_3'^{(-)}}{6m_3} + \frac{\kappa_1^{(-)}-\kappa_1'^{(-)}}{6m_1} + \frac{\kappa_2^{(-)}-\kappa_2'^{(-)}}{6m_1}\end{pmatrix} , \qquad (6.114)\\
\rho_{3\downarrow\uparrow} &= A_3\begin{pmatrix}\frac{\kappa_3'^{(+)}}{6m_3} - \frac{\kappa_1'^{(+)}-\kappa_1^{(+)}}{6m_1} - \frac{\kappa_2'^{(+)}-\kappa_2^{(+)}}{6m_1} & \cdot\\ \cdot & \frac{\kappa_3^{(+)}}{6m_3} - \frac{\kappa_1'^{(+)}-\kappa_1^{(+)}}{6m_1} - \frac{\kappa_2'^{(+)}-\kappa_2^{(+)}}{6m_1}\end{pmatrix} , \qquad (6.115)\\
\rho_{3\downarrow\downarrow} &= A_3\begin{pmatrix}\frac{2}{3} & \cdot\\ \cdot & \frac{1}{3}\end{pmatrix} , \qquad (6.116)
\end{aligned}$$

where off-diagonal elements are irrelevant and

$$\begin{aligned}
A_1 &= \psi_{1S1S}(\vec{K}_{13},\vec{Q}_3\,)\psi_{1S1S}(\vec{K}_{1'3},\vec{Q}'_3\,)^* , \qquad (6.117)\\
A_3 &= \psi_{1S1S}(\vec{K}_{12},\vec{Q}_3\,)\psi_{1S1S}(\vec{K}_{12},\vec{Q}_{3'}\,)^* . \qquad (6.118)
\end{aligned}$$

6.5.2 Form factors

Using the wave functions given in Sec. 6.5.1 I calculate the current matrix elements for the ground states of *ccb* and *bbc*. The results for quark 1 and quark 3 are, *cf.* Eq. (6.56),

$$J_1^+ = 2P^+ \begin{bmatrix} 1 & -\frac{q^{(-)}}{\sqrt{2}M_{123}}\left(\frac{2}{3\beta_1}-1\right) \\ -\frac{q^{(+)}}{\sqrt{2}M_{123}}\left(\frac{2}{3\beta_1}-1\right) & 1 \end{bmatrix} e^{-\frac{1}{8}(\nu_{12}+4\beta_3^2\nu_{3(12)})Q^2} , \quad (6.119)$$

$$J_1^1 = \frac{P^1+P'^1}{2P^+}J_1^+ - iq^2\frac{2}{3\beta_1}\begin{bmatrix}1&0\\0&-1\end{bmatrix} e^{-\frac{1}{8}(\nu_{12}+4\beta_3^2\nu_{3(12)})Q^2} , \quad (6.120)$$

$$J_1^2 = \frac{P^2+P'^2}{2P^+}J_1^+ + iq^1\frac{2}{3\beta_1}\begin{bmatrix}1&0\\0&-1\end{bmatrix} e^{-\frac{1}{8}(\nu_{12}+4\beta_3^2\nu_{3(12)})Q^2} , \quad (6.121)$$

and

$$J_3^+ = 2P^+ \begin{bmatrix} 1 & -\frac{q^{(-)}}{\sqrt{2}M_{123}}\left(\frac{-1}{3\beta_3}-1\right) \\ -\frac{q^{(+)}}{\sqrt{2}M_{123}}\left(\frac{-1}{3\beta_3}-1\right) & 1 \end{bmatrix} e^{-\frac{1}{2}(1-\beta_3)^2\nu_{3(12)}Q^2} , \quad (6.122)$$

$$J_3^1 = \frac{P^1+P'^1}{2P^+}J_3^+ - iq^2\frac{-1}{3\beta_3}\begin{bmatrix}1&0\\0&-1\end{bmatrix} e^{-\frac{1}{2}(1-\beta_3)^2\nu_{3(12)}Q^2} , \quad (6.123)$$

$$J_3^2 = \frac{P^2+P'^2}{2P^+}J_3^+ + iq^1\frac{-1}{3\beta_3}\begin{bmatrix}1&0\\0&-1\end{bmatrix} e^{-\frac{1}{2}(1-\beta_3)^2\nu_{3(12)}Q^2} . \quad (6.124)$$

Therefore, from J_1^+ and J_3^+,

$$F_1^{(1)}(Q^2) = e^{-\frac{1}{8}(\nu_{12}+4\beta_3^2\nu_{3(12)})Q^2} , \quad (6.125)$$

$$F_2^{(1)}(Q^2) = \left(\frac{2M}{3m_1}-\frac{M}{M_{123}}\right) e^{-\frac{1}{8}(\nu_{12}+4\beta_3^2\nu_{3(12)})Q^2} , \quad (6.126)$$

$$F_1^{(3)}(Q^2) = e^{-\frac{1}{2}(1-\beta_3)^2\nu_{3(12)}Q^2} , \quad (6.127)$$

$$F_2^{(3)}(Q^2) = \left(-\frac{M}{3m_3}-\frac{M}{M_{123}}\right) e^{-\frac{1}{2}(1-\beta_3)^2\nu_{3(12)}Q^2} . \quad (6.128)$$

and

$$G_M^{(1)}(Q^2) = \left(\frac{2M}{3m_1}-\frac{M-M_{123}}{M_{123}}\right) e^{-\frac{1}{8}(\nu_{12}+4\beta_3^2\nu_{3(12)})Q^2} , \quad (6.129)$$

$$G_M^{(3)}(Q^2) = \left(-\frac{M}{3m_3}-\frac{M-M_{123}}{M_{123}}\right) e^{-\frac{1}{2}(1-\beta_3)^2\nu_{3(12)}Q^2} . \quad (6.130)$$

Similarly as for the vector quarkonia, currents $J_1^\perp$ and $J_3^\perp$ do not have the expected form of Eqs. (6.53) and (6.54). Using only the diagonal terms of $J_1^\perp$ and $J_3^\perp$, the magnetic form factors are, $G_M^{(1)}(0) = 2/(3\beta_1)$ and $G_M^{(3)}(0) = -1/(3\beta_3)$. Therefore, the extraction of the magnetic form factor is ambiguous, but the ambiguity goes away when $M \to M_{123}$.

6.6 Summary of charge radii and moments

Using the form factors of scalar and pseudoscalar quarkonia, Eqs. (6.90)–(6.92), the charge radii are,

$$\eta(1S): \quad r_1^2 = 3(1-\beta_1)^2\nu , \quad (6.131)$$

$$\eta(2S): \quad r_1^2 = 7(1-\beta_1)^2\nu , \quad (6.132)$$

$$\chi_0(1P): \quad r_1^2 = 5(1-\beta_1)^2\nu . \quad (6.133)$$

$c\bar{c}$					
	$\eta_c(1S)$	$\chi_{c0}(1P)$	$\eta_c(2S)$	J/ψ	$\psi(2S)$
$\sqrt{r_1^2}$ [fm]	0.249	0.322	0.381	0.257	0.385
BLFQ [97]	0.207	0.265	0.386	0.212	0.387
CI [100]	0.210			0.261	
Lattice [101]	0.251	0.308		0.257	
DSE [102]	0.219			0.228	
$b\bar{b}$					
	$\eta_b(1S)$	$\chi_{b0}(1P)$	$\eta_b(2S)$	$\Upsilon(1S)$	$\Upsilon(2S)$
$\sqrt{r_1^2}$ [fm]	0.1521	0.1963	0.2323	0.1535	0.2331
BLFQ [97]	0.126	0.192	0.237	0.126	0.239
CI [100]	0.110			0.195	
$c\bar{b}$					
	$B_c(1S)$	$\chi_{bc0}(1P)$	$B_c(2S)$	$B_c^*(1S)$	$B_c^*(2S)$
$\sqrt{r_c^2}$ [fm]	0.337	0.435	0.515	0.342	0.516
$\sqrt{r_b^2}$ [fm]	0.105	0.136	0.160	0.106	0.161
$\sqrt{r^2}$ [fm]	0.282	0.364	0.430	0.286	0.433

Table 6.1: Summary of charge radii of mesons. The number of digits that I provide is adjusted to make visible the difference between radii of vector and pseudoscalar particles.

The charge radii of vector quarkonia, based on Eqs. (6.97)–(6.102), are

$$\Upsilon(1S): \qquad r_1^2 = 3(1-\beta_1)^2\nu + \frac{m_2}{m_1 M_{12} M} - \frac{M - M_{12}}{M_{12} M^2} , \tag{6.134}$$

$$\Upsilon(2S): \qquad r_1^2 = 7(1-\beta_1)^2\nu + \frac{m_2}{m_1 M_{12} M} - \frac{M - M_{12}}{M_{12} M^2} . \tag{6.135}$$

The above formulas apply also to ψ and B_c^* mesons. To obtain formulas for r_2^2 the exchange of indices $1 \leftrightarrow 2$ is necessary. Table 6.1 presents the results for charge radii of mesons and baryons respectively. I used the values of quark masses, and other relevant parameters, that were found in Chapter 5. The results are compared with Basis Light Front Quantization (BLFQ) calculations [97], Contact Interaction (CI) calculations [100], Lattice [101], and Dyson-Schwinger equations [102]. Where comparison is possible my results agree rather well with the literature. The agreement is surprisingly good with lattice QCD calculations, where relative differences are smaller than 5% (in case of η_c and J/ψ they are much smaller).

Using Eqs. (6.125)–(6.128), the baryon charge radii are,

$$r_1^2 = \frac{3\nu_{12}}{4} + 3\beta_3^2\nu_{3(12)} + \frac{m_1 + 2m_3}{2m_1 M_{123} M} , \tag{6.136}$$

$$r_3^2 = 3(1-\beta_3)^2\nu_{3(12)} - \frac{m_1 + 2m_3}{m_3 M_{123} M} , \tag{6.137}$$

where ν_{12} and $\nu_{3(12)}$ are defined below Eq. (5.16). Furthermore, in accord with Eq. (6.48), the total radius squared is a weighted mean,

$$r^2 = \frac{2Q_{f_1} r_1^2 + Q_{f_3} r_3^2}{2Q_{f_1} + Q_{f_3}} . \tag{6.138}$$

For *bbc* system, which is electrically neutral, I define r^2 in the same way, but without dividing by the total charge. The result for such r^2, in principle, could be negative, but it turns out positive,

	Ω_{ccc}	Ω_{ccb}	Ω_{bbc}	Ω_{bbb}
$\sqrt{r_c^2}$ [fm]	0.31	0.35	0.32	
$\sqrt{r_b^2}$ [fm]		0.18	0.20	0.19
$\sqrt{r^2}$ [fm]	0.31	0.39	0.20	0.19
Lattice [93], $\sqrt{\langle r_E \rangle_c}$ [fm]	0.29			

Table 6.2: Summary of charge radii of baryons.

	μ_1	BLFQ [97]	CI [100]	Lattice [101]	DSE [102]
J/ψ	2 ± 0.13	1.952(3)	2.047	2.10(3)	2.13(4)
$\psi(2S)$	2 ± 0.54	2.05(2)			
$\Upsilon(1S)$	2 ± 0.02	1.985(1)	2.012		
$\Upsilon(2S)$	2 ± 0.14	1.992(1)			

Table 6.3: Summary of magnetic dipole moments of charmonia and bottomonia and comparison with some results available in literature. My estimation of error is $\mu_1 \cdot (M - M_{12})/M_{12}$.

therefore, I can take the square root. Table 6.2 presents the results for the radii r_1, r_3 and r of ground states of all *four* systems *bbb*, *bbc*, *ccb* and *ccc*. For single-flavor baryons I use Eqs. (6.136) and (6.137), but I drop the last terms (proportional to $m_1 + 2m_3$), because they depend on the spin structure of the state and I do not know them, however, they are rather small, see radii of η and Υ states for comparison. The agreement of *ccc* radius with lattice calculation is quite good, even though I used only the approximate formula.

The magnetic dipole moments of vector quarkonia (the contribution from quark 1), using Eqs. (6.98) and Eqs. (6.101), are

$$\mu_1 \;=\; \frac{M}{m_1} - 2\frac{M - M_{12}}{M_{12}} \;=\; 2 - \frac{m_1 - m_2}{m_1 M_{12}} M \;. \tag{6.139}$$

For baryons Eqs. (6.129) and (6.130) are used and give,

$$\mu \;=\; 2Q_q \left(\frac{2M}{3m_1} - \frac{M - M_{123}}{M_{123}} \right) + Q_{q'} \left(-\frac{M}{3m_3} - \frac{M - M_{123}}{M_{123}} \right) \;. \tag{6.140}$$

Additionally, I give uncertainties that are related to the ambiguities of extraction of form factors. I assume fixed relative uncertainty that is the ratio of binding energy to the sum of masses of quarks. Tables 6.3 and 6.4 summarize my results and compare them with literature. The comparison shows that magnetic moments of charmonia and bottomonia agree very well within the uncertainties of my calculation with other theoretical approaches. For mixed-flavor systems my results have systematically bigger magnitudes, which is an indication that calculation for these systems probably needs to be improved.

	μ	[103]	[104]	[104]	[105]	[106, 107]
$B_c^{+*}(1S)$	3.25 ± 0.07	2.88				2.57
$B_c^{+*}(2S)$	3.24 ± 0.35	2.65				
Ω_{ccb}	5.16 ± 0.46		4.49	4.62	4.69	4.03
Ω_{bbc}	-2.77 ± 0.09		-2.45	-2.39	-2.39	-2.24

Table 6.4: Summary of magnetic dipole moments of $c\bar{b}$ particles and baryons and comparison with some results found in literature. My estimation of error is $\mu \cdot (M - M_{12})/M_{12}$ for mesons and $\mu \cdot (M - M_{123})/M_{123}$ for baryons.

Chapter 7

Structure functions

7.1 Introduction

In this chapter I study deep inelastic scattering (DIS) of electrons off heavy quarkonia and triply-heavy baryons. Experimental study of such processes is presently not achievable because of short life times of such hadrons and difficulty in their production (especially for the triply-heavy baryons, which have not been observed yet). Therefore, my theoretical investigation is intended to be a short review of possibilities that front form of dynamics, complemented with renormalization group procedure for effective particles, offers in this field of studies.

Figure 7.1 illustrates the DIS process to be described [108]. An electron with four-momentum k scatters on a hadron with four-momentum P and transfers to the hadron very large four-momentum q (illustrated as an exchange of a virtual photon). As a result of the interaction, electron acquires four-momentum k' and the hadron is most of the times disintegrated into a lot of particles in the final state X. The analysis is inclusive and only the electron momenta k and k' are measured (I limit the discussion to scattering of unpolarized particles). Therefore, the cross section includes the sum over all possible X and it is described using two variables,

$$Q^2 = -q^2 \tag{7.1}$$

and

$$x = \frac{Q^2}{2P\cdot q}\,, \tag{7.2}$$

or x and

$$y = \frac{P\cdot q}{P\cdot k}\,. \tag{7.3}$$

Conventionally, one introduces also ν, which is the loss of energy of the electron in the frame, in which the hadron is at rest, so that $P\cdot q = M\nu$. In one-photon-exchange approximation the cross section factorizes,

$$\frac{d\sigma}{dxdy} = \frac{2\pi y\alpha_{\rm em}}{Q^4} L_{\mu\nu}W^{\mu\nu}\,, \tag{7.4}$$

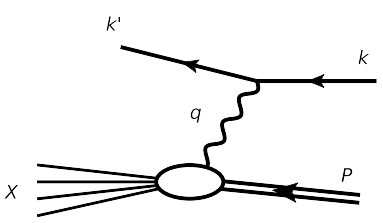

Figure 7.1: Deep inelastic scattering

where $\alpha_{\rm em}$ is the electromagnetic coupling constant, $L_{\mu\nu}$ is the leptonic tensor and $W^{\mu\nu}$ is the hadronic tensor. The leptonic tensor has a known form [21], while the hadronic tensor is unknown and depends on the internal structure of the hadron. Formal definition of the hadronic tensor is,

$$W^{\mu\nu} = \frac{1}{2s+1}\sum_{\sigma=-s}^{s}\frac{1}{4\pi}\int d^4z e^{iqz}\langle P,\sigma|\left[\hat{J}^\mu(z),\hat{J}^\nu(0)\right]|P,\sigma\rangle \tag{7.5}$$

$$= \frac{1}{2s+1}\sum_{\sigma=-s}^{s}\frac{1}{4\pi}\sum_X(2\pi)^4\delta^{(4)}(P+q-P_X)\langle P,\sigma|\hat{J}^\mu(0)|X\rangle\langle X|\hat{J}^\nu(0)|P,\sigma\rangle\ , \tag{7.6}$$

where s is the spin of the hadron and the sum over X is the sum over all possible intermediate states X, with momentum P_X. The Dirac delta in the second form of $W^{\mu\nu}$ expresses the energy-momentum conservation condition for the scattering process. In the calculations that follow I will always assume that $q^+ = 0$. Conservation of electromagnetic current implies,

$$q_\mu W^{\mu\nu} = q_\nu W^{\mu\nu} = 0\ . \tag{7.7}$$

The standard parametrization of the hadronic tensor is,

$$W^{\mu\nu} = -\left(g^{\mu\nu}-\frac{q^\mu q^\nu}{q^2}\right)W_1+\left(P^\mu-\frac{P\cdot q}{q^2}q^\mu\right)\left(P^\nu-\frac{P\cdot q}{q^2}q^\nu\right)\frac{W_2}{M^2}\ , \tag{7.8}$$

where real functions W_1 and W_2 depend on the invariants of the deep inelastic scattering and are called structure functions. Bjorken [109] predicted that in the limit of very large momentum and energy transfer, $Q^2\to\infty$, $\nu\to\infty$, but with ratio Q^2/ν fixed (called the Bjorken limit), one can define structure functions,

$$F_1(x) = \lim_{Q^2\to\infty,\ \nu\to\infty} W_1\ , \tag{7.9}$$

$$F_2(x) = \lim_{Q^2\to\infty,\ \nu\to\infty} \frac{\nu}{M}W_2\ , \tag{7.10}$$

which depend only on x – the result known as Bjorken scaling. The scaling was confirmed experimentally, but it was also realized that in QCD these functions obtain corrections that depend logarithmically on Q^2 [43, 44, 45, 46].

In the process one can distinguish two vastly different momentum scales. The scale of the probing photon is Q and it is very big. The Compton wave length $1/Q$ is very small and the photon sees the structure of the hadron at these small distance scales, hence, the scattering is called "deep" [110]. On the other hand, the scale of the bound state is $\lambda_{\rm hadron}$ and it is small. For heavy quarkonia it is given in Eqs. (5.11) and (5.12). For representing a proton as a state of just three quarks it should probably be on the order of the scale of strong interactions $\Lambda_{\rm QCD}$. To describe the process comprehensively one needs to be able to describe physical pictures that correspond to these scales in one framework. The RGPEP provides necessary tools. Equation (7.6) may be written in terms of different degrees of freedom, particles with different effective sizes $s = 1/\lambda$ (not to be confused with the total spin s of the particle, which is used in this chapter). The exact solutions would not depend on λ, but approximate calculations need the proper choice of the degrees of freedom. Therefore, given a particle one should ascribe to it a size that is relevant for that particle in the physical process of interest. For example, the effective constituent quarks that form a bound state in a simple way, such as quarks b or c in heavy quarkonium in Chapter 4, move slowly and are large, *i.e.*, they correspond to small $\lambda = \lambda_{\rm hadron}$. On the other hand, very energetic photon has very small Compton wave length and should have $\lambda\sim Q$, hence, size $s\sim s_{\rm Compton} = 1/Q$. Because it is so small it cannot interact with big constituent quarks. However, in RGPEP one can express degrees of freedom at one scale in terms of degrees of freedom at another scale. Using Eq. (3.20),

$$b_Q = \mathcal{U}_Q b_\infty \mathcal{U}_Q^\dagger = \mathcal{U}_Q\mathcal{U}_\lambda^\dagger b_\lambda \mathcal{U}_\lambda\mathcal{U}_Q^\dagger \equiv \mathcal{W}_{Q\lambda}b_\lambda\mathcal{W}_{Q\lambda}^\dagger\ , \tag{7.11}$$

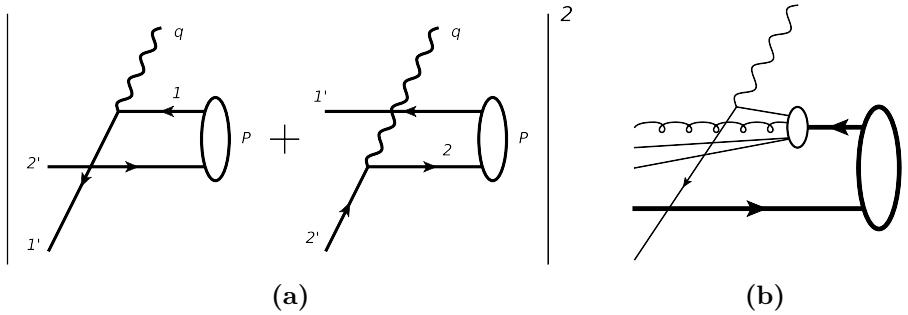

Figure 7.2: (a) The leading contribution to the hadronic tensor of quarkonia in DIS. (b) Example of a scaling violating contribution. The thick lines represent effective big quarks at the small scale λ of the bound state formation. Thin lines represent small particles at large scale Q relevant to the scattering process. The two kinds of particles are related with each other by the RGPEP unitary transformation $\mathcal{W}$ represented by the small blob.

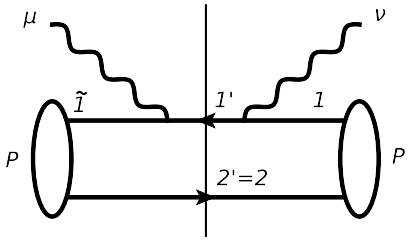

Figure 7.3: Quark 1 contribution to the hadronic tensor.

where I use the momentum scale to label the operators instead of t, hence, b_∞ is the point-like quark operator. Transformation $\mathcal{W}_{Q\lambda}$ expresses particles of size $1/Q$ in terms of particles of size $1/\lambda$ [58, 111]. Therefore, in Eq. (7.6) one can express the hadron state $|P,\sigma\rangle$ in terms of big quarks with $\lambda = \lambda_{\rm hadron}$, while the current operators with small quarks with $\lambda = Q$. Then the quarks of one kind are expressed in terms of the other quarks using $\mathcal{W}$, see Fig 7.2b. This is an exciting line of research, because the bigger Q the more small particles could "fit" into the big constituent-like quarks, hence, allowing for the description of scaling violations with simultaneous description of bound states. It is also conceivable that phenomenon of exhausting the available volume by increasing the number of partons, called saturation, can be addressed. In addition, it is argued [58] that large Q^2 evolution could be connected with evolution in x [47, 48]. In view of that I present rather modest results, in which I assume $\mathcal{W} \approx 1$.

7.2 Quarkonia

I limit the discussion to pseudoscalar and scalar quarkonia, however, the same results apply also to vector quarkonia – the spin structure of the state practically does not matter. The sum over intermediate states in Eq. (7.6) should in principle be performed over the physical particles that come out of the interaction, that is, in terms of hadrons. That would very much complicate the analysis of DIS. However, in the Bjorken limit I replace,

$$\sum_X |X\rangle\langle X|\ \delta^{(4)}(P+q-P_X) \quad \to \quad \int_{1'2'} b^\dagger_{1'} d^\dagger_{2'} |0\rangle\langle 0| d_{2'} b_{1'}\ \delta^{(4)}(P+q-p_{1'}-p_{2'})\ , \qquad (7.12)$$

where instead of hadrons I sum over quarks, see Fig. 7.2a. The replacement $P_X \to p_{1'} + p_{2'}$ is valid only approximately in the Bjorken limit when the struck quark takes all of the large photon momentum and masses of particles can be neglected. The electromagnetic current operator is defined in Eq. (6.2) and the quarkonium state in Eq. (4.15). Equation (7.6) may be imagined as the square of the scattering amplitude. In the Bjorken limit the interference term between quark

and antiquark vanishes, and one can consider contributions from quark and antiquark separately. The quark contribution is, see Fig. 7.3,

$$\begin{aligned} W^{\mu\nu} &= \frac{Q_q^2}{4\pi}\int [1'2'] \sum_{\sigma_{1'}\sigma_{2'}}\sum_{\sigma_{\tilde{1}}}\sum_{\sigma_1} \tilde{\delta}_{1'2'.P}(2\pi)\delta(P^- + q^- - p_{1'}^- - p_{2'}^-) \\ &\times \psi_{\sigma_{\tilde{1}}\sigma_{2'}}(x_1,\kappa_1)^* \frac{j^\mu_{\tilde{1}1'} j^\nu_{1'1}}{x_1^2} \psi_{\sigma_1\sigma_{2'}}(x_1,\kappa_1) \ , \end{aligned} \tag{7.13}$$

where Q_q is the electric charge of the quark and I split the four-dimensional Dirac delta into momentum conservation delta and FF-energy conservation delta. I define,

$$[\tilde{\rho}_1]_{\sigma_1\sigma_{\tilde{1}}} = \sum_{\sigma_{2'}} \psi_{\sigma_1\sigma_{2'}}(x_1,\kappa_1)\psi_{\sigma_{\tilde{1}}\sigma_{2'}}(x_1,\kappa_1)^* \ , \tag{7.14}$$

which differs from Eq. (6.17) in the momentum of the wave functions that build the matrix. Using the matrices defined in Eqs. (6.14)–(6.16) and $\tilde{\rho}_1$ the hadronic tensor takes the form,

$$W^{\mu\nu} = \frac{Q_q^2}{4\pi}\int [12]\tilde{\delta}_{12.P}\frac{1}{x_1^2}\mathrm{Tr}[\tilde{\rho}_1(\mathbf{j}^\mu)^\dagger \mathbf{j}^\nu]\ (2\pi)\delta(P^- + q^- - p_{1'}^- - p_2^-) \ . \tag{7.15}$$

In the Bjorken limit, the FF-energy conservation delta simplifies,

$$(2\pi)\delta(P^- + q^- - p_{1'}^- - p_2^-) \ \to \ \frac{2\pi x^2 P^+}{Q^2}\delta(x_1 - x) \ . \tag{7.16}$$

For $\eta(1S)$ and $\eta(2S)$ the matrix $\tilde{\rho}_1$ is proportional to unit matrix (neglecting small, relativistic corrections), see Eq. (6.74). For χ_0 the matrix $\tilde{\rho}_1$ is not diagonal, however, off-diagonal elements of $\tilde{\rho}_1$ are not relevant, because the current matrices $\mathbf{j}^\mu$ are diagonal and in Eq. (7.15) I compute trace. Moreover,

$$\psi_{1P_{-1}}(\vec{k})\psi_{1P_{-1}}(\vec{k})^* = \psi_{1P_{+1}}(\vec{k})\psi_{1P_{+1}}(\vec{k})^* \ , \tag{7.17}$$

hence, effectively, $\tilde{\rho}_1$ is also proportional to unit matrix, *cf.* Eq. (6.76). Therefore,

$$\mathrm{Tr}[\tilde{\rho}_1(\mathbf{j}^\mu)^\dagger \mathbf{j}^\nu] = \frac{1}{2} f(x_1,\kappa_1)\tilde{V}^{\mu\nu} \ , \tag{7.18}$$

where

$$f(x_1,\kappa_1) = \begin{cases} |\psi_{nS}(x_1,\kappa_1)|^2 \ , & \text{for } \eta(nS) \ , \\ \frac{2|\psi_{1P_{+1}}(x_1,\kappa_1)|^2 + |\psi_{1P_0}(x_1,\kappa_1)|^2}{3} \ , & \text{for } \chi_0(1P) \ , \end{cases} \tag{7.19}$$

and

$$\tilde{V}^{\mu\nu} = \mathrm{Tr}[(\mathbf{j}^\mu)^\dagger \mathbf{j}^\nu] = \mathrm{Tr}[\gamma^\mu(\not{p}_{1'} + m_1)\gamma^\nu(\not{p}_1 + m_1)] \tag{7.20}$$

$$= 4\left[p_{1'}^\mu p_1^\nu + p_{1'}^\nu p_1^\mu - g^{\mu\nu}(p_{1'}\cdot p_1 - m_1^2)\right] \ . \tag{7.21}$$

Algebraic manipulations lead to,

$$\tilde{V}^{\mu\nu} = 2q_1^2\left(g^{\mu\nu} - \frac{q_1^\mu q_1^\nu}{q_1^2}\right) + 8\left(p_1^\mu - \frac{p_1\cdot q_1}{q_1^2}q_1^\mu\right)\left(p_1^\nu - \frac{p_1\cdot q_1}{q_1^2}q_1^\nu\right) \ , \tag{7.22}$$

where

$$q_1^\mu = p_{1'}^\mu - p_1^\mu \ . \tag{7.23}$$

Four-vector q_1^μ differs from q^μ in the energy component only, $q_1^- \neq q^-$. This is because $P^- \neq p_1^- + p_2^-$. Both contractions, $q_{1\nu}\tilde{V}^{\mu\nu}$ and $q_{1\mu}\tilde{V}^{\mu\nu}$ are zero, but for the hadronic tensor to be conserved contractions with q^μ are required to vanish, while

$$q_\mu \tilde{V}^{\mu\nu} \neq 0 \neq q_\nu \tilde{V}^{\mu\nu} \ . \tag{7.24}$$

To guarantee that the conditions of current conservation are satisfied one can redefine currents [112],

$$J^\mu \ \ \rightarrow \ \ J^\mu - \frac{J\cdot q}{q^2} q^\mu \ . \tag{7.25}$$

The redefinition implies substitution $\tilde{V}^{\mu\nu} \rightarrow V^{\mu\nu}$, where

$$V^{\mu\nu} \ = \ \tilde{V}^{\mu\nu} - \tilde{V}^{\alpha\nu}\frac{q_\alpha q^\mu}{q^2} - \tilde{V}^{\mu\beta}\frac{q_\beta q^\nu}{q^2} + \tilde{V}^{\alpha\beta} q_\alpha q_\beta \frac{q^\mu q^\nu}{q^2} \ , \tag{7.26}$$

and fulfills $q_\mu V^{\mu\nu} = 0 = q_\nu V^{\mu\nu}$. For $q^+ = 0$,

$$\begin{aligned} V^{\mu\nu} \ &= \ 2q^2\left(g^{\mu\nu} - \frac{q^\mu q^\nu}{q^2}\right) \\ &+ \ 8\left(p_1^\mu - \frac{p_1\cdot q}{q^2}q^\mu - \frac{p_1\cdot q_1}{q^2}\sigma^\mu\right)\left(p_1^\nu - \frac{p_1\cdot q}{q^2}q^\nu - \frac{p_1\cdot q_1}{q^2}\sigma^\nu\right) \ , \end{aligned} \tag{7.27}$$

where

$$\sigma^\mu \ = \ q_1^\mu - q^\mu \ , \tag{7.28}$$

has only one nonzero component, σ^-. Focusing only on + and $\perp$ components,

$$V^{++} \ = \ 8(p_1^+)^2 \ , \tag{7.29}$$

$$V^{+i} \ = \ 8p_1^+\left(p_1^i - \frac{p_1\cdot q}{q^2}q^i\right) \ , \tag{7.30}$$

$$V^{ij} \ = \ -2q^2\left(\delta^{ij} + \frac{q^i q^j}{q^2}\right) + 8\left(p_1^i - \frac{p_1\cdot q}{q^2}q^i\right)\left(p_1^j - \frac{p_1\cdot q}{q^2}q^j\right) \ . \tag{7.31}$$

These expressions already resemble Eq. (7.8), except they have p_1 instead of P. Using the relative momenta, I have, $p_1^+ = x_1 P^+$ and,

$$p_1^i - \frac{p_1\cdot q}{q^2}q^i \ = \ x_1\left(P^i - \frac{P\cdot q}{q^2}q^i\right) + \kappa_1^i + \frac{\kappa_1^\perp q^\perp}{q^2}q^i \ . \tag{7.32}$$

The part that contains $\kappa_1^\perp$ integrates to zero in W^{+i} components (because the rest of the integrand is a function of κ_1^2). For W^{ij} components under integration sign one can replace,

$$\left(\kappa_1^i + \frac{\kappa_1^\perp q^\perp}{q^2}q^i\right)\left(\kappa_1^j + \frac{\kappa_1^\perp q^\perp}{q^2}q^j\right) \ \ \rightarrow \ \ \frac{1}{2}\kappa_1^2\left(\delta^{ij} + \frac{q^i q^j}{q^2}\right) \ , \tag{7.33}$$

where, in order to derive that rule, one has to remember that $q^2 = -(q^\perp)^2$.

Collecting the above manipulations of $V^{\mu\nu}$, I arrive at the expression for $W^{\mu\nu}$ that for + and $\perp$ components has the form of Eq. (7.8) with,

$$W_1 \ = \ \frac{Q_q^2}{4\pi}\int [12]\tilde{\delta}_{12.P}\frac{2\kappa_1^2 - q^2}{x_1^2} f(x_1,\kappa_1)\ (2\pi)\delta(P^- + q^- - p_{1'}^- - p_2^-) \ , \tag{7.34}$$

$$\frac{W_2}{M^2} \ = \ \frac{Q_q^2}{4\pi}\int [12]\tilde{\delta}_{12.P}\ 4\ f(x_1,\kappa_1)\ (2\pi)\delta(P^- + q^- - p_{1'}^- - p_2^-) \ . \tag{7.35}$$

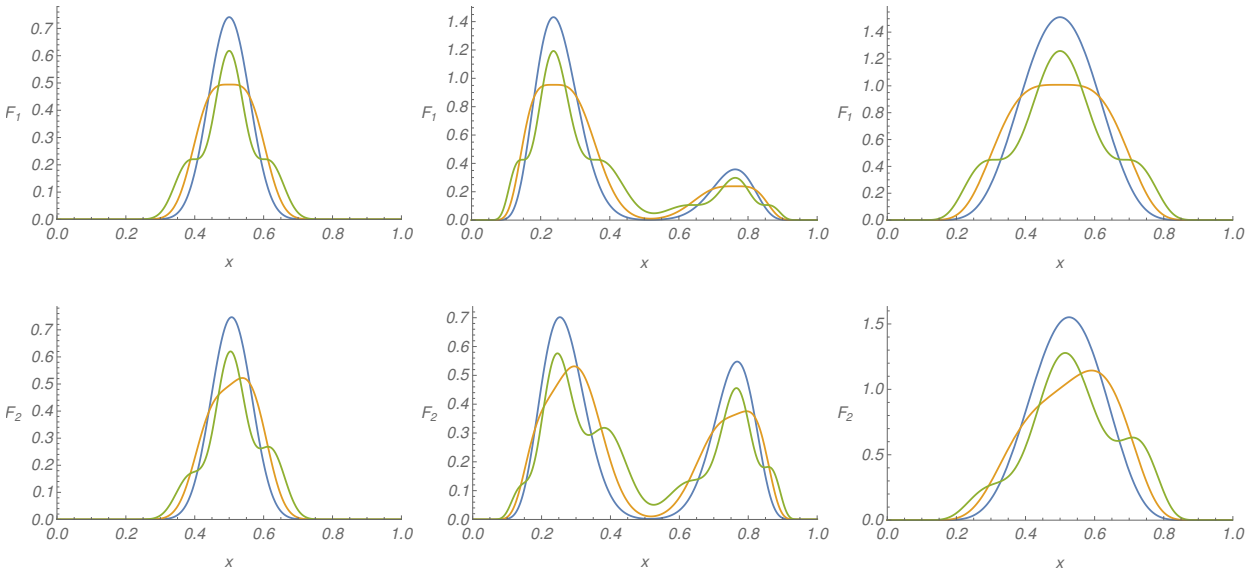

Figure 7.4: Structure functions $F_1(x)$ and $F_2(x)$ for (a) bottomonia, (b) B_c particles, (c) charmonia. On each plot, the highest curve (blue) represents the $1S$ state, the curve with the widest top (orange) represents the $1P$ state, and the curve with steps (green) represents the $2S$ state.

Therefore, the structure functions from Eqs. (7.9) and (7.10) are,

$$F_1(x,Q^2) = \frac{1}{2}Q_q^2\int [12]P^+\tilde{\delta}_{12.P}\ f(x_1,\kappa_1)\ \delta(x_1-x)\ , \tag{7.36}$$

$$F_2(x,Q^2) = xQ_q^2\int [12]P^+\tilde{\delta}_{12.P}\ f(x_1,\kappa_1)\ \delta(x_1-x)\ , \tag{7.37}$$

where f is defined in Eq. (7.19). These F_1 and F_2 do not depend on Q^2, as expected in the leading approximation, where Bjorken scaling should hold. Moreover, they are related through the well-known Callan-Gross relation [113],

$$F_2 = 2xF_1\ . \tag{7.38}$$

Integrating over x_1 first and then taking the nonrelativistic limit of the integral, I obtain,

$$F_1(x,Q^2) = \frac{1}{2}Q_q^2\int \frac{d^2k^\perp}{(2\pi)^2}\frac{M_{12}}{2\pi}\ |\psi(\vec{k})|^2\Big|_{k^z=k^z(x)}\ , \tag{7.39}$$

where, $M_{12}=m_1+m_2$ and in accord with Eq. (4.45),

$$k^z(x) = \sqrt{\frac{\beta_1\beta_2}{x(1-x)}}(m_1+m_2)(x-\beta_1)\ . \tag{7.40}$$

Using the eigenfunctions of the harmonic oscillator, Eq. (5.4), the expressions for the structure function F_1 for different quarkonia states are (only the contribution from quark 1 are shown for contribution from quark 2 one has to exchange $\beta_1 \leftrightarrow \beta_2$),

$$1S: \quad F_1(x) = \frac{1}{2}Q_q^2\ e^{-2\nu k^z(x)^2}\sqrt{\nu(m_1+m_2)^2}\sqrt{\frac{2}{\pi}}\ , \tag{7.41}$$

$$1P: \quad F_1(x) = \frac{1}{2}Q_q^2\ e^{-2\nu k^z(x)^2}\left(\frac{2}{3}+\frac{4}{3}\nu k^z(x)^2\right)\sqrt{\nu(m_1+m_2)^2}\sqrt{\frac{2}{\pi}}\ , \tag{7.42}$$

$$2S: \quad F_1(x) = \frac{1}{2}Q_q^2\ e^{-2\nu k^z(x)^2}\left(\frac{5}{6}-\frac{4}{3}\nu k^z(x)^2+\frac{8}{3}\nu^2 k^z(x)^4\right)\sqrt{\nu(m_1+m_2)^2}\sqrt{\frac{2}{\pi}}\ . \tag{7.43}$$

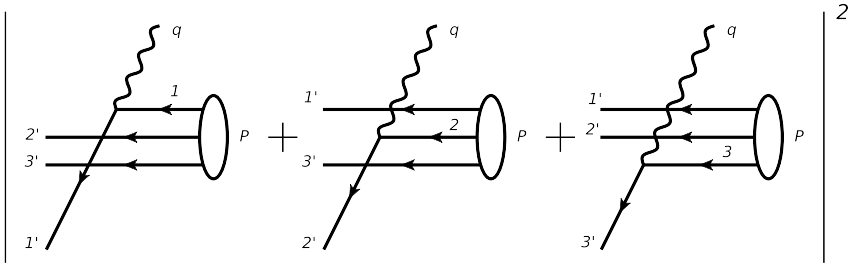

Figure 7.5: Leading contribution to the hadronic tensor of baryons in DIS.

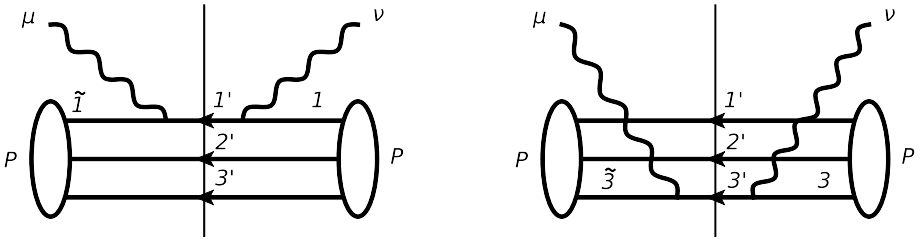

Figure 7.6: Contributions to hadronic tensor from quarks 1 (left) and 3 (right).

Figure 7.4 presents plots of the structure functions for mesons. For $c\bar{b}$ mesons the left peak is due to the charm quark contribution and the right peak is due to bottom quark contribution. The individual quark contributions include squared charges of the quarks, therefore, the left peak is higher. The flat tops of F_1 for $1P$ states arise because wave function is zero at $|\vec{k}\,| = 0$. The steps of F_1 for $2S$ states are an effect of zero of the wave function at some $|\vec{k}\,| > 0$.

7.3 Baryons

Similarly as for quarkonia, the sum over intermediate states in Eq. (7.6) is replaced with the sum over final quarks, and the delta function is approximated by the delta of free quarks instead of free hadrons,

$$\sum_X |X\rangle\langle X|\ \delta^{(4)}(P+q-P_X) \quad \to \quad \frac{1}{n!}\int_{1'2'3'} b^\dagger_{1'} b^\dagger_{2'} b^\dagger_{3'} |0\rangle\langle 0| b_{3'} b_{2'} b_{1'}\ \delta^{(4)}(P+q-p_{1'}-p_{2'}-p_{3'})\ , \tag{7.44}$$

where n is the number of identical quarks. Baryon states are given in Eqs. (4.25) and (4.26). I focus on mixed-flavor baryons, but the results apply for single-flavor baryons too. Contributions from separate quarks add on the level of the scattering amplitude, which is then squared to obtain cross section, see Fig. 7.5. In the Bjorken limit the interference terms vanish, and quarks contribute separately, see Fig. 7.6. From Eq. (7.6),

$$\begin{aligned} W^{\mu\nu} &= \frac{1}{2}\sum_\sigma 2\frac{Q_q^2}{4\pi}\int [1'2'3'] \sum_{\sigma_{1'}\sigma_{2'}\sigma_{3'}} \sum_{\sigma_{\tilde{1}}\sigma_1} (2\pi)^4\delta^{(4)}(P+q-p_{1'}-p_{2'}-p_{3'})\psi^{\sigma\,*}_{\sigma_{\tilde{1}}\sigma_{2'}\sigma_{3'}} \frac{j^\mu_{\tilde{1}1'} j^\nu_{1'1}}{x_1^2} \psi^\sigma_{\sigma_1\sigma_{2'}\sigma_{3'}} \\ &+ \frac{1}{2}\sum_\sigma \frac{Q_{q'}^2}{4\pi}\int [1'2'3'] \sum_{\sigma_{1'}\sigma_{2'}\sigma_{3'}} \sum_{\sigma_{\tilde{3}}\sigma_3} (2\pi)^4\delta^{(4)}(P+q-p_{1'}-p_{2'}-p_{3'})\psi^{\sigma\,*}_{\sigma_{1'}\sigma_{2'}\sigma_{\tilde{3}}} \frac{j^\mu_{\tilde{3}3'} j^\nu_{3'3}}{x_3^2} \psi^\sigma_{\sigma_{1'}\sigma_{2'}\sigma_3}\ , \end{aligned} \tag{7.45}$$

where all wave functions are functions of $x_{1/12}$, $\kappa_{1/12}$, x_3, and κ_3. To simplify the notation I define, matrices whose components are enumerated with spin indices,

$$[\tilde{\rho}_{1\sigma'\sigma}]_{\sigma_1\sigma_{\tilde{1}}} = \sum_{\sigma_{2'}\sigma_{3'}} \psi^{\sigma}_{\sigma_1\sigma_{2'}\sigma_{3'}}\psi^{\sigma'*}_{\sigma_{\tilde{1}}\sigma_{2'}\sigma_{3'}} , \tag{7.46}$$

$$[\tilde{\rho}_{3\sigma'\sigma}]_{\sigma_3\sigma_{\tilde{3}}} = \sum_{\sigma_{1'}\sigma_{2'}} \psi^{\sigma}_{\sigma_{1'}\sigma_{2'}\sigma_3}\psi^{\sigma'*}_{\sigma_{1'}\sigma_{2'}\sigma_{\tilde{3}}} , \tag{7.47}$$

which differ from Eqs. (6.27) and (6.28) in momentum arguments, which here are the same for each wave function on the right hand side. Using Eqs. (6.29)–(6.34),

$$\begin{aligned} W^{\mu\nu} &= 2\frac{Q_q^2}{4\pi}\int [123]\tilde{\delta}_{123.P}\frac{1}{x_1^2}\mathrm{Tr}[\rho_{1,\sigma\sigma'}(\mathbf{j}_1^\mu)^\dagger \mathbf{j}_1^\nu](2\pi)\delta(P^- + q^- - p_{1'}^- - p_2^- - p_3^-) \\ &+ \frac{Q_{q'}^2}{4\pi}\int [123]\tilde{\delta}_{123.P}\frac{1}{x_3^2}\mathrm{Tr}[\rho_{3,\sigma\sigma'}(\mathbf{j}_3^\mu)^\dagger \mathbf{j}_3^\nu](2\pi)\delta(P^- + q^- - p_1^- - p_2^- - p_{3'}^-) . \end{aligned} \tag{7.48}$$

Because current matrices $\mathbf{j}_1^\mu$ and $\mathbf{j}_3^\mu$ are diagonal, only diagonal terms of $\tilde{\rho}_{1,\sigma\sigma}$ and $\tilde{\rho}_{3,\sigma\sigma}$ matter. Furthermore, $\tilde{\rho}_{1,\uparrow\uparrow} + \tilde{\rho}_{1,\downarrow\downarrow}$ and $\tilde{\rho}_{3,\uparrow\uparrow} + \tilde{\rho}_{3,\downarrow\downarrow}$ are proportional to unity matrix. Therefore,

$$\frac{1}{2}\sum_\sigma \mathrm{Tr}[\tilde{\rho}_{1,\sigma\sigma}(\mathbf{j}_1^\mu)^\dagger \mathbf{j}_1^\nu] = \frac{1}{2}|\psi_{1S1S}(x_{1/12},\kappa_{1/12},x_3,\kappa_3)|^2\ \tilde{V}_1^{\mu\nu} , \tag{7.49}$$

$$\frac{1}{2}\sum_\sigma \mathrm{Tr}[\tilde{\rho}_{3,\sigma\sigma}(\mathbf{j}_3^\mu)^\dagger \mathbf{j}_3^\nu] = \frac{1}{2}|\psi_{1S1S}(x_{1/12},\kappa_{1/12},x_3,\kappa_3)|^2\ \tilde{V}_3^{\mu\nu} . \tag{7.50}$$

For spin-3/2 ground states of baryons, the left hand side changes, $\frac{1}{2}$ is replaced with $\frac{1}{4}$, and the sum goes from $\sigma = -3/2$ to $\sigma = 3/2$, but new $\tilde{\rho}$ matrices sum up to value twice as big as for spin 1/2 and the right hand side is exactly the same. From here on, the reasoning and calculations continue in a way very much resembling the calculations in the quarkonium case. Therefore, I already write the results,

$$\begin{aligned} W_1 &= 2\frac{Q_q^2}{4\pi}\int [123]\tilde{\delta}_{123.P}\frac{2\kappa_1^2 - q^2}{x_1^2}\ f\ (2\pi)\delta(P^- + q^- - p_{1'}^- - p_2^- - p_3^-) \\ &+ \frac{Q_{q'}^2}{4\pi}\int [123]\tilde{\delta}_{123.P}\frac{2\kappa_3^2 - q^2}{x_3^2}\ f\ (2\pi)\delta(P^- + q^- - p_1^- - p_2^- - p_{3'}^-) , \end{aligned} \tag{7.51}$$

$$\begin{aligned} \frac{W_2}{M^2} &= 2\frac{Q_q^2}{4\pi}\int [123]\tilde{\delta}_{123.P}\ 4f\ (2\pi)\delta(P^- + q^- - p_{1'}^- - p_2^- - p_3^-) \\ &+ \frac{Q_{q'}^2}{4\pi}\int [123]\tilde{\delta}_{123.P}\ 4f\ (2\pi)\delta(P^- + q^- - p_1^- - p_2^- - p_{3'}^-) , \end{aligned} \tag{7.52}$$

where

$$f = |\psi_{1S1S}(x_{1/12},\kappa_{1/12},x_3,\kappa_3)|^2 . \tag{7.53}$$

Energy conservation deltas simplify in the Bjorken limit, *e.g.*, $\delta(P^- + q^- - p_1^- - p_2^- - p_{3'}^-) \approx \delta(q^- - p_{3'}^-) \approx (x^2P^+/Q^2)\delta(x_3 - x)$. The structure functions are then,

$$F_1(x,Q^2) = 2\cdot\frac{1}{2}Q_q^2\int [123]P^+\tilde{\delta}_{123.P}\ f\ \delta(x_1 - x) + \frac{1}{2}Q_{q'}^2\int [123]P^+\tilde{\delta}_{123.P}\ f\ \delta(x_3 - x) , \tag{7.54}$$

$$F_2(x,Q^2) = 2\cdot xQ_q^2\int [123]P^+\tilde{\delta}_{123.P}\ f\ \delta(x_1 - x) + xQ_{q'}^2\int [123]P^+\tilde{\delta}_{123.P}\ f\ \delta(x_3 - x) , \tag{7.55}$$

Again, these F_1 and F_2 do not depend on Q^2 and fulfill Callan-Gross relation. In the nonrelativistic limit,

$$\begin{aligned} F_1(x,Q^2) &= 2\cdot\frac{1}{2}Q_q^2\int\frac{d^2Q_1}{(2\pi)^2}\int\frac{d^3K_{23}}{(2\pi)^3}\frac{M_{123}}{2\pi}\,|\psi_{1S1S}|^2\Big|_{Q_{\tilde{1}}^z = Q_{\tilde{1}}^z(x)} \\ &+ \frac{1}{2}Q_{q'}^2\int\frac{d^2Q_3}{(2\pi)^2}\int\frac{d^3K_{12}}{(2\pi)^3}\frac{M_{123}}{2\pi}\,|\psi_{1S1S}|^2\Big|_{Q_{\tilde{3}}^z = Q_{\tilde{3}}^z(x)} , \end{aligned} \tag{7.56}$$

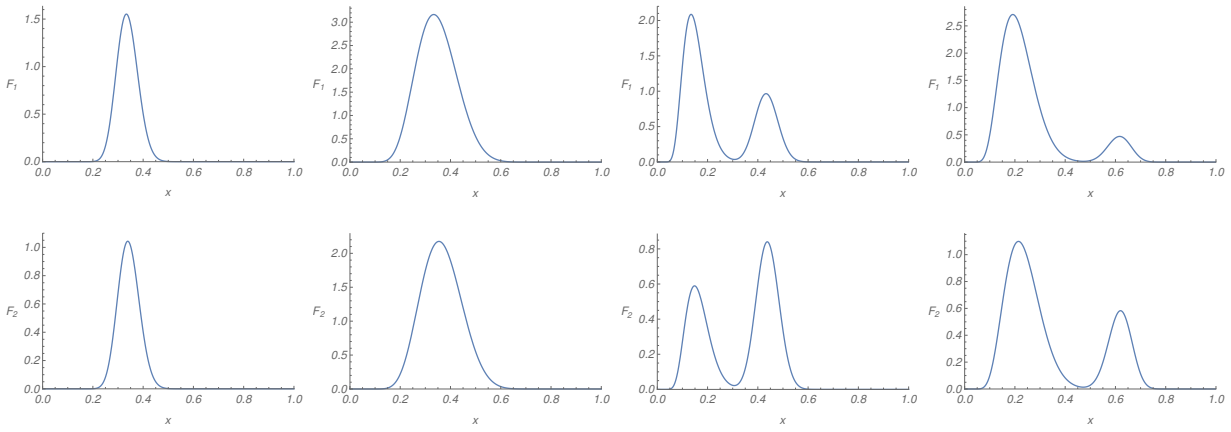

(a) **(b)** **(c)** **(d)**

Figure 7.7: Structure functions $F_1(x)$ and $F_2(x)$ for (a) *bbb*, (b) *ccc*, (c) *bbc*, and (d) *ccb* particles.

where in the first integral wave function needs to be expressed in terms of $\vec{K}_{23}$ and $\vec{Q}_1$ through,

$$\vec{K}_{12} = -\frac{1}{2}\vec{K}_{23} + \frac{1}{2(\beta_1+\beta_3)}\vec{Q}_1 \ , \tag{7.57}$$

$$\vec{Q}_3 = -\vec{K}_{23} - \frac{\beta_3}{\beta_1+\beta_3}\vec{Q}_1 \ , \tag{7.58}$$

and

$$Q_i^z(x) = \sqrt{\frac{\beta_i(1-\beta_i)}{x(1-x)}}M_{123}(x-\beta_i) \ . \tag{7.59}$$

The final result for the ground state of QQQ' (and QQQ) is,

$$\begin{aligned} F_1(x) &= 2\cdot\frac{1}{2}Q_q^2\ e^{-\frac{8\nu_{12}\nu_{3(12)}}{\nu_{12}+4\nu_{3(12)}}[Q_1^z(x)]^2}\ 2M_{123}\sqrt{\frac{\nu_{12}\nu_{3(12)}}{\nu_{12}+4\nu_{3(12)}}}\ \sqrt{\frac{2}{\pi}} \\ &+ \frac{1}{2}Q_{q'}^2\ e^{-2\nu_{3(12)}[Q_3^z(x)]^2}M_{123}\sqrt{\nu_{3(12)}}\sqrt{\frac{2}{\pi}} \ . \end{aligned} \tag{7.60}$$

Figure 7.7 presents the results for the structure functions of baryons. The left peaks in mixed-flavor baryons correspond to charm quarks and are usually higher than right peaks that correspond to bottom quarks, because charm quark has electric charge twice as big as the bottom quark (up to sign). The structure functions of single-flavor baryons are peaked in the vicinity of $x \sim 1/3$ as expected, because on average all three quarks share momentum equally.

Approximations I adopted are too crude for my results to reproduce qualitative features like logarithmic evolution in Q^2 and other. For example, the structure functions that I calculated fall off exponentially near $x \sim 1$ instead of according to a power law [114]. However, $x \sim 1$ means large momentum Q^z, while baryon wave functions in nonrelativistic approximations are supposed to be good only for momenta small compared to hadron mass. Similarly for $x \approx 0$ the description needs to include more Fock sectors to aim at reproducing data.

Chapter 8

Conclusion

8.1 Summary of theory and results

The thesis presents a study of bound states of heavy quarks in heavy-flavor QCD (a theory without light quarks). The theory is written in the FF of Hamiltonian dynamics, with the canonical Hamiltonian as a starting point that needs regularization and renormalization. It is renormalized using renormalization group procedure for effective particles. The RGPEP operates with the concept of effective particles whose size is a scale parameter of renormalization group transformation. The renormalized Hamiltonian, written in terms of creation and annihilation operators for effective particles, is finite when the regularization cutoff on transverse momenta is sent to infinity. Asymptotic freedom follows and allows one to compute the renormalized Hamiltonian in perturbation theory at hadronic scales. I limit the calculation to the terms that are of second order in the effective coupling constant. The renormalized Hamiltonian eigenvalue equation, written in the whole Fock space of effective particles, is replaced by the eigenvalue equation written in terms of only two sectors of the Fock space – one containing the minimal quark content ($Q\bar{Q}$ for mesons and QQQ for baryons), and the other one that in addition to the quarks contains also just one effective gluon. The replacement is made plausible by the additional step, which is the assumption that in the reduced eigenvalue equation the gluon has mass, which is allowed to be a function of the gluon momentum relative to the quarks. In contrast to sectors with gluons, sectors with extra quark-antiquark pairs may be safely omitted because the renormalized Hamiltonian does not allow interactions to change invariant masses of states by much more than the RGPEP scale parameter. The sector with one massive gluon is then eliminated using the perturbative procedure of Bloch. The resulting effective Hamiltonians for $Q\bar{Q}$ and QQQ states contain the RGPEP form factors in interaction vertices and can be approximated by the form they take in the nonrelativistic limit. Finally, the effective approximate Hamiltonians turn out to contain the Coulomb potentials and harmonic oscillator potentials between quarks. Using the effective Hamiltonians, approximate masses and wave functions of heavy hadrons are found.

I calculated the mass spectra of mesons and baryons and I derived formulas for their electromagnetic form factors in elastic scattering and their structure functions in the electron deep inelastic scattering off them. Masses of quarks at the corresponding RGPEP scale parameters were fitted to the masses of the three lightest spin-1 states (excluding 1^{+-} states) in each of the meson families – bottomonia and charmonia. The coupling constant was evaluated using the leading asymptotic freedom formula for two flavors. The results for masses of ground states of bbb and ccc baryons contain no free parameters and they agree well with predictions of other theoretical approaches. The excitation spectrum is in a qualitative agreement with lattice QCD studies. Therefore, these results constitute a firm foothold for future studies of bound states in QCD with one flavor of heavy quarks using our method. The results for ccb and bbc baryons, as well as $c\bar{b}$ and $b\bar{c}$ mesons, bear some theoretical uncertainty due to the universal mass shift that appears because of significant scale difference between bottom and charm quark masses. The shift depends strongly on the gluon mass ansatz and may be of the order of spin-splittings. This suggests that systems with two differ-

ent mass scales probably need more complicated renormalization-group scale setting than the one we used. There may also be some other terms than the gluon mass in the effective Hamiltonians that become important when masses of quarks in a bound state differ significantly. These other terms will have to be found and one needs to check if they cancel the ansatz-dependent universal mass shift for hadrons built from different quarks. Future studies will provide the required insight. Present calculations predict that in ccb the two charm quarks form a tight diquark, while in bbc the bottom quarks are bound with each other more loosely than with the charm quark.

I calculated the form factors of the hadrons I found and I used them to compute the radii of these hadrons. My results for the radii agree well with results found in literature and especially good agreement is obtained with the lattice calculations wherever comparison is possible. I also calculated magnetic moments of baryons and vector quarkonia. Comparison with literature shows that for systems that involve only one flavor of quarks my results agree with other theoretical predictions, and for systems that involve both charm and bottom quarks the moments are larger than those predicted using other methods.

The hadron structure functions I computed in a simplified way. I neglected the huge difference between the scale of quark binding and the scale of the virtual photon in deep inelastic scattering (formally infinite). My calculations show interesting features, such as dependence of the structure function shape on the wave function nodes. However, my calculations of the structure functions can be considered merely a demonstration of potential utility of the method, because I approximated the transformation that connects effective particles at two different RGPEP scales, that of DIS and that of bound-state formation, by identity. Corrections due to scale evolution are not included.

8.2 Foreseeable corrections

One direction of future studies, which I am convinced are necessary, is the fourth-order calculation of the renormalized Hamiltonian. They could allow us, I believe, to remove the gluon-mass ansatz or move it to the sector with two effective gluons. The resulting effective Hamiltonians will contain all interaction terms that are of order k^2/m^2 with respect to the Coulomb potential, including all the Breit-Fermi spin-dependent interactions, and improving the accuracy of calculations. Wave functions obtained from effective Hamiltonians accurate to fourth order of perturbation theory, and third-order photon-quark vertex, should provide more realistic results for elastic form factors of heavy hadrons than my calculations. However, to construct fully relativistic scattering amplitudes, it is also necessary to study the full set of renormalized operators that form the Poincare algebra. The full set includes the spatial rotation operators that are needed for rotating the states in a way that properly includes interactions.

Another line of foreseeable research concerns nonperturbative calculations that involve Hamiltonians acting on spaces composed of at least two Fock sectors. Such calculations are needed to obtain reliable results for highly excited states. Such states may have large components in sectors with gluons, and hence, may be not describable using perturbative elimination of sectors with gluons. For example, in the bottomonium family of states already $\Upsilon(3S)$, whose mass is by 895 MeV larger than the mass of $\Upsilon(1S)$, may be considered highly excited.

The serious problem that one probably has to face is that gluons in QCD are massless. In perturbation theory this fact implies that sectors with gluons have norms that diverge with the small-x cutoff. The gluon mass ansatz that I adopted is not sufficient to guarantee that the nonperturbative eigenvalue problem in two sectors does not depend on the ansatz. Depending on the exact form of the gluon mass ansatz, either the one-sector effective eigenvalue equation is free from small-x divergences or the norm of the higher component of the eigenstate (the one with the one massive gluon) in the two-sector problem is free from small-x divergences, but not both. However, this conclusion, based on perturbative calculation of gluon component, does not take into account other interactions that are present in the sector with the gluon. The nonperturbatively calculated norm is not known.

An important direction of future studies is a calculation of structure functions that uses trans-

formation $\mathcal{W}_{Q\lambda}$, which relates particles at the scale of the momentum transfer Q to the particles at the scale of quark binding λ. As explained in Chapter 7 such calculation would aim to establish the evolution of structure functions in the framework of renormalized Hamiltonian dynamics of effective particles.

Renormalization group procedure for effective particles can in principle be applied to describe also light particles like proton. However, substantial development of the method is needed in the area of nonperturbative solutions of the RGPEP equation, since at the mass scales of light quarks the coupling constant is not small. Moreover, the quantitative explanation of chiral symmetry breaking in the FF of Hamiltonian QCD is still missing.

Appendix A

Symmetric wave functions of baryons

In the case of three identical quarks wave functions of baryons have to be fully antisymmetric and because the color wave function is fully antisymmetric, the spin-momentum wave function needs to be fully symmetric. The prescriptions of how to construct fully symmetric spin-momentum wave functions from spin and momentum wave functions are given in Table 5.2. Here I list their explicit forms, but only for the states of highest angular momentum projection on the z axis in each multiplet. The ground state is,

$$\left|0\omega,\frac{3}{2}^{+},J_z\right\rangle \;=\; |1S1S\rangle|J_z\rangle\;, \tag{A.1}$$

where $J_z = +3/2, +1/2, -1/2, -3/2$. The states of the first band of harmonic oscillator are,

$$\begin{aligned}
\left|1\omega,\frac{3}{2}^{-},+\frac{3}{2}\right\rangle &= \frac{1}{\sqrt{2}}|1P_1 1S\rangle\left|+\frac{1}{2}A\right\rangle - \frac{1}{\sqrt{2}}|1S1P_1\rangle\left|+\frac{1}{2}S\right\rangle\;, &\text{(A.2)}\\
\left|1\omega,\frac{1}{2}^{-},+\frac{1}{2}\right\rangle &= -\frac{1}{\sqrt{6}}|1P_0 1S\rangle\left|+\frac{1}{2}A\right\rangle + \frac{1}{\sqrt{3}}|1P_1 1S\rangle\left|-\frac{1}{2}A\right\rangle\\
&+ \frac{1}{\sqrt{6}}|1S1P_0\rangle\left|+\frac{1}{2}S\right\rangle - \frac{1}{\sqrt{3}}|1S1P_1\rangle\left|-\frac{1}{2}S\right\rangle\;. &\text{(A.3)}
\end{aligned}$$

The symmetric states of the second band of excitations of harmonic oscillators are,

$$\begin{aligned}
\left|A_{\frac{3}{2}^{+}},+\frac{3}{2}\right\rangle &= |2S1S\rangle_{+}\left|+\frac{3}{2}\right\rangle\;, &\text{(A.4)}\\
\left|B_{\frac{1}{2}^{+}},+\frac{1}{2}\right\rangle &= \frac{1}{\sqrt{2}}|2S1S\rangle_{-}\left|+\frac{1}{2}S\right\rangle - \frac{1}{\sqrt{2}}|0,0\rangle\left|+\frac{1}{2}A\right\rangle\;, &\text{(A.5)}\\
\left|C_{\frac{7}{2}^{+}},+\frac{7}{2}\right\rangle &= |1D_2 1S\rangle_{+}\left|+\frac{3}{2}\right\rangle\;, &\text{(A.6)}\\
\left|C_{\frac{5}{2}^{+}},+\frac{5}{2}\right\rangle &= -\sqrt{\frac{3}{7}}|1D_1 1S\rangle_{+}\left|+\frac{3}{2}\right\rangle + \sqrt{\frac{4}{7}}|1D_2 1S\rangle_{+}\left|+\frac{1}{2}\right\rangle\;, &\text{(A.7)}\\
\left|C_{\frac{3}{2}^{+}},+\frac{3}{2}\right\rangle &= \sqrt{\frac{1}{5}}|1D_0 1S\rangle_{+}\left|+\frac{3}{2}\right\rangle - \sqrt{\frac{2}{5}}|1D_1 1S\rangle_{+}\left|+\frac{1}{2}\right\rangle + \sqrt{\frac{2}{5}}|1D_2 1S\rangle_{+}\left|-\frac{1}{2}\right\rangle\;, &\text{(A.8)}\\
\left|C_{\frac{1}{2}^{+}},+\frac{1}{2}\right\rangle &= -\sqrt{\frac{1}{10}}|1D_{-1} 1S\rangle_{+}\left|+\frac{3}{2}\right\rangle + \sqrt{\frac{1}{5}}|1D_0 1S\rangle_{+}\left|+\frac{1}{2}\right\rangle\\
&- \sqrt{\frac{3}{10}}|1D_1 1S\rangle_{+}\left|-\frac{1}{2}\right\rangle + \sqrt{\frac{2}{5}}|1D_2 1S\rangle_{+}\left|-\frac{3}{2}\right\rangle\;, &\text{(A.9)}
\end{aligned}$$

$$\left|D_{\frac{5}{2}^+},+\frac{5}{2}\right\rangle = \frac{1}{\sqrt{2}}|1D_2 1S\rangle_-\left|+\frac{1}{2}S\right\rangle - \frac{1}{\sqrt{2}}|2,+2\rangle\left|+\frac{1}{2}A\right\rangle , \tag{A.10}$$

$$\begin{aligned}\left|D_{\frac{3}{2}^+},+\frac{3}{2}\right\rangle &= -\sqrt{\frac{1}{10}}|1D_1 1S\rangle_-\left|+\frac{1}{2}S\right\rangle + \sqrt{\frac{2}{5}}|1D_2 1S\rangle_-\left|-\frac{1}{2}S\right\rangle \\ &+ \sqrt{\frac{1}{10}}|2,+1\rangle\left|+\frac{1}{2}A\right\rangle - \sqrt{\frac{2}{5}}|2,+2\rangle\left|-\frac{1}{2}A\right\rangle ,\end{aligned} \tag{A.11}$$

where

$$|2S1S\rangle_\pm = \frac{|2S1S\rangle \pm |1S2S\rangle}{\sqrt{2}} , \tag{A.12}$$

$$|1D_m 1S\rangle_\pm = \frac{|1D_m 1S\rangle \pm |1S1D_m\rangle}{\sqrt{2}} . \tag{A.13}$$

For the purposes of App. B I list also $L = 0$ states of the fourth band of excited states of the harmonic oscillators in baryons [62],

$$|E\rangle = \left(\sqrt{\frac{5}{8}}|3S1S\rangle_+ + \sqrt{\frac{3}{8}}|2S2S\rangle\right)\left|+\frac{3}{2}\right\rangle , \tag{A.14}$$

$$|F\rangle = \left(\sqrt{\frac{15}{36}}|3S1S\rangle_+ - \sqrt{\frac{1}{36}}|2S2S\rangle + \sqrt{\frac{20}{36}}|1D1D_{L=0}\rangle\right)\left|+\frac{3}{2}\right\rangle , \tag{A.15}$$

$$|G\rangle = \frac{1}{\sqrt{2}}|3S1S\rangle_-\left|+\frac{1}{2}S\right\rangle - \frac{1}{\sqrt{2}}|2P1P_{L=0}\rangle_+\left|+\frac{1}{2}A\right\rangle , \tag{A.16}$$

$$\begin{aligned}|H\rangle &= \frac{1}{\sqrt{2}}\left(-\sqrt{\frac{3}{12}}|3S1S\rangle_+ + \sqrt{\frac{5}{12}}|2S2S\rangle + \sqrt{\frac{4}{12}}|1D1D_{L=0}\rangle\right)\left|+\frac{1}{2}S\right\rangle \\ &- \frac{1}{\sqrt{2}}|2P1P_{L=0}\rangle_-\left|+\frac{1}{2}A\right\rangle ,\end{aligned} \tag{A.17}$$

where

$$|3S1S\rangle_\pm = \frac{|3S1S\rangle \pm |1S3S\rangle}{\sqrt{2}} , \tag{A.18}$$

$$|2P1P_{L=0}\rangle_\pm = \frac{|2P1P_{L=0}\rangle \pm |1P2P_{L=0}\rangle}{\sqrt{2}} . \tag{A.19}$$

Appendix B

Test of magnitude of Coulomb interactions in baryons

In Chapter 5 I solve Eq. (4.94) by treating Coulomb interactions as perturbations and I do it in the first order of perturbation theory. The unperturbed wave functions are constructed from harmonic oscillator wave functions. To test if such approach is justified, I calculate the effective Hamiltonian in the basis of all states that have zero orbital angular momentum, $L = 0$, and whose unperturbed energies reach 4ω, and diagonalize it. I compare the resulting energies with the first order results. The states that I have to take into account are the ground state, the second-band states A and B, and fourth-band states listed in App. A. I group those states into two groups: spin-3/2 and positive parity states $|0\omega\rangle$, $|A\rangle$, $|E\rangle$ and $|F\rangle$, and spin-1/2 and positive parity states $|B\rangle$, $|G\rangle$ and $|H\rangle$. Hamiltonian matrix elements between any state from one group and any state from the other group are zero, because we neglect spin interactions. Furthermore, in each group, there are no interactions between states with different spin projections on z axis, they are degenerated and Coulomb potential cannot introduce splittings between them. Therefore, I can restrict my attention to subspaces composed of states with the highest possible spin projection on z-axis. The Coulomb interaction in the subspace of the $3/2^+$ states is described by the Hamiltonian matrix,

$$V^{3/2^+}_{L=0,IJ} \;=\; \langle I|\hat{V}_C|J\rangle \;=\; -\frac{2}{3}\alpha\sqrt{\frac{2m\omega}{\pi}}\tilde{V}^{3/2^+}_{L=0,IJ}\;, \tag{B.1}$$

where $I, J = 0\omega, A, E, F$, and

$$\tilde{V}^{3/2^+}_{L=0} \;=\; 3\begin{array}{c}\left[\begin{array}{cccc} \frac{131}{192} & \frac{169}{192\sqrt{6}} & -\frac{7}{48\sqrt{3}} & \frac{1}{8} \\ \frac{169}{192\sqrt{6}} & \frac{329}{384} & -\frac{23}{48\sqrt{2}} & \frac{\sqrt{3}}{8\sqrt{2}} \\ -\frac{7}{48\sqrt{3}} & -\frac{23}{48\sqrt{2}} & \frac{11}{12} & -\frac{1}{2\sqrt{3}} \\ \frac{1}{8} & \frac{\sqrt{3}}{8\sqrt{2}} & -\frac{1}{2\sqrt{3}} & 1 \end{array}\right] \begin{array}{c} F \\ E \\ A \\ 0\omega \end{array} \\ F \quad E \quad A \quad 0\omega \end{array} \tag{B.2}$$

$$\;=\; 3\left[\begin{array}{cccc} 0.6823 & 0.3593 & -0.0842 & 0.1250 \\ 0.3593 & 0.8568 & -0.3388 & 0.1531 \\ -0.0842 & -0.3388 & 0.9167 & -0.2887 \\ 0.1250 & 0.1531 & -0.2887 & 1.0000 \end{array}\right]. \tag{B.3}$$

The Coulomb interaction in the subspace of $1/2^+$ states B, G and H is described by the Hamiltonian matrix,

$$V^{1/2^+}_{L=0,IJ} \;=\; \langle I|\hat{V}_C|J\rangle \;=\; -\frac{2}{3}\alpha\sqrt{\frac{2m\omega}{\pi}}\tilde{V}^{1/2^+}_{L=0,IJ}\;, \tag{B.4}$$

where $I, J = B, G, H$, and

$$\tilde{V}^{1/2^+}_{L=0} = 3 \begin{bmatrix} \frac{1321}{1920} & \frac{1}{64} & \frac{\sqrt{5}}{32} \\ \frac{1}{64} & \frac{361}{480} & -\frac{19}{48\sqrt{5}} \\ \frac{\sqrt{5}}{32} & -\frac{19}{48\sqrt{5}} & \frac{19}{24} \end{bmatrix} \begin{matrix} H \\ G \\ B \end{matrix} = 3 \begin{bmatrix} 0.6880 & 0.01562 & 0.06988 \\ 0.01562 & 0.7521 & -0.1770 \\ 0.06988 & -0.1770 & 0.7917 \end{bmatrix}. \quad \text{(B.5)}$$
$$H \quad G \quad B$$

The unperturbed Hamiltonians are

$$H^{(0)}_{3/2^+} = \begin{bmatrix} 7\omega & & & \\ & 7\omega & & \\ & & 5\omega & \\ & & & 3\omega \end{bmatrix}, \qquad H^{(0)}_{1/2^+} = \begin{bmatrix} 7\omega & & \\ & 7\omega & \\ & & 5\omega \end{bmatrix}, \quad \text{(B.6)}$$

where off-diagonal elements are zero. In the zeroth order the eigenvectors are $|0\omega\rangle$, $|A\rangle$, $|E\rangle$, $|F\rangle$ and $|B\rangle$, $|G\rangle$, $|H\rangle$, and their energies are given by the diagonal elements of unperturbed Hamiltonians. In the first order of perturbation theory only the diagonal elements of the interaction Hamiltonian are taken into account, with the exception of states that are degenerated in the unperturbed Hamiltonian. States E, F, G and H are degenerated, therefore, the first order perturbation theory is equivalent to diagonalizing the following matrices,

$$H^{(1)}_{3/2^+} = H^{(0)}_{3/2^+} - 2\alpha\sqrt{\frac{2m\omega}{\pi}} \begin{bmatrix} \frac{131}{192} & \frac{169}{192\sqrt{6}} & & \\ \frac{169}{192\sqrt{6}} & \frac{329}{384} & & \\ & & \frac{11}{12} & \\ & & & 1 \end{bmatrix}, \quad \text{(B.7)}$$

$$H^{(1)}_{1/2^+} = H^{(0)}_{1/2^+} - 2\alpha\sqrt{\frac{2m\omega}{\pi}} \begin{bmatrix} \frac{1321}{1920} & \frac{1}{64} & \\ \frac{1}{64} & \frac{361}{480} & \\ & & \frac{19}{24} \end{bmatrix}. \quad \text{(B.8)}$$

As a result, I obtain energies that are listed in Table B.1. The eigenstates of the fourth-band subspace are $|E'\rangle$, $|F'\rangle$, $|G'\rangle$ and $|H'\rangle$. Quark masses and harmonic oscillator frequencies are taken from the fits presented in Chapter 5. A better estimate for eigenstates of Eq. (4.94) is obtained by diagonalizing the full Hamiltonians,

$$H_{3/2^+} = H^{(0)}_{3/2^+} + V^{3/2^+}_{L=0}, \quad \text{(B.9)}$$

$$H_{1/2^+} = H^{(0)}_{1/2^+} + V^{1/2^+}_{L=0}. \quad \text{(B.10)}$$

The results for the energies are listed in Table B.1, which presents comparison between the two methods of calculating the energies. The difference is small enough to justify applicability of the first order perturbation theory. It is also worth mentioning that the energies of the states would shift further if one included states from higher and higher bands of harmonic oscillator, however, these shifts quickly become very small because of RGPEP form factor that accompanies the Coulomb potential in Eq. (4.94).

	Energies of states [MeV]						
	0ω	A	E'	F'	B	G'	H'
First order perturbation theory, *bbb*	253.8	756.5	1123	1452	812.0	1294	1325
Diagonalization of Hamiltonian matrix, *bbb*	207.0	747.9	1172	1458	797.9	1302	1331
First order perturbation theory, *ccc*	436.0	1026	1494	1790	1076	1648	1676
Diagonalization of Hamiltonian matrix, *ccc*	404.6	1019	1528	1794	1066	1654	1680

Table B.1: Comparison of the two ways of computing energies of *bbb* and *ccc* baryons.

Appendix C

List of masses of mesons and baryons

Here I provide the complete list of formulas for masses of heavy mesons and baryons that are plotted in Figs. 5.1, 5.2 and 5.3.

The masses of mesons are computed using the following equation,

$$M = (m_1 + m_2)\sqrt{1 + \frac{2E}{m_1 + m_2}} , \tag{C.1}$$

where E for different meson states are,

$$E_{1S} = \frac{3}{2}\omega - \frac{4}{3}\alpha\sqrt{\frac{2}{\pi\nu}} , \tag{C.2}$$

$$E_{2S} = \frac{7}{2}\omega - \frac{10}{9}\alpha\sqrt{\frac{2}{\pi\nu}} , \tag{C.3}$$

$$E_{3S} = \frac{11}{2}\omega - \frac{89}{90}\alpha\sqrt{\frac{2}{\pi\nu}} , \tag{C.4}$$

$$E_{1P} = \frac{5}{2}\omega - \frac{8}{9}\alpha\sqrt{\frac{2}{\pi\nu}} , \tag{C.5}$$

$$E_{2P} = \frac{9}{2}\omega - \frac{4}{5}\alpha\sqrt{\frac{2}{\pi\nu}} , \tag{C.6}$$

$$E_{1D} = \frac{7}{2}\omega - \frac{32}{45}\alpha\sqrt{\frac{2}{\pi\nu}} , \tag{C.7}$$

$$E_{2D} = \frac{11}{2}\omega - \frac{208}{315}\alpha\sqrt{\frac{2}{\pi\nu}} . \tag{C.8}$$

The masses of baryons are computed using the following equation,

$$M = (m_1 + m_2 + m_3)\sqrt{1 + \frac{2E}{m_1 + m_2 + m_3}} , \tag{C.9}$$

where E for different baryon states are,

$$E = \omega_{12}\left(2k_{12} + l_{12} + \frac{3}{2}\right) + \omega_{3(12)}\left(2k_{3(12)} + l_{3(12)} + \frac{3}{2}\right) + V , \tag{C.10}$$

and V is the expectation value of Coulomb interaction terms computed in the harmonic oscillator eigenstates. For example, state $1P1P_{L=0}$ has $k_{3(12)} = k_{12} = 0$, $l_{3(12)} = l_{12} = 1$, and the binding energy E is,

$$E^{L=0}_{1P1P} = \frac{5}{2}\omega_{12} + \frac{5}{2}\omega_{3(12)} + V^{L=0}_{1P1P} . \tag{C.11}$$

It is convenient to define,

$$V = -\frac{2}{3}\alpha\sqrt{\frac{2}{\pi\nu_{12}}}\tilde{V} \tag{C.12}$$

and

$$x = \frac{4\nu_{3(12)}}{\nu_{12}} = \frac{\omega_{12}}{\beta_3\omega_{3(12)}} \, . \tag{C.13}$$

For the states composed of three identical quarks listed in Table 5.2,

$$\tilde{V}_{1S1S} = 3 \, , \tag{C.14}$$
$$\tilde{V}_{1\omega} = \frac{5}{2} \, , \tag{C.15}$$
$$\tilde{V}_{A} = \frac{11}{4} \, , \tag{C.16}$$
$$\tilde{V}_{B} = \frac{19}{8} \, , \tag{C.17}$$
$$\tilde{V}_{C} = \frac{23}{10} \, , \tag{C.18}$$
$$\tilde{V}_{D} = \frac{43}{20} \, . \tag{C.19}$$

For states with only the two first quarks identical listed in Table 5.1,

$$\tilde{V}_{1S1S} = 1 + \frac{4}{\sqrt{1+x}} \, , \tag{C.20}$$
$$\tilde{V}_{1P1S} = \frac{2}{3} + \frac{4\,(3x+2)}{3(1+x)^{3/2}} \, , \tag{C.21}$$
$$\tilde{V}_{1S1P} = 1 + \frac{4(2x+3)}{3(1+x)^{3/2}} \, , \tag{C.22}$$
$$\tilde{V}^{L=0}_{1P1P} = \frac{2}{3} + \frac{4(2x^2+7x+2)}{3(1+x)^{5/2}} \, , \tag{C.23}$$
$$\tilde{V}^{L=1}_{1P1P} = \frac{2}{3} + \frac{8}{3\sqrt{x+1}} \, , \tag{C.24}$$
$$\tilde{V}^{L=2}_{1P1P} = \frac{2}{3} + \frac{8\left(5x^2+13x+5\right)}{15(x+1)^{5/2}} \, , \tag{C.25}$$
$$\tilde{V}_{1D1S} = \frac{8}{15} + \frac{4\left(15x^2+20x+8\right)}{15(1+x)^{5/2}} \, , \tag{C.26}$$
$$\tilde{V}_{1S1D} = 1 + \frac{4\left(8x^2+20x+15\right)}{15(1+x)^{5/2}} \, , \tag{C.27}$$
$$\tilde{V}_{2S1S} = \frac{5}{6} + \frac{2\left(6x^2+8x+5\right)}{3(1+x)^{5/2}} \, , \tag{C.28}$$
$$\tilde{V}_{1S2S} = 1 + \frac{2\left(5x^2+8x+6\right)}{3(1+x)^{5/2}} \, . \tag{C.29}$$

Bibliography

[1] D. J. Gross and F. Wilczek, "Ultraviolet Behavior of Nonabelian Gauge Theories," Phys. Rev. Lett. **30** (1973) 1343–1346.

[2] H. D. Politzer, "Reliable Perturbative Results for Strong Interactions?," Phys. Rev. Lett. **30** (1973) 1346–1349.

[3] M. Gómez-Rocha and S. D. Głazek, "Asymptotic freedom in the front-form Hamiltonian for quantum chromodynamics of gluons," Phys. Rev. **D92** no. 6, (2015) 065005, arXiv:1505.06688 [hep-ph].

[4] S. D. Glazek, "Perturbative formulae for relativistic interactions of effective particles," Acta Phys. Polon. **B43** (2012) 1843–1862, arXiv:1204.4760 [hep-th].

[5] K. G. Wilson, T. S. Walhout, A. Harindranath, W.-M. Zhang, R. J. Perry, and S. D. Glazek, "Nonperturbative QCD: A Weak coupling treatment on the light front," Phys. Rev. **D49** (1994) 6720–6766, arXiv:hep-th/9401153 [hep-th].

[6] S. D. Głazek, M. Gómez-Rocha, J. More, and K. Serafin, "Renormalized quark–antiquark Hamiltonian induced by a gluon mass ansatz in heavy-flavor QCD," Phys. Lett. **B773** (2017) 172–178, arXiv:1705.07629 [hep-ph].

[7] K. Serafin, M. Gómez-Rocha, J. More, and S. D. Głazek, "Approximate Hamiltonian for baryons in heavy-flavor QCD," Eur. Phys. J. **C78** no. 11, (2018) 964, arXiv:1805.03436 [hep-ph].

[8] P. A. M. Dirac, "Forms of Relativistic Dynamics," Rev. Mod. Phys. **21** (1949) 392–399.

[9] S. J. Brodsky, H.-C. Pauli, and S. S. Pinsky, "Quantum chromodynamics and other field theories on the light cone," Phys. Rept. **301** (1998) 299–486, arXiv:hep-ph/9705477 [hep-ph].

[10] S. J. Brodsky, C. D. Roberts, R. Shrock, and P. C. Tandy, "Confinement contains condensates," Phys. Rev. **C85** (2012) 065202, arXiv:1202.2376 [nucl-th].

[11] S. D. Glazek, "Fermion mass mixing and vacuum triviality in the renormalization group procedure for effective particles," Phys. Rev. **D87** no. 12, (2013) 125032, arXiv:1305.3702 [hep-th].

[12] F. J. Dyson, "The S matrix in quantum electrodynamics," Phys. Rev. **75** (1949) 1736–1755.

[13] J. S. Schwinger, "On the Green's functions of quantized fields. 1.," Proc. Nat. Acad. Sci. **37** (1951) 452–455.

[14] C. D. Roberts and A. G. Williams, "Dyson-Schwinger equations and their application to hadronic physics," Prog. Part. Nucl. Phys. **33** (1994) 477–575, arXiv:hep-ph/9403224 [hep-ph].

[15] G. Eichmann, H. Sanchis-Alepuz, R. Williams, R. Alkofer, and C. S. Fischer, "Baryons as relativistic three-quark bound states," Prog. Part. Nucl. Phys. **91** (2016) 1–100, arXiv:1606.09602 [hep-ph].

[16] T. Hilger, M. Gómez-Rocha, A. Krassnigg, and W. Lucha, "Aspects of open-flavour mesons in a comprehensive DSBSE study," Eur. Phys. J. **A53** no. 10, (2017) 213, arXiv:1702.06262 [hep-ph].

[17] S. Strauss, C. S. Fischer, and C. Kellermann, "Analytic structure of the Landau gauge gluon propagator," Phys. Rev. Lett. **109** (2012) 252001, arXiv:1208.6239 [hep-ph].

[18] E. L. Solis, C. S. R. Costa, V. V. Luiz, and G. Krein, "Quark propagator in Minkowski space," Few Body Syst. **60** no. 3, (2019) 49, arXiv:1905.08710 [hep-ph].

[19] K. G. Wilson, "Confinement of Quarks," Phys. Rev. **D10** (1974) 2445–2459. [,319(1974)].

[20] S. Aoki et al., "Review of lattice results concerning low-energy particle physics," Eur. Phys. J. **C74** (2014) 2890, arXiv:1310.8555 [hep-lat].

[21] **Particle Data Group** Collaboration, M. Tanabashi et al., "Review of Particle Physics," Phys. Rev. **D98** no. 3, (2018) 030001.

[22] X. Ji, "Parton Physics on a Euclidean Lattice," Phys. Rev. Lett. **110** (2013) 262002, arXiv:1305.1539 [hep-ph].

[23] C. Alexandrou, K. Cichy, M. Constantinou, K. Hadjiyiannakou, K. Jansen, F. Steffens, and C. Wiese, "Updated Lattice Results for Parton Distributions," Phys. Rev. **D96** no. 1, (2017) 014513, arXiv:1610.03689 [hep-lat].

[24] E. Eichten, K. Gottfried, T. Kinoshita, K. D. Lane, and T.-M. Yan, "Charmonium: The Model," Phys. Rev. **D17** (1978) 3090. [Erratum: Phys. Rev.D21,313(1980)].

[25] S. Capstick and N. Isgur, "Baryons in a Relativized Quark Model with Chromodynamics," Phys. Rev. **D34** (1986) 2809. [AIP Conf. Proc.132,267(1985)].

[26] S. Capstick and W. Roberts, "Quark models of baryon masses and decays," Prog. Part. Nucl. Phys. **45** (2000) S241–S331, arXiv:nucl-th/0008028 [nucl-th].

[27] G. F. de Teramond and S. J. Brodsky, "Hadronic spectrum of a holographic dual of QCD," Phys. Rev. Lett. **94** (2005) 201601, arXiv:hep-th/0501022 [hep-th].

[28] G. F. de Teramond and S. J. Brodsky, "Light-Front Holography: A First Approximation to QCD," Phys. Rev. Lett. **102** (2009) 081601, arXiv:0809.4899 [hep-ph].

[29] S. D. Glazek and A. P. Trawiński, "Model of the AdS/QFT duality," Phys. Rev. **D88** no. 10, (2013) 105025, arXiv:1307.2059 [hep-ph].

[30] A. P. Trawiński, S. D. Głazek, S. J. Brodsky, G. F. de Téramond, and H. G. Dosch, "Effective confining potentials for QCD," Phys. Rev. **D90** no. 7, (2014) 074017, arXiv:1403.5651 [hep-ph].

[31] W. E. Caswell and G. P. Lepage, "Effective Lagrangians for Bound State Problems in QED, QCD, and Other Field Theories," Phys. Lett. **167B** (1986) 437–442.

[32] N. Brambilla, A. Pineda, J. Soto, and A. Vairo, "Potential NRQCD: An Effective theory for heavy quarkonium," Nucl. Phys. **B566** (2000) 275, arXiv:hep-ph/9907240 [hep-ph].

[33] M. A. Shifman, A. I. Vainshtein, and V. I. Zakharov, "QCD and Resonance Physics. Theoretical Foundations," Nucl. Phys. **B147** (1979) 385–447.

[34] M. A. Shifman, A. I. Vainshtein, and V. I. Zakharov, "QCD and Resonance Physics: Applications," Nucl. Phys. **B147** (1979) 448–518.

[35] J. P. Vary, H. Honkanen, J. Li, P. Maris, S. J. Brodsky, A. Harindranath, G. F. de Teramond, P. Sternberg, E. G. Ng, and C. Yang, "Hamiltonian light-front field theory in a basis function approach," Phys. Rev. **C81** (2010) 035205, arXiv:0905.1411 [nucl-th].

[36] Y. Li, P. Maris, and J. P. Vary, "Quarkonium as a relativistic bound state on the light front," Phys. Rev. **D96** no. 1, (2017) 016022, arXiv:1704.06968 [hep-ph].

[37] J. M. Cornwall, "Dynamical Mass Generation in Continuum QCD," Phys. Rev. **D26** (1982) 1453.

[38] A. C. Aguilar, D. Binosi, C. T. Figueiredo, and J. Papavassiliou, "Evidence of ghost suppression in gluon mass scale dynamics," Eur. Phys. J. **C78** no. 3, (2018) 181, arXiv:1712.06926 [hep-ph].

[39] I. L. Bogolubsky, E. M. Ilgenfritz, M. Muller-Preussker, and A. Sternbeck, "Lattice gluodynamics computation of Landau gauge Green's functions in the deep infrared," Phys. Lett. **B676** (2009) 69–73, arXiv:0901.0736 [hep-lat].

[40] G. Parisi and R. Petronzio, "On Low-Energy Tests of QCD," Phys. Lett. **94B** (1980) 51–53.

[41] C. Bloch, "Sur la théorie des perturbations des états liés," Nucl. Phys. **6** (1958) 329 – 347. http://www.sciencedirect.com/science/article/pii/0029558258901160.

[42] K. G. Wilson, "A Model Of Coupling Constant Renormalization," Phys. Rev. **D2** (1970) 1438.

[43] V. N. Gribov and L. N. Lipatov, "Deep inelastic electron scattering in perturbation theory," Phys. Lett. **37B** (1971) 78–80.

[44] V. N. Gribov and L. N. Lipatov, "Deep inelastic e p scattering in perturbation theory," Sov. J. Nucl. Phys. **15** (1972) 438–450. [Yad. Fiz.15,781(1972)].

[45] Y. L. Dokshitzer, "Calculation of the Structure Functions for Deep Inelastic Scattering and e+ e- Annihilation by Perturbation Theory in Quantum Chromodynamics.," Sov. Phys. JETP **46** (1977) 641–653. [Zh. Eksp. Teor. Fiz.73,1216(1977)].

[46] G. Altarelli and G. Parisi, "Asymptotic Freedom in Parton Language," Nucl. Phys. **B126** (1977) 298–318.

[47] E. A. Kuraev, L. N. Lipatov, and V. S. Fadin, "The Pomeranchuk Singularity in Nonabelian Gauge Theories," Sov. Phys. JETP **45** (1977) 199–204. [Zh. Eksp. Teor. Fiz.72,377(1977)].

[48] I. I. Balitsky and L. N. Lipatov, "The Pomeranchuk Singularity in Quantum Chromodynamics," Sov. J. Nucl. Phys. **28** (1978) 822–829. [Yad. Fiz.28,1597(1978)].

[49] S. D. Glazek and T. Maslowski, "Renormalized Poincare algebra for effective particles in quantum field theory," Phys. Rev. **D65** (2002) 065011, arXiv:hep-th/0110185 [hep-th].

[50] A. Casher and L. Susskind, "Chiral magnetism (or magnetohadrochironics)," Phys. Rev. **D9** (1974) 436–460.

[51] K. Serafin, "Relativistic Model of Hamiltonian Renormalization for Bound States and Scattering Amplitudes," Few Body Syst. **58** no. 3, (2017) 125, arXiv:1705.03844 [hep-ph].

[52] L. D. Landau and E. M. Lifshitz, Quantum Mechanics: Non-Relativistic Theory, vol. 3 of Course of Theoretical Physics. Pergamon Press, New York, 1977.

[53] S. M. Dawid, R. Gonsior, J. Kwapisz, K. Serafin, M. Tobolski, and S. D. Głazek, "Renormalization group procedure for potential $-g/r^2$," Phys. Lett. **B777** (2018) 260–264, arXiv:1704.08206 [quant-ph].

[54] S. D. Glazek and K. G. Wilson, "Renormalization of Hamiltonians," Phys. Rev. **D48** (1993) 5863–5872.

[55] S. D. Glazek, "Similarity renormalization group approach to boost invariant Hamiltonian dynamics," Acta Phys. Polon. **B29** (1998) 1979–2064, arXiv:hep-th/9712188 [hep-th].

[56] F. Bloch and A. Nordsieck, "Note on the Radiation Field of the electron," Phys. Rev. **52** (1937) 54–59.

[57] A. C. Aguilar, D. Binosi, and J. Papavassiliou, "The Gluon Mass Generation Mechanism: A Concise Primer," Front. Phys.(Beijing) **11** no. 2, (2016) 111203, arXiv:1511.08361 [hep-ph].

[58] S. D. Glazek, "Reinterpretation of gluon condensate in dynamics of hadronic constituents," Acta Phys. Polon. **B42** (2011) 1933–2010, arXiv:1106.6100 [hep-th].

[59] S. D. Glazek and K. G. Wilson, "Asymptotic freedom and bound states in Hamiltonian dynamics," Phys. Rev. **D57** (1998) 3558–3566, arXiv:hep-th/9707028 [hep-th].

[60] S. D. Glazek and J. Mlynik, "Optimization of perturbative similarity renormalization group for Hamiltonians with asymptotic freedom and bound states," Phys. Rev. **D67** (2003) 045001, arXiv:hep-th/0210110 [hep-th].

[61] M. Gómez-Rocha, T. Hilger, and A. Krassnigg, "Effects of a dressed quark-gluon vertex in vector heavy-light mesons and theory average of the B_c^* meson mass," Phys. Rev. **D93** no. 7, (2016) 074010, arXiv:1602.05002 [hep-ph].

[62] G. Karl and E. Obryk, "On wave functions for three-body systems," Nucl. Phys. **B8** (1968) 609–621.

[63] N. Isgur and G. Karl, "Positive Parity Excited Baryons in a Quark Model with Hyperfine Interactions," Phys. Rev. **D19** (1979) 2653. [Erratum: Phys. Rev.D23,817(1981)].

[64] J. D. Bjorken, "Is the ccc a new deal for baryon spectroscopy?," AIP Conf. Proc. **132** (1985) 390–403.

[65] M. Tsuge, T. Morii, and J. Morishita, "Baryon Spectrum in the Potential Model With Relativistic Corrections," Mod. Phys. Lett. **A1** (1986) 131. [Erratum: Mod. Phys. Lett.A2,283(1987)].

[66] B. Silvestre-Brac, "Spectrum and static properties of heavy baryons," Few Body Syst. **20** (1996) 1–25.

[67] Y. Jia, "Variational study of weakly coupled triply heavy baryons," JHEP **10** (2006) 073, arXiv:hep-ph/0607290 [hep-ph].

[68] A. P. Martynenko, "Ground-state triply and doubly heavy baryons in a relativistic three-quark model," Phys. Lett. **B663** (2008) 317–321, arXiv:0708.2033 [hep-ph].

[69] W. Roberts and M. Pervin, "Heavy baryons in a quark model," Int. J. Mod. Phys. **A23** (2008) 2817–2860, arXiv:0711.2492 [nucl-th].

[70] J. Vijande, A. Valcarce, and H. Garcilazo, "Constituent-quark model description of triply heavy baryon nonperturbative lattice QCD data," Phys. Rev. **D91** no. 5, (2015) 054011, arXiv:1507.03735 [hep-ph].

[71] G. Yang, J. Ping, P. G. Ortega, and J. Segovia, "Triply-heavy baryons in a constituent quark model," arXiv:1904.10166 [hep-ph].

[72] F. Giannuzzi, "Doubly heavy baryons in a Salpeter model with AdS/QCD inspired potential," Phys. Rev. **D79** (2009) 094002, arXiv:0902.4624 [hep-ph].

[73] Z. Ghalenovi, A. A. Rajabi, S.-x. Qin, and D. H. Rischke, "Ground-State Masses and Magnetic Moments of Heavy Baryons," Mod. Phys. Lett. **A29** (2014) 1450106, arXiv:1403.4582 [hep-ph].

[74] Z. Shah and A. K. Rai, "Masses and Regge trajectories of triply heavy Ω_{ccc} and Ω_{bbb} baryons," Eur. Phys. J. **A53** no. 10, (2017) 195.

[75] W. Ponce, "Heavy Quarks in a Spherical Bag," Phys. Rev. **D19** (1979) 2197.

[76] P. Hasenfratz, R. R. Horgan, J. Kuti, and J. M. Richard, "Heavy Baryon Spectroscopy in the QCD Bag Model," Phys. Lett. **94B** (1980) 401–404.

[77] A. Bernotas and V. Simonis, "Heavy hadron spectroscopy and the bag model," Lith. J. Phys. **49** (2009) 19–28, arXiv:0808.1220 [hep-ph].

[78] K.-W. Wei, B. Chen, and X.-H. Guo, "Masses of doubly and triply charmed baryons," Phys. Rev. **D92** no. 7, (2015) 076008, arXiv:1503.05184 [hep-ph].

[79] K.-W. Wei, B. Chen, N. Liu, Q.-Q. Wang, and X.-H. Guo, "Spectroscopy of singly, doubly, and triply bottom baryons," Phys. Rev. **D95** no. 11, (2017) 116005, arXiv:1609.02512 [hep-ph].

[80] J.-R. Zhang and M.-Q. Huang, "Deciphering triply heavy baryons in terms of QCD sum rules," Phys. Lett. **B674** (2009) 28–35, arXiv:0902.3297 [hep-ph].

[81] Z.-G. Wang, "Analysis of the Triply Heavy Baryon States with QCD Sum Rules," Commun. Theor. Phys. **58** (2012) 723–731, arXiv:1112.2274 [hep-ph].

[82] T. M. Aliev, K. Azizi, and M. Savci, "Masses and Residues of the Triply Heavy Spin-1/2 Baryons," JHEP **04** (2013) 042, arXiv:1212.6065 [hep-ph].

[83] T. M. Aliev, K. Azizi, and M. Savcı, "Properties of triply heavy spin-3/2 baryons," J. Phys. **G41** (2014) 065003, arXiv:1404.2091 [hep-ph].

[84] F. J. Llanes-Estrada, O. I. Pavlova, and R. Williams, "A First Estimate of Triply Heavy Baryon Masses from the pNRQCD Perturbative Static Potential," Eur. Phys. J. **C72** (2012) 2019, arXiv:1111.7087 [hep-ph].

[85] H. Sanchis-Alepuz, R. Alkofer, G. Eichmann, and R. Williams, "Model Comparison of Delta and Omega Masses in a Covariant Faddeev Approach," PoS **QCD-TNT-II** (2011) 041, arXiv:1112.3214 [hep-ph].

[86] S.-X. Qin, C. D. Roberts, and S. M. Schmidt, "Poincaré-covariant analysis of heavy-quark baryons," Phys. Rev. **D97** no. 11, (2018) 114017, arXiv:1801.09697 [nucl-th].

[87] Z. S. Brown, W. Detmold, S. Meinel, and K. Orginos, "Charmed bottom baryon spectroscopy from lattice QCD," Phys. Rev. **D90** no. 9, (2014) 094507, arXiv:1409.0497 [hep-lat].

[88] S. Meinel, "Excited-state spectroscopy of triply-bottom baryons from lattice QCD," Phys. Rev. **D85** (2012) 114510, arXiv:1202.1312 [hep-lat].

[89] R. A. Briceno, H.-W. Lin, and D. R. Bolton, "Charmed-Baryon Spectroscopy from Lattice QCD with $N_f = 2 + 1 + 1$ Flavors," Phys. Rev. **D86** (2012) 094504, arXiv:1207.3536 [hep-lat].

[90] M. Padmanath, R. G. Edwards, N. Mathur, and M. Peardon, "Spectroscopy of triply-charmed baryons from lattice QCD," Phys. Rev. **D90** no. 7, (2014) 074504, arXiv:1307.7022 [hep-lat].

[91] **PACS-CS** Collaboration, Y. Namekawa et al., "Charmed baryons at the physical point in 2+1 flavor lattice QCD," Phys. Rev. **D87** no. 9, (2013) 094512, arXiv:1301.4743 [hep-lat].

[92] C. Alexandrou, V. Drach, K. Jansen, C. Kallidonis, and G. Koutsou, "Baryon spectrum with $N_f = 2 + 1 + 1$ twisted mass fermions," Phys. Rev. **D90** no. 7, (2014) 074501, arXiv:1406.4310 [hep-lat].

[93] K. U. Can, G. Erkol, M. Oka, and T. T. Takahashi, "Look inside charmed-strange baryons from lattice QCD," Phys. Rev. **D92** no. 11, (2015) 114515, arXiv:1508.03048 [hep-lat].

[94] J. Carbonell, B. Desplanques, V. A. Karmanov, and J. F. Mathiot, "Explicitly covariant light front dynamics and relativistic few body systems," Phys. Rept. **300** (1998) 215–347, arXiv:nucl-th/9804029 [nucl-th].

[95] R. G. Arnold, C. E. Carlson, and F. Gross, "Elastic electron-Deuteron Scattering at High-Energy," Phys. Rev. **C21** (1980) 1426.

[96] V. B. Berestetskii, E. M. Lifshitz, and L. P. Pitaevskii, Quantum Electrodynamics, vol. 4 of Course of Theoretical Physics. Pergamon Press, Oxford, 1982.

[97] L. Adhikari, Y. Li, M. Li, and J. P. Vary, "Form factors and generalized parton distributions of heavy quarkonia in basis light front quantization," Phys. Rev. **C99** no. 3, (2019) 035208, arXiv:1809.06475 [hep-ph].

[98] S. D. Glazek and J. M. Namyslowski, "Nucleon Wave Function with Running Quark Masses," Acta Phys. Polon. **B19** (1988) 569–587.

[99] B. L. Ioffe, "Calculation of Baryon Masses in Quantum Chromodynamics," Nucl. Phys. **B188** (1981) 317–341. [Erratum: Nucl. Phys.B191,591(1981)].

[100] K. Raya, M. A. Bedolla, J. J. Cobos-Martínez, and A. Bashir, "Heavy quarkonia in a contact interaction and an algebraic model: mass spectrum, decay constants, charge radii and elastic and transition form factors," Few Body Syst. **59** no. 6, (2018) 133, arXiv:1711.00383 [nucl-th].

[101] J. J. Dudek, R. G. Edwards, and D. G. Richards, "Radiative transitions in charmonium from lattice QCD," Phys. Rev. **D73** (2006) 074507, arXiv:hep-ph/0601137 [hep-ph].

[102] M. S. Bhagwat and P. Maris, "Vector meson form factors and their quark-mass dependence," Phys. Rev. **C77** (2008) 025203, arXiv:nucl-th/0612069 [nucl-th].

[103] T. A. Lahde, "Exchange current operators and electromagnetic dipole transitions in heavy quarkonia," Nucl. Phys. **A714** (2003) 183–212, arXiv:hep-ph/0208110 [hep-ph].

[104] R. Dhir, C. S. Kim, and R. C. Verma, "Magnetic Moments of Bottom Baryons: Effective mass and Screened Charge," Phys. Rev. **D88** (2013) 094002, arXiv:1309.4057 [hep-ph].

[105] A. Faessler, T. Gutsche, M. A. Ivanov, J. G. Korner, V. E. Lyubovitskij, D. Nicmorus, and K. Pumsa-ard, "Magnetic moments of heavy baryons in the relativistic three-quark model," Phys. Rev. **D73** (2006) 094013, arXiv:hep-ph/0602193 [hep-ph].

[106] V. Simonis, "Improved predictions for magnetic moments and M1 decay widths of heavy hadrons," arXiv:1803.01809 [hep-ph].

[107] V. Šimonis, "Magnetic properties of ground-state mesons," Eur. Phys. J. **A52** no. 4, (2016) 90, arXiv:1604.05894 [hep-ph].

[108] R. G. Roberts, The Structure of the proton: Deep inelastic scattering. Cambridge Monographs on Mathematical Physics. Cambridge University Press, 1994.

[109] J. D. Bjorken, "Asymptotic Sum Rules at Infinite Momentum," Phys. Rev. **179** (1969) 1547–1553.

[110] A. D. Martin, "Proton structure, Partons, QCD, DGLAP and beyond," Acta Phys. Polon. **B39** (2008) 2025–2062, arXiv:0802.0161 [hep-ph].

[111] A. P. Trawiński, Hadron light-front wave functions based on AdS/QCD duality. PhD thesis, Warsaw U., 2016-05. http://depotuw.ceon.pl/handle/item/1640?locale-attribute=en.

[112] R. P. Feynman, Photon-hadron interactions. Reading, 1973.

[113] C. G. Callan, Jr. and D. J. Gross, "High-energy electroproduction and the constitution of the electric current," Phys. Rev. Lett. **22** (1969) 156–159.

[114] R. P. Feynman, "Very high-energy collisions of hadrons," Phys. Rev. Lett. **23** (1969) 1415–1417. [,494(1969)].

I gra gitara...